

**DOKUZ EYLUL UNIVERSITY
GRADUATE SCHOOL OF NATURAL AND APPLIED
SCIENCES**

**DETERMINATION OF ANIONS IN
GEOHERMAL WATERS WITH ION
CHROMATOGRAPHY AND BICARBONATE
WITH SPECTROSCOPIC METHOD**

by

Merve ZEYREK

August, 2008

İZMİR

**DETERMINATION OF ANIONS IN
GEOHERMAL WATERS WITH ION
CHROMATOGRAPHY AND BICARBONATE
WITH SPECTROSCOPIC METHOD**

**A Thesis Submitted to the
Graduate School of Natural and Applied Sciences of Dokuz Eylül
University
In Partial Fulfillment of the Requirements for the Master of Science
of Chemistry in
Chemistry, Applied Chemistry Program**

**by
Merve ZEYREK**

**August, 2008
İZMİR**

M.Sc THESIS EXAMINATION RESULT FORM

We have read the thesis entitled “**DETERMINATION OF ANIONS IN GEOTHERMAL WATERS WITH ION CHROMATOGRAPHY AND BICARBONATE WITH SPECTROSCOPIC METHOD**” completed by **MERVE ZEYREK** under supervision of **ASSOCIATE PROFESSOR KADRIYE ERTEKİN** and we certify that in our opinion it is fully adequate, in scope and in quality, as a thesis for the degree of Master of Science.

Doç. Dr. Kadriye Ertekin

Supervisor

Prof. Dr. Kadir YURDAKOÇ

(Jury Member)

Prof. Dr. Ali Çelik

(Jury Member)

Prof.Dr. Cahit HELVACI

Director

Graduate School of Natural and Applied Sciences

ACKNOWLEDGMENTS

I would like to express sincere gratitude to my supervisor Associated Professor Dr.Kadriye Ertekin for providing the fascinating subject, for her valuable support during this thesis and for the great working conditions at our laboratory.

Funding for this research was provided by the TUBITAK (Multi-Disciplinary Earthquake Researches in High Risk Regions of Turkey Representing Different Tectonic Regimes – TURDEP Project) and Scientific Research Funds of Dokuz Eylul University.

I want to thank to Professor Sedat Inan, Professor Zafer Akc1g, Associated Professor Mustafa Akgun, Assistant Professor Orhan Polat and Doctor Cemil Seyis for their valuable orientations.

I gratefully acknowledge that my personal funding was provided by the Scientific Research Council of Turkey (TUBITAK-BİDEB).

I also gratefully acknowledge the extensive helps of my colleagues M Sc. student Sibel Kacmaz, Ph. D. student Sibel Derinkuyu and M Sc. student R.Erim Ongun during experimental studies and sampling respectively.

Finally, I want to thank to my parents and my engaged for their tolerant attitude to my working effort during the elaboration of this dissertation and for their incessant support during all the years of my studies.

Merve ZEYREK

DETERMINATION OF ANIONS IN GEOTHERMAL WATERS WITH ION CHROMATOGRAPHY AND BICARBONATE WITH SPECTROSCOPIC METHOD

ABSTRACT

This thesis consists of two complimentary chapters. In the first part, simultaneous ion chromatographic analysis of seven different anions (Fluoride, Chloride, Nitride, Bromide, Nitrate, Phosphate, Sulfate) in real groundwater samples were performed by ion chromatography method. Some validation tests and the optimum conditions for the determination of anions were studied. Analysis of anions was performed by injection of samples to the chromatographic system after filtration and/or dilution. The precision and accuracy of the method were tested at three different concentration levels for each standard. Recovery studies were performed by adding standards in to the geothermal groundwater and drinking water samples. For groundwater samples recovery tests was performed between two successive months. Precision was also assessed as the percentage relative standard deviation (% RSD) of both repeatability (within-day) and reproducibility (between-day and different concentrations) for groundwater samples. SD and RSD values of 220 real groundwater samples acquired during 8 months were evaluated.

In the second part, bicarbonate (HCO_3^-) analysis in groundwater samples was performed by spectrophotometric, titrimetric and potentiometric methods. New indicator dyes namely [N, N'-bis(4-dimethylaminobenzylidene)benzene-1,4-diamine (Y-10), 4-[4-(dimethylamino) phenylmethylene]amino acetophenone (Y-11) and 4-(4-(dimethylamino)phenyl)methyleneamino benzonitrile (Y-13)] were offered for absorption based analysis of HCO_3^- anion.

The indicator dyes were characterized in the different solvents of ethanol (EtOH), dichloromethane (DCM), tetrahydrofuran (THF) and Toluene/Ethanol (To: EtOH) mixture (80:20)), in solid matrix of PVC and in Ionic Liquid media. Maximum absorption wavelength (λ_{abs}) and molar extinction coefficients (ϵ) of the indicators were determined with Uv-Vis spectrophotometer in all of the employed matrices. Acidity constant values of three different indicator dyes were calculated in ethanol and polyvinylchloride for HCO_3^- sensing purposes. Cross sensitivities of the indicator dyes to other cations was also tested and evaluated.

Keywords: Ion chromatography, groundwater analysis, chromatographic groundwater analysis, anion analysis, HCO_3^- analysis, spectral HCO_3^- analysis

JEOTERMAL SU ÖRNEKLERİNDE ANYONLARIN İYON KROMATOĞRAFİ VE BİKARBONATIN SPEKTROSKOPİK METHOD İLE TAYİNİ

ÖZ

Bu tez iki tamamlayıcı bölümden oluşmaktadır. Birinci bölümde gerçek yeraltı suyu örneklerinde yedi farklı anyonun (Florür, Klorür, Nitrit, Bromür, Nitrat, Fosfat ve Sülfat) eşzamanlı analizleri iyon kromatografi metoduyla gerçekleştirilmiştir. Bazı validasyon testleri ve anyonların analizi için optimum koşullar araştırılmıştır. Anyonların analizi filtrasyon ve/veya seyreltme işlemlerinden sonra örneklerin cihaza enjeksiyonu ile gerçekleştirilmiştir. Methodun kesinliği ve doğruluğu her bir standart için üç farklı konsantrasyon düzeyinde incelenmiştir. Gerikazanım çalışmaları standartların yeraltı suyu ve içme suyu örneklerine eklenmesiyle yapılmıştır. Yeraltı suyu örneklerinde gerikazanım testleri ardışık iki ay ara ile toplanan örnekler üzerinde gerçekleştirilmiştir. Yeraltı suyu örnekleri için kesinlik aynı zamanda gün içi ve günler arası tekrarlanabilirliğin % bağıl standart sapması (%RSD) olarak da araştırılmıştır. Standart sapma ve bağıl standart sapma değerleri sekiz ay boyunca toplanan 220 adet gerçek yeraltı suyu örneğinde değerlendirilmiştir.

İkinci kısımda yeraltı suyu örneklerinde bikarbonat (HCO_3^-) analizi spektrofotometrik, titrimetrik ve potasyometrik methodlarla gerçekleştirilmiştir. [N,N'-bis(4-dimetilaminobenziliden)benzen-1,4-diamin (Y-10), 4-[4-(dimetilamino)fenilmetilen]aminoasetofenon (Y-11) ve 4-(4-(dimetilamino)fenil)metilenamino benzonitril (Y-13)] boyaları HCO_3^- iyonunun spektrofotometrik analizi için önerilmiştir. İndikatör boyalar, etanol, diklorometan, tetrahidrofuran, toluen-etanol karışımı (80:20)çözücülerinde, katı matriks olan PVC de ve iyonik sıvı içerisinde karakterize edilmiştir.

İndikatör boyaların maksimum absorpsiyon dalga boyu (λ_{abs}) ve molar absorptivite katsayıları (ϵ) yukarıda söz edilen tüm matrislerde UV-Vis spektrofotometresi ile belirlenmiştir. Boyar maddelerin asitlik sabitleri HCO_3^- analizinde kullanılabilirliğini araştırmak amacıyla belirlenmiştir. Diğer metal katyonlarına olan yanıtları da test edilip değerlendirilmiştir.

Anahtar Kelimeler: İyon kromatografi, yeraltı suyu analizi, kromatografik yeraltı suyu analizi, anyon analizi, HCO_3^- analizi, spektal HCO_3^- analizi

CONTENTS	Page
THESIS EXAMINATION RESULT FORM.....	ii
ACKNOWLEDGEMENTS.....	iii
ABSTRACT.....	iv
ÖZ.....	v
CHAPTER ONE – INTRODUCTION.....	1
1.1 Groundwater Composition.....	1
1.2 Techniques for Groundwater Analysis.....	4
CHAPTER TWO -ION CHROMATOGRAPHY BASED STUDIES.....	5
2.1 Historical Development of Ion Chromatography	8
2.2 Types of Ion Chromatography	8
2.2.1 Ion-Exclusion Chromatography (HPICE).....	8
2.2.2 Ion-Pair Chromatography (MPIC)	8
2.2.3 Ion-Exchange Chromatography (HPIC)	8
2.3 Advantages of Ion Chromatography	9
2.3.1 Speed	9
2.3.2 Sensitivity.....	10
2.3.3 Selectivity.....	10
2.3.4 Simultaneous Detection	11
2.3.5 Stability of the Separator Columns	11
2.4 Principle of Ion Chromatographic Separation and Detection	11
2.4.1 Requirements for Separation.....	12
2.4.2 Basis for Separation.....	12
2.4.3 Separation.....	13
2.4.3.1 Equilibration.....	14
2.4.3.2 Sample Application and Wash.....	14
2.4.3.3 Elution and Regeneration.....	16
2.4.3.4 Detection	18

2.5 Ion-Exchange Equilibria.....	19
2.6 Components of an Ion Chromatography (IC) Instrument.....	22
2.6.1 Eluent Delivery	23
2.6.1.1 Degassing the Eluent.....	24
2.6.2 Pumps	24
2.6.3 Pressure.....	26
2.6.4 Injector.....	26
2.6.5 Column Oven.....	27
2.6.6 IC Column	27
2.6.7 Ion-Exchange Packing.....	28
2.6.7.1 Polymeric Resins.....	29
2.6.7.1.1 Substrate and Cross-Linking	29
2.6.7.1.2 Chemical Functionalization	31
2.6.7.2 Polyacrylate Anion Exchangers	32
2.6.7.3 Quaternary Phosphonium Resins	33
2.6.7.4 Latex Agglomerated Ion Exchangers.....	33
2.6.7.5 Silica-Based Anion Exchangers.....	36
2.6.8 Suppressors.....	36
2.6.8.1 Fiber Suppressors	36
2.6.8.2 Membrane Suppressors	37
2.6.8.3 Electrolytic Suppressors.....	39
2.6.8.3.1 Suppressed Anion Chromatography.....	40
2.6.8.3.2 Non-Suppressed Anion Chromatography	42
2.6.9 Detectors	44
2.6.9.1 Conductivity Detectors	44
2.6.9.2 Ultraviolet-Visible Detectors	46
2.6.9.3 Electrochemical Detectors	48
2.6.9.4 Refractive Index Detection	49
2.6.9.5 Other Detectors	49
2.7 Experimental Method and Instrumentation.....	50
2.7.1 Instrument	50
2.7.2 Reagents	51

2.7.3 Preparation of the Solutions	52
2.7.4 Pretreatment of Samples	52
2.8 Results and Discussion.....	52
2.8.1 Analysis of Seven Anion Standards.....	52
2.8.2 Method Validation Studies and Accuracy.....	61
2.8.2.1 Recovery Studies with Real Ground Water Samples.....	63
2.8.2.2 Statistical Assessment of Recovery Results of Groundwater Samples	67
2.8.3 Reproducibility.....	70
2.8.3.1 Reproducibility of Replicate Injections	71
2.8.3.2 Reproducibility Studies of Intraday	73
2.8.3.3 Reproducibility Studies between Months	74
2.8.4 Analysis of Groundwater Samples of Pamukkale Location with Ion Chromatography.....	76
 CHAPTER THREE –INTRODUCTION	87
 3.1 UV-Vis spectrophotometric Method.....	87
3.2 Basic principles of UV-Vis spectrophotometric Method.....	88
3.2.1 The electromagnetic Spectrum.....	88
3.2.2 Wavelength and Frequency.....	88
3.2.3 Transmittance and Absorbance	89
3.2.4 Theory of UV-Visible Spectra	89
3.2.5 Luminescence.....	91
3.2.5.1 Mechanism of Luminescence.....	91
3.2.6 Experimental Method and Instrumentation.....	93
3.2.6.1 Reagents	93
3.2.6.2 Preparation of the Buffer Solutions.....	95
3.2.6.3 Construction of the Sensing Films	96
3.2.6.4 Preparation of Ionic Liquid Media.....	97
3.3 Absorption Based Spectral Characterization of the Employed Indicator Dyes	98

3.3.1 pKa Calculations of Y10, Y11 and Y 13 in the Solvent of EtOH	101
3.3.2 pKa Calculations of Y 10, Y 11 and Y 13 in PVC Matrix	104
3.4 Emission Based HCO ₃ ⁻ tests of the PVC Doped Indicator Dyes	106
3.4.1 Calibration Graph of PVC doped Y 10, Y 11 and Y 13 Dyes for HCO ₃ ⁻	108
3.4.2 HCO ₃ ⁻ Analysis in Real-Groundwater Samples.....	112
3.5 Ionic Liquid Media Based Studies	114
3.6 Response of PVC Doped Y 10, Y 11 and Y 13 to Different Cations and Anions	118
 CHAPTER FOUR-CONCLUSION	120
 REFERANCES.....	124

CHAPTER ONE

INTRODUCTION

1.1 Groundwater Composition (Stumm & Morgan, 1970)

During the hydrogeological cycle, water interacts continuously matter. The processes dissolution and precipitation, oxidation and reduction acid-base and coordinative interactions are the same in the nature as in the laboratory.

The actual natural water systems usually consist of numerous minerals and often a gas phase in addition to the aqueous phase.

Natural waters indeed are open and dynamic systems with variable inputs and outputs of mass and energy for which the state of equilibrium is a result.

Equilibrium and near equilibrium conditions are more likely to prevail in ground waters than in surfaces waters because a relatively large surface area of solid minerals is exposed to slowly moving water.

Phosphorus occurs in ground waters almost exclusively in the form of inorganic orthophosphates ($\text{H}_2\text{PO}_4^{-1}$) and (HPO_4^{2-}) in the near natural pH range. Phosphate concentrations cannot exceed 10^{-6} M because of the solubility limitation by hydroxylapatite.

Similarly total iron and manganese concentrations encountered in ground waters as soluble species can be predicted from solubility equilibria. A ground water saturated with MnCO_3 , FeCO_3 and CaCO_3 should contain soluble $[\text{Mn}^{2+}]$, $[\text{Fe}^{3+}]$ and $[\text{Ca}^{2+}]$.

Unless special precautions are taken, the measured pH value may not represent the actual pH of the water in the aquifer such discrepancy may result in an apparent super saturation.

The concentration of dissolved oxygen and carbon dioxide in a ground water near it is source of recharge reflect the partial pressures of O₂ and CO₂ in the soil gas which usually is an reached with CO₂ because of respiratory activity of micro organisms (Stumm & Morgan, 1970).

Typically soil solutions contain CO₂ concentrations representative of partial pressures between 10⁻¹ and 10⁻² atm. Respiratory production of CO₂ accompanied by a concordant consumption of oxygen but because O₂ is present at much higher concentrations than CO₂, the O₂ content changes relatively little. Hence, the partial pressure level of a ground water in contact. The amount and character of the mineral matter dissolved by precipitation depend upon the chemical composition and physical structure of the rocks with which they have been in contact, temperature, the pressure, the duration of the contact, the materials already in solution, hydrogen- and hydroxyl-ion concentrations (pH), and redox potential (Eh). The solvent action of the water is assisted by the presence in solution of carbon dioxide, derived from the atmosphere as the water fell as precipitation, or from the soil through which it passes, where it is formed by organic processes (Stumm & Morgan, 1970).

Most of the major, secondary, minor, and trace constituents dissolved in ground water and information concerning ranges of concentration are given below (Walton, 1970).

Table 1.1 Dissolved constituents in groundwater

Major Constituents (Range of Concentration 1.0 to 1.000 ppm)	
Sodium	Bicarbonate
Calcium	Sulfate
Magnesium	Chloride
Silica	

Secondary Constituents (Range of Concentration 0.01 to 10.0 ppm)	
Iron	Carbonate
Strontium	Nitrate
Potassium	Fluoride
Boron	

Minor Constituents (Range of Concentration 0.00001 to 0.1 ppm)	
Antimony	Lithium
Aluminum	Manganese
Arsenic	Molybdenum
Barium	Nickel
Bromide	Phosphate
Cadmium	Rubidium
Chromium	Selenium
Cobalt	Titanium
Copper	Uranium
Germanium	Vanadium
Iodide	Zinc
Lead	

Trace Constituents (Range of Concentration Generally Less Than 0.001 ppm)	
Beryllium	Ruthenium
Bismuth	Scandium
Cerium	Silver
Cesium	Thallium
Gallium	Thorium
Gold	Tin
Indium	Tungsten
Lanthanum	Ytterbium
Niobium	Yttrium
Platinum	Zirconium
Radium	

1.2 Techniques for Groundwater Analysis

Accurate analysis of ground water samples is a very important subject of environmental studies. Many classical methods have been proposed for determination of anions in water samples, among them the most important ones are spectrophotometric (Dahlen, Karlsson, Backstrom, Hagberg, & Pettersson, 2000; Parvinen, & Lajunen, 1999), atomic absorption spectrometry (AAS), an inductively coupled plasma-atomic emission spectrometry (ICP-AES) (Ozcan, & Yilmaz, 2005; Liu, Wu, Li, & Ga, 1999; Muller, 1999; Chakrapani, Murty, Mohanta, & Rangaswamy, 1998), electrochemical (voltametric, ion-selective electrodes, amperometric, and coulometric), titration and gravimetric methods (Komy, 1993; Soto-Chinchilla, Garcia-Campana, Gamiz-Gracia, & Cruces-Blanco, 2006). In general, these methods are time- and labour-consuming and sometimes even impossible to apply because of such restrictions as large volume of sample needed, the effect of the matrix or unsatisfactory selectivity. Recently, some instrumental analytical methods for simultaneous analysis have been proposed: The ion chromatography method offers good reproducibility, high sensitivity, is selective and gives results in a short time (Polesello, Valsecchi, Cavalli, & Reschiotto, 2001; Niedzielski, 2005; Samatya, Kabay, Yuksel, Arda, & Yuksel, 2006; Vaaramaa, & Lehto, 2003). Nevertheless, determination of complex matrices requires sample-pretreatment or sophisticated assemblies.

CHAPTER TWO

ION CHROMATOGRAPHY BASED STUDIES

2.1 Historical Development of Ion Chromatography

“Chromatography” is the general term for a variety of physico-chemical separation techniques, all of which have in common the distribution of a component between a mobile phase and a stationary phase. The various chromatographic techniques are subdivided according to the physical state of these two phases (Weiss, 2004).

Ion chromatography refers to modern and efficient methods of separating and determining ions based upon ion-exchange resins. Ion chromatography was first developed in the mid-1970s, when it was shown that anion or cation mixtures can be readily resolved on HPLC columns packed with anion-exchange or cation exchange resins (Skoog, & Leary, 1992). Ion Chromatography (IC) was introduced in 1975 by Small, Stevens, and Bauman as a new analytical method. Within a short period of time, ion chromatography evolved from a new detection scheme for a few selected inorganic anions and cations to a versatile analytical technique for ionic species in general. For a sensitive detection of ions via their electrical conductance, the separator column effluent was passed through a “suppressor” column. This suppressor column chemically reduces the eluent background conductance, while at the same time increasing the electrical conductance of the analyte ions (Weiss, 2004).

In 1979, Fritz et al. described an alternative separation and detection scheme for inorganic anions, in which the separator column is directly coupled to the conductivity cell. As a prerequisite for this chromatographic setup, low capacity ion-exchange resins must be employed, so that low ionic strength eluents can be used. In addition, the eluent ions should exhibit low equivalent conductance, thus enabling sensitive detection of the sample components.

At the end of the 1970s, ion chromatographic techniques were used to analyze organic ions for the first time. The requirement for a quantitative analysis of organic acids brought about an ion chromatographic method based on the ion exclusion process that was first described by Wheaton and Bauman in 1953 (Weiss, 2004).

The 1980s witnessed the development of high efficiency separator columns with particle diameters between 5 μm and 8 μm , which resulted in a significant reduction of analysis time. In addition, separation methods based on the ion pair process were introduced as an alternative to ion-exchange chromatography, because they allow the separation and determination of both anions and cations.

Since the beginning of the 1990s, column development has aimed to provide stationary phases with special selectivity. In inorganic anion analysis, stationary phases were developed that allow the separation of fluoride from the system void and the analysis of the most important mineral acids as well as oxyhalides such as chlorite, chlorate, and bromate in the same run. Moreover, high capacity anion exchangers are under development that will enable analysis of, for example, trace anionic impurities in concentrated acids and salinary samples. Problem solutions of this kind are especially important for the semiconductor industry, seawater analysis, and clinical chemistry. In inorganic cation analysis, simultaneous analysis of alkali- and alkaline-earth metals is of vital importance, and can only be realized within an acceptable time frame of 15 minutes by using weak acid cation exchangers. Of increasing importance is the analysis of aliphatic amines, which can be carried out on similar stationary phases by adding organic solvents to the acid eluent (Weiss, 2004).

The scope of ion chromatography was considerably enlarged by newly designed electrochemical and spectrophotometric detectors. A milestone of this development was the introduction of a pulsed amperometric detector in 1983, allowing a very sensitive detection of carbohydrates, amino acids, and divalent sulfur compounds.

A growing number of applications utilizing post-column derivatization in combination with photometric detection opened the field of polyphosphate, polyphosphonate, and transition metal analysis for ion chromatography, thus providing a powerful extension to conventional titrimetric and atomic spectrometry methods (Weiss, 2004).

These developments made ion chromatography an integral part of both modern inorganic and organic analysis.

Even though ion chromatography is still the preferred analytical method for inorganic and organic ions, meanwhile, ion analyses are also carried out with capillary electrophoresis (CE), which offers certain advantages when analyzing samples with extremely complex matrices. In terms of detection, only spectrometric methods such as UV/Vis and fluorescence detection are commercially available. Because inorganic anions and cations as well as aliphatic carboxylic acids cannot be detected very sensitively or cannot be detected at all, applications of CE are rather limited as compared to IC, with the universal conductivity detection being employed in most cases (Weiss, 2004).

Dasgupta et al. as well as Avdalovic et al. independently succeeded to miniaturize a conductivity cell and a suppressor device down to the scale required for CE. Since the sensitivity of conductivity detection does not suffer from miniaturization, detection limits achieved for totally dissociated anions and low molecular weight organics compete well with those of ion chromatography techniques. Thus, capillary electrophoresis with suppressed conductivity detection can be regarded as a complementary technique for analyzing small ions in simple and complex matrices (Weiss, 2004).

2.2 Types of Ion Chromatography

Modern ion chromatography as an element of liquid chromatography is based on three different separation mechanisms, which also provide the basis for the nomenclature in use (Weiss, 2004).

2.2.1 Ion-Exclusion Chromatography (HPICE) (High Performance Ion Chromatography Exclusion)

The separation mechanism in ion-exclusion chromatography is governed by Donnan exclusion, steric exclusion, sorption processes and, depending on the type of separator column, by hydrogen bonding (Weiss, 2004).

2.2.2 Ion-Pair Chromatography (MPIC) (Mobile Phase Ion Chromatography)

The dominating separation mechanism in ion-pair chromatography is adsorption. The stationary phase consists of a neutral porous divinylbenzene resin of low polarity and high specific surface area. The selectivity of the separator column is determined by the mobile phase (Weiss, 2004).

2.2.3 Ion-Exchange Chromatography (HPIC) (High Performance Ion Chromatography)

This separation method is based on ion exchange processes occurring between the mobile phase and ion-exchange groups bonded to the support material. In highly polarizable ions, additional non-ionic adsorption processes contribute to the separation mechanism. The stationary phase consists of polystyrene, ethylvinylbenzene, or methacrylate resins co-polymerized with divinylbenzene and modified with ion-exchange groups. Ion-exchange chromatography is used for the separation of both inorganic and organic anions and cations. Separation of anions is accomplished with quaternary ammonium groups attached to the polymer, whereas

sulfonate-, carboxyl-, or phosphonate groups are used as ion exchange sites for the separation of cations (Weiss, 2004).

2.3 Advantages of Ion Chromatography

The name "ion chromatography" applies to any modern method for chromatographic separation of ions. Normally, such separations are performed on a column packed with a solid ion-exchange material. Ion chromatography is considered to be an indispensable tool in a modern analytical laboratory. Complex mixtures of anions or cations can usually be separated and quantitative amounts of the individual ions measured in a relatively short time. Higher concentrations of sample ions may require some dilution of the sample before introduction into the ion-chromatographic instrument, ion chromatography is also a superb way to determine ions present at concentrations down to at least the low part per billion ($\mu\text{g/L}$) range (Fritz, & Gjerde, 2000).

Ion Chromatography offers the following advantages:

- Speed
- Sensitivity
- Selectivity
- Simultaneous detection
- Stability of the separator columns

2.3.1 Speed

The time necessary to perform an analysis becomes an increasingly important aspect, because enhanced manufacturing costs for high quality products and additional environmental efforts have lead to a significant increase in the number of samples to be analyzed (Weiss, 2004).

With the introduction of high efficiency separator columns for ion exchange, ion-exclusion, and ion-pair chromatography in recent years, the average Analysis time could be reduced to about 10 minutes. Today, a baseline-resolved separation of the seven most important inorganic anions requires only three minutes (Weiss, 2004).

2.3.2 Sensitivity

The introduction of microprocessor technology, in combination with modern high efficiency stationary phases, makes it a routine task to detect ions in the medium and lower $\mu\text{g/L}$ concentration range without pre-concentration. The detection limit for simple inorganic anions and cations is about $10 \mu\text{g/L}$ based on an injection volume of $50 \mu\text{L}$. The total amount of injected sample lies in the lower ng range. Even ultra pure water, required for the operation of power plants or for the production of semiconductors, may be analyzed for its anion and cation content after pre-concentration with respective concentrator columns. With these pre-concentration techniques, the detection limit could be lowered to the ng/L range. However, it should be emphasized that the instrumentation for measuring such incredibly low amounts is rather sophisticated. In addition, high demands have to be met in the creation of suitable environmental conditions (Weiss, 2004).

2.3.3 Selectivity

The selectivity of ion chromatographic methods for analyzing inorganic and organic anions and cations is ensured by the selection of suitable separation and detection systems. Regarding conductivity detection, the suppression technique is of vital importance, because the respective counter ions of the analyte ions as a potential source of interferences are exchanged against hydronium and hydroxide ions, respectively. New developments in the field of post-column derivatization show that specific compound classes such as transition metals, alkaline-earth metals, polyvalent anions, silicate, etc. can be detected with high selectivity. Such examples explain why sample preparation for ion chromatographic analyses usually involves

only a simple dilution and filtration of the sample. This high degree of selectivity facilitates the identification of unknown sample components (Weiss, 2004).

2.3.4 Simultaneous Detection

A major advantage of ion chromatography is its ability to simultaneously detect multiple sample components. Anion and cation profiles may be obtained within a short time; such profiles provide information about the sample composition and help to avoid time-consuming tests. However, the ability of ion chromatographic techniques for simultaneous quantitation is limited by extreme concentration differences between various sample components. For example, the major and minor components in a wastewater matrix may only be detected simultaneously if the concentration ratio is <1000:1. Otherwise, the sample must be diluted and analyzed in a separate chromatographic run (Weiss, 2004).

2.3.5 Stability of the Separator Columns

The stability of separator columns very much depends on the type of the packing material being used. Resin materials such as polystyrene/divinylbenzene copolymers prevail as support material in ion chromatography. The high pH stability of these resins allows the use of strong acids and bases as eluent, which is a prerequisite for the widespread applicability of this method. Strong acids and bases, on the other hand, can also be used for rinsing procedures (Weiss, 2004).

2.4 Principle of Ion Chromatographic Separation and Detection

2.4.1 Requirements for Separation

The ion-exchange resins used in modern chromatography are smaller in size but have a lower capacity than older resins. Columns packed with these newer resins have more theoretical plates than older columns. For this reason, successful

separations can now be obtained even when there are only small differences in retention times of the sample ions (Fritz, & Gjerde, 2000).

The major requirements of systems used in modern ion chromatography can be summarized as follows:

1. An efficient cation- or anion-exchange column with as many theoretical plates as possible.
2. An eluent that provides reasonable differences in retention times of sample ions.
3. A resin-eluent system that attains equilibrium quickly so that kinetic peak broadening is eliminated or minimized.
4. Elution conditions such that retention times are in a convenient range-not too short or too long.
5. An eluent and resin those are compatible with a suitable detector.

2.4.2 Basis for Separation

The basis for separation in ion chromatography lies in differences in the exchange equilibrium between the various sample anions and the eluent ion. For example, ions can be separated on a cation-anion exchange resin columns with a dilute solution as the eluent (mobile phase). Introduction of the sample causes ions to be taken up in a band (zone) near the top of the column by ion exchange (Fritz, & Gjerde, 2000).

Both of ions of mobile phase and sample components in ionic composition compete with each other for attaching to the opposite charge resin. The sample ions bind to the counter ions of the resin. While the ions which strongly tied up to the resin retain inside the column for long time; neutral or unavailable charged ions move faster down and leave the column first (Figure 2.1).

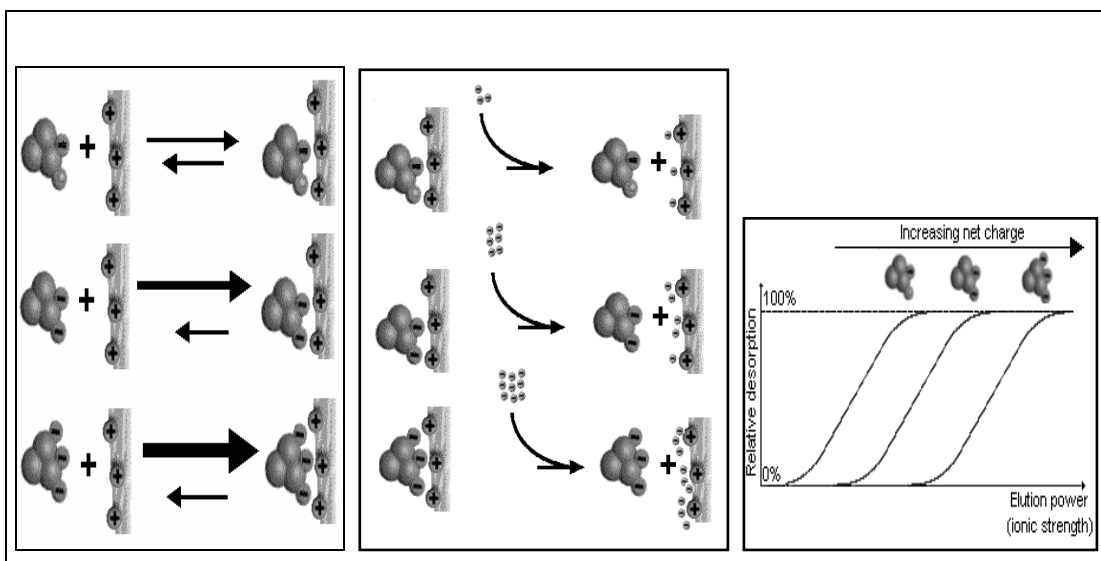


Figure 2.1 The differences in the exchange equilibrium between the various sample anions and the eluent ion (taken from http://www5.gelifesciences.com/APTRIX/upp00919.nsf/Content/LabSep_EduC~LC_tech~IEX~IEXBasic~IEXTheSepM?OpenDocument&hometitle=LabSep)

2.4.3 Separation

Separation in ion exchange chromatography depends upon the reversible adsorption of charged solute molecules to immobilized ion exchanged groups of opposite charged. Most ion-exchanged experiments are performed in four main stages: (taken from http://www.rmpr.cnrs.fr/j1pr/5__TECHNIQUES_DE_PURIFICATION/ION_EXCHANGE.SWF)

- Equilibration
- Sample application and wash
- Elution and Regeneration
- Detection

2.4.3.1 Equilibration

To perform a separation, the eluent is first pumped through the system until equilibrium is reached, as evidenced by a stable baseline. The time needed for equilibrium to be reached may vary from a couple of minutes to an hour or longer, depending on the type of resin and eluent that is used. During this step the ion-exchange sites will be converted to the E^- form: Resin- $Q^+ E^-$. There may also be a second equilibrium in which some E^- is adsorbed on the resin surface but not at specific ion-exchange sites (Figure 2.2). In such cases the adsorption is likely to occur as an ion pair, such as $E-Na^+$ or $E-H^+$ (Fritz, & Gjerde, 2000).

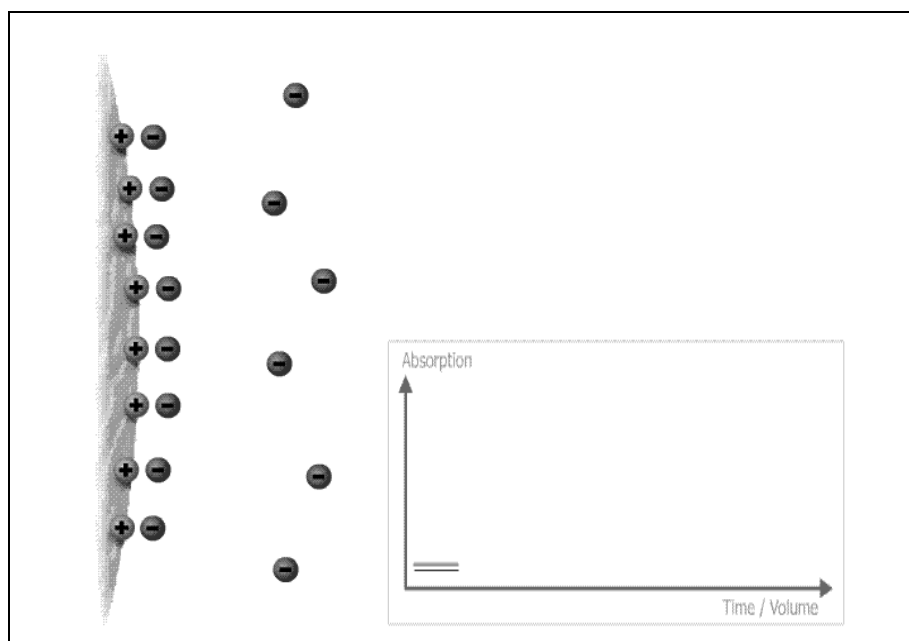
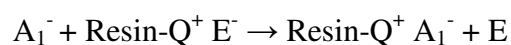


Figure 2.2 Equilibration (taken from http://www.rmpr.cnrs.fr/j1pr/5__TECHNIQUES_DE_PURIFICATION/ION_EXCHANGE.SWF)

2.4.3.2 Sample Application and Wash

An analytical sample can be injected into the system as soon as a steady baseline has been obtained (Figure 2.3). A sample containing anions A_1^- , A_2^- , A_3^- A_i^- undergoes ion-exchange with the exchange sites near the top of the chromatography column (Fritz, & Gjerde, 2000).



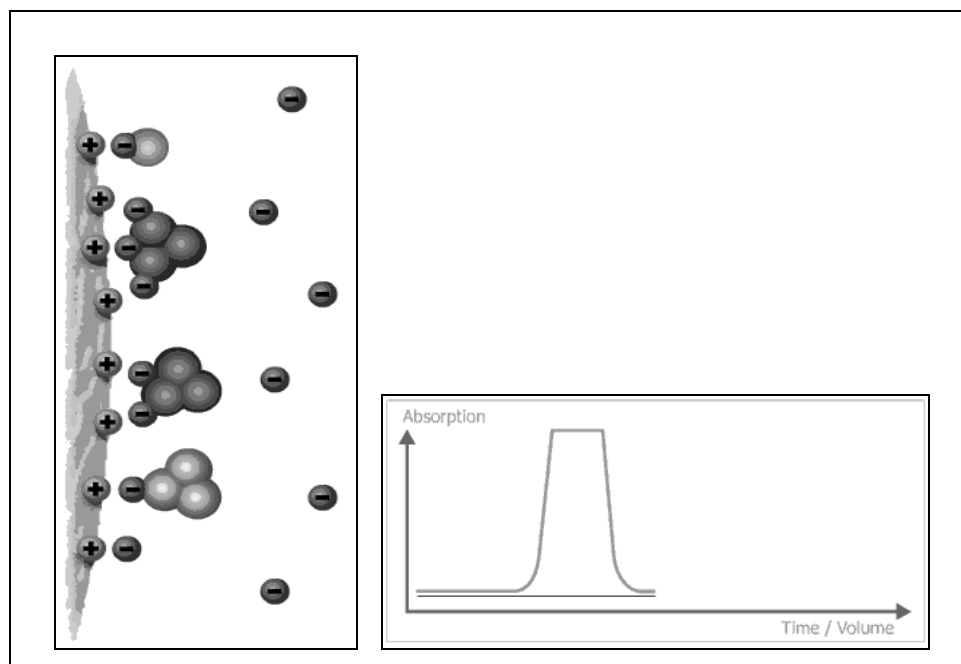


Figure 2.3 Sample application (taken from http://www.rmpr.cnrs.fr/j1pr/5__TECHNIQUES_DE_PURIFICATION/ION_EXCHANGE.SWF)

If the total anion concentration of the sample happens to be exactly the same as that of the eluent being pumped through the system, the total ion concentration in the solution at the top of the column will remain unchanged. However, if the total ion concentration of the sample is greater than that of the eluent, the concentration of E^- will increase in the solution at the top of the column due to the exchange reaction shown above (Figure 2.4). This zone of higher E^- concentration will create a ripple effect as the zone passes down the column and through the detector. This will show up as the first peak in the chromatogram, which is called the injection peak.

A sample of lower total ionic concentration than that of the eluent will create a zone of lower E^- concentration that will ultimately show up as a negative injection peak. The magnitude of the injection peak (either positive or negative) can be used to estimate the total ionic concentration of the sample compared with that of the eluent. Sometimes the total ionic concentration of the sample is adjusted to match that of the eluent in order to eliminate or reduce the size of the injection peak. The intensity of the injection peak may give an idea regarding the concentration of the analyte. In case of a small injection peak, the analyte concentration can be concluded as high.

Conversely, a high injection peak can be indicator of a small analyte concentration on an ion chromatogram (Fritz, & Gjerde, 2000).

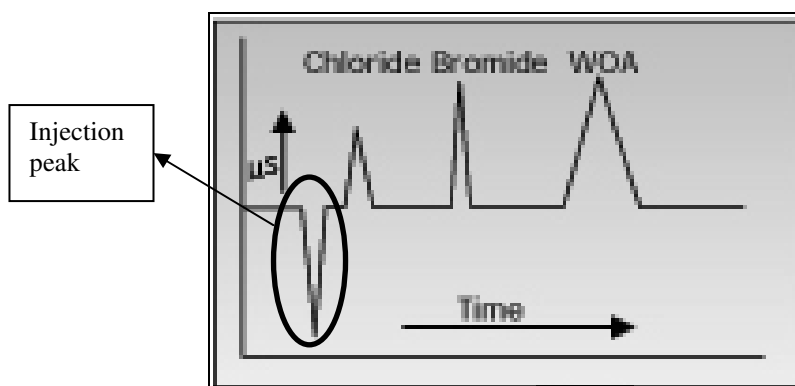
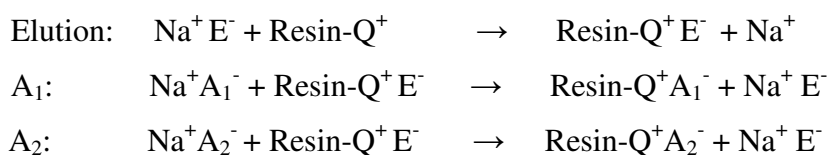


Figure 2.4 The injection peak (taken from http://www.residues.com/ion_chromatography.html)

Behind the zone in the column due to sample injection, the total anion concentration in the column solution again becomes constant and is equal to the E^- concentration in the eluent. However, continuous ion exchange will occur as the various sample anions compete with E^- for the exchange sites on the resin. As eluent, containing E^- continues to be pumped through the column, the sample anions will be pushed down the column. The separation is based on differences in the ion-exchange equilibrium of the various sample anions with the eluent anion, E^- . Thus, if sample ion A_1^- has a lower affinity for the resin than ion A_2^- , then A_1^- will move at a faster rate through the column than A_2^- (Fritz, & Gjerde, 2000).

2.4.3.3 Elution and Regeneration

In the elution step, pumping eluent through the column results in multiple ion-exchange equilibria along the column in which the sample ions and eluent ions compete for ion-exchange sites next to the Resin-Q^+ groups.



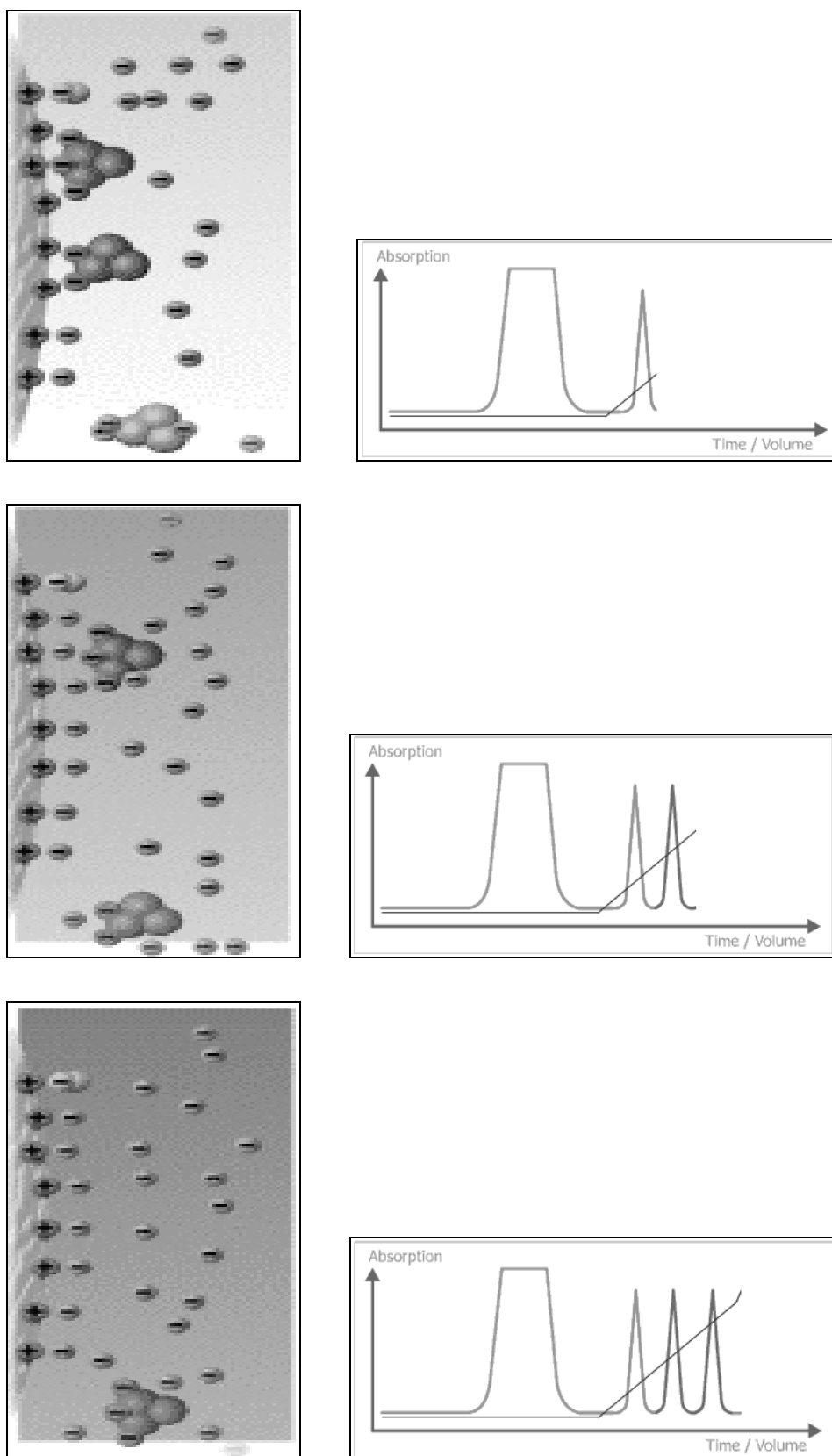


Figure 2.5 Elution (taken from http://www.rmpr.cnrs.fr/j1pr/5__TECHNIQUES_DE_PURIFICATION/ION_EXCHANGE.SWF)

The net result is that both A_1^- and A_2^- move down the column. If A_1^- has a greater affinity for the Q^+ sites than A_2^- has, the A_1^- moves at a slower rate (Figure 2.5). Due to their differences in rate of movement, A_1^- and A_2^- are gradually resolved into separate zones or bands (Fritz, & Gjerde, 2000).

The solid phase in each of these zones contains some E^- as well as the sample ion, A_1^- or A_2^- . Likewise, the liquid phase contains some E^- as well as A_1^- or A_2^- . The total anionic concentration ($A_1^- + E^-$ or $A_2^- + E^-$) is equal to that of the eluent in each zone (Fritz, & Gjerde, 2000).

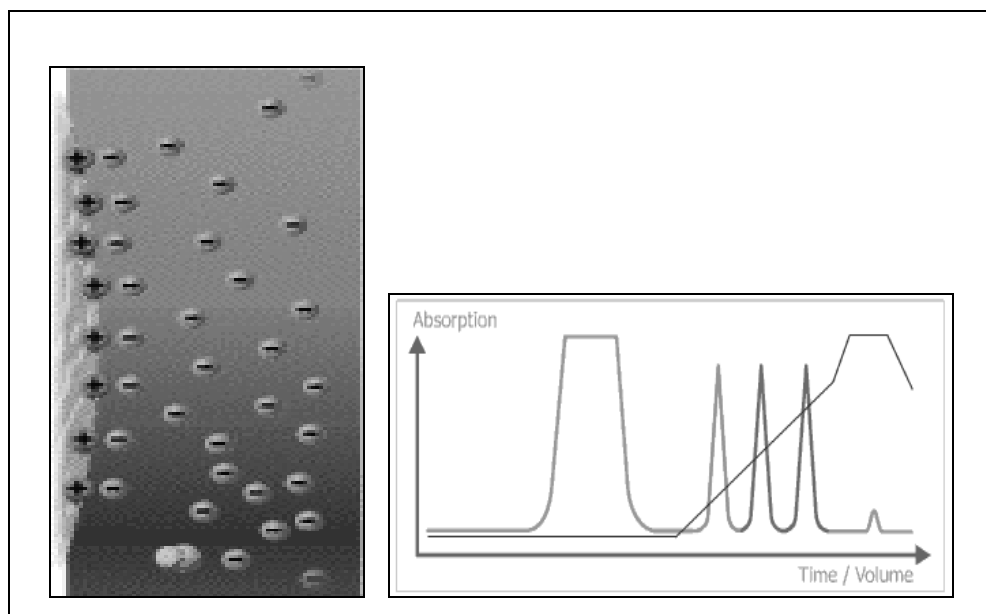


Figure 2.6 Regeneration (taken from http://www.rmpr.cnrs.fr/j1pr/5__TECHNIQUES_DE_PURIFICATION/ION_EXCHANGE.SWF)

2.4.3.4 Detection

Continued elution with eluent causes the sample ions to leave the column and pass through a small detector cell. If a conductivity detector is used, the conductance of all of the anions, plus that of the cations will contribute to the total conductance. If the total ionic concentration remains constant, how can a signal be obtained when a sample anion zone passes through the detector? The answer is that the equivalent conductance of A_1^- and A_2^- is much lower than that of E^- . The net result is a decrease

in the conductance measured when the A_1^- and A_2^- zones pass through the detector (Fritz, & Gjerde, 2000).

The total ionic concentration of the initial sample zone was higher than that of the eluent. This zone of higher ionic concentration will be displaced by continued pumping of eluent through the column until it passes through the detector. This will cause an increase in conductance and a peak in the recorded chromatogram called an injection peak. If the total ionic concentration of the injected sample is lower than that of the eluent, an injection peak of lower conductance will be observed. The injection peak can be eliminated by balancing the conductance of the injected sample with that of the eluent. Strasburg et al. studied injection peaks in some detail (Strasburg, Fritz, Berkowitz, & Schmuckler, 1989).

In suppressed anion chromatography, the effluent from the ion exchange column comes into contact with a cation-exchange device (Catex- H^+) just before the liquid stream passes into the detector.

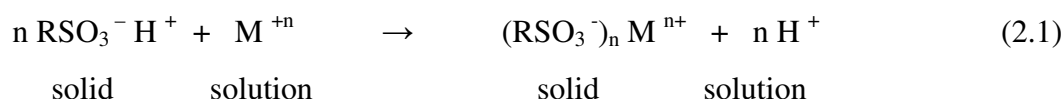
The background conductance of the eluent entering the detector is thus very low because virtually all ions have been removed by the suppressor unit. However, when a sample zone passes through the detector, the conductance is high due to the conductance of the A_1^- or A_2^- and the even higher conductance of the H^+ associated with the anion (Fritz, & Gjerde, 2000).

2.5 Ion-Exchange Equilibria

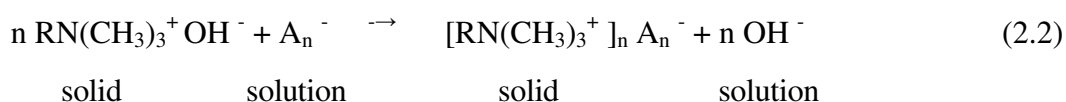
Ion-exchange processes are based upon exchange equilibria between ions in solution and ions of like sign on the surface of an essentially insoluble, high-molecular-weight solid. Natural ion exchangers, such as clays and zeolites, have been recognized and used for several decades. Synthetic ion-exchange resins were first produced in the mid-1930s for water softening, water deionization, and solution purification. The most common active sites for cation exchange resins are the sulfonic acid group $-SO_3\sim H^+$, a strong acid, and the carboxylic acid group $-COO\sim H^+$, a weak acid. Anionic exchangers contain quaternary amine groups

—N(CH₃)₃⁺ OH⁻ or primary amine groups —NH₃⁺ OH⁻; the former is a strong base and the latter a weak one (Skoog, & Leary, 1992).

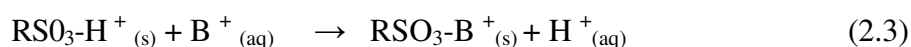
When a sulfonic acid ion exchanger is brought in contact with an aqueous solvent containing a cation M⁺, exchange equilibria is set up that can be described by



where RSO₃-H⁺ represents one of many sulfonic acid groups attached to a large polymer molecule. Similarly, a strong base exchanger interacts with the anion A⁻ as shown by the reaction (Skoog, & Leary, 1992).



As an example of the application of the mass-action law to ion-exchange equilibria, we will consider the reaction between a singly charged ion B⁺ with a sulfonic acid resin held in a chromatographic column. Initial retention of B⁺ ions at the head of the column occurs because of the reaction



Here, the (s) and (aq) emphasize that the system contains a solid and an aqueous phase. Elution with a dilute solution of hydrochloric acid shifts the equilibrium in Equation 2.3 to the left causing part of the B⁺ ions in the stationary phase to be transferred into the mobile phase. These ions then move down the column in a series of transfers between the stationary and mobile phases (Skoog, & Leary, 1992).

The equilibrium constant K_{cx} for the exchange reaction shown in Equation 2.3 takes the form

$$\frac{[\text{RSO}_3^-\text{B}^+]_s \times [\text{H}^+]_{\text{aq}}}{[\text{RSO}_3^-\text{H}^+]_s \times [\text{B}^+]_{\text{aq}}} = K_{\text{ex}} \quad (2.4)$$

Here, $[\text{RSO}_3^-\text{B}^+]_s$ and $[\text{RSO}_3^-\text{H}^+]_s$ are concentrations (strictly activities) of B^+ and H^+ in the solid phase. Rearranging yields;

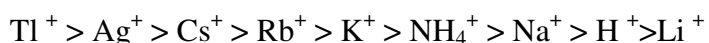
$$\frac{[\text{RSO}_3^-\text{B}^+]_s}{[\text{B}^+]_{\text{aq}}} = K_{\text{ex}} \times \frac{[\text{RSO}_3^-\text{H}^+]_s}{[\text{H}^+]_{\text{aq}}} \quad (2.5)$$

During the elution, the aqueous concentration of hydrogen ions is much larger than the concentration of the singly charged B^+ ions in the mobile phase. Furthermore, the exchanger has an enormous number of exchange sites relative to the number of B^+ ions being retained. Thus, the overall concentrations $[\text{H}^+]_{\text{aq}}$ and $[\text{RSO}_3^-\text{H}^+]_s$ are not affected significantly by shifts in the equilibrium 2.3. Therefore, when $[\text{RSO}_3^-\text{H}^+]_s \gg [\text{RSO}_3^-\text{B}^+]_s$ and $[\text{H}^+]_{\text{aq}} \gg [\text{B}^+]_{\text{aq}}$ the right-hand side of Equation 2.5 is substantially constant, and we can write

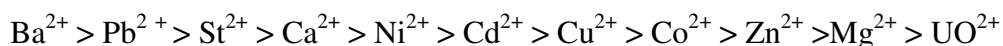
$$\frac{[\text{RSO}_3^-\text{B}^+]_s}{[\text{B}^+]_{\text{aq}}} = K = \frac{C_s}{C_m} \quad (2.6)$$

Note that K_{ex} in Equation 2.4 represents the affinity of the resin for the ion B^+ relative to another ion (here, H^+). Where K_{ex} is large, a strong tendency exists for the solid phase to retain B^+ ; where K_{ex} is small, the reverse obtains. By selecting a common reference ion such as H^+ , distribution ratios for different ions on a given type of resin can be experimentally compared. Such experiments reveal that polyvalent ions are much more strongly held than singly charged species, within a given charge group. However, differences appear that are related to the size of the hydrated ion as well as to other properties. Thus, for a typical sulfonated cation

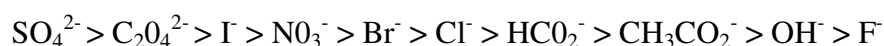
exchange resin, values for K_{ex} decrease in the order



For divalent cations, the order is



For anions, K_{ex} for a strong base resin decreases in the order



This sequence is somewhat dependent upon type of resin and reaction conditions and should thus be considered only approximate (Skoog, & Leary, 1992).

2.6 Components of an Ion Chromatography (IC) Instrument

The Ion Chromatography system performs ion analyses using suppressed or non-suppressed conductivity detection. An ion chromatography system typically consists of a liquid eluent, a high-pressure pump, a sample injector, a guard and separator column, a chemical suppressor, a conductivity cell, and a data collection system (Figure 2.7).

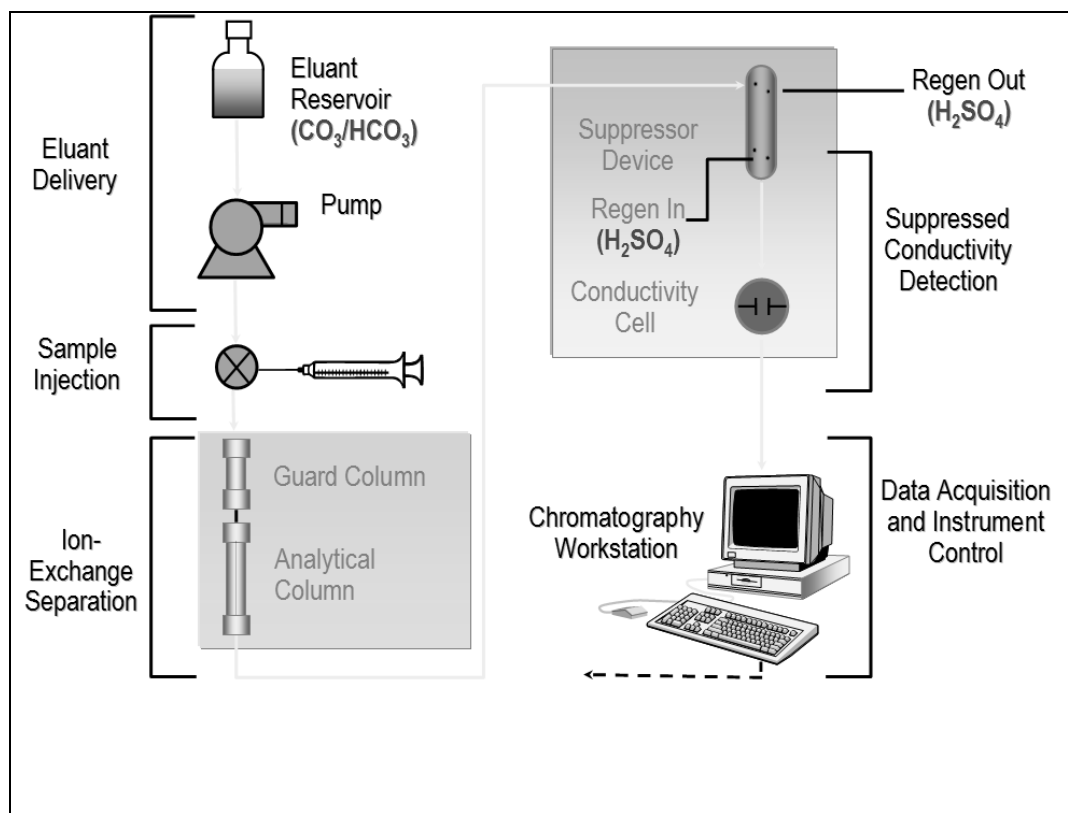


Figure 2.7 The ion chromatography system configuration (Courtesy of Dionex Corporation)

Before running a sample, the ion chromatography system is calibrated using a standard solution. By comparing, the data obtained from a sample to that obtained from the known standard, sample ions can be identified and quantitated. The data collection system, typically a computer running chromatography software, produces a chromatogram (a plot of the detector output vs. time). The chromatography software converts each peak in the chromatogram to a sample concentration and produces a printout of the results (Dionex, 2007).

2.6.1. Eluent Delivery

Eluent, a liquid that helps to separate the sample ions, carries the sample through the ion chromatography system. This means that the eluent composition and concentration remain constant throughout the run (Dionex, 2007).

2.6.1.1 Degassing the Eluent

Degassing the eluent is important because air can get trapped in the check valve, causing the pump to lose its prime. Loss of prime results in erratic eluent flow or no flow at all. Sometimes only one pump head will lose its prime and the pressure will fluctuate in rhythm with the pump stroke. Another reason for removing dissolved air from the eluent is that air can result in changes in the effective concentration of the eluent (Fritz, & Gjerde, 2000).

2.6.2 Pumps

The pump pushes the eluent and sample through the guard and separator columns (Dionex, 2007). IC pumps are designed around an eccentric cam that is connected to a piston (Figure 2.8). The rotation of the motor is transferred into the reciprocal movement of the piston. A pair of check valves controls the direction of flow through the pump head. A pump seal surrounding the piston body keeps the eluent from leaking out of the pump head (Fritz, & Gjerde, 2000).

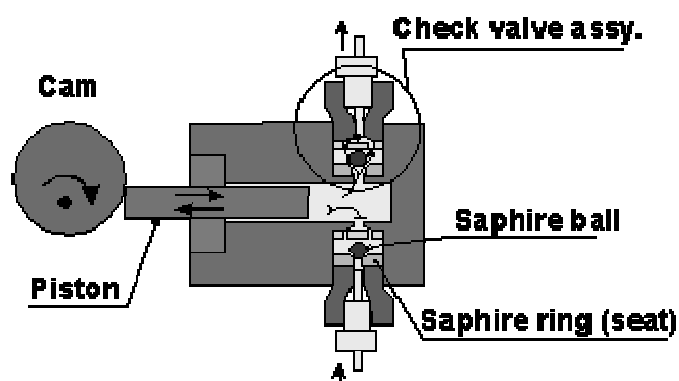


Figure 2.8 IC pump head, piston, and cam (taken from http://hplc.chem.shu.edu/NEW/HPLC_Book/Instrumentation/pmp_recip.html#RECIPROCATING%20%20PISTON%20PUMPS)

In single-headed reciprocating pumps, the eluent is delivered to the column for only half of the pumping cycle. A pulse dampener is used to soften the spike of pres-

sure at the peak of the pumping cycle and to provide an eluent flow when the pump is refilling. Use of a dual head pump is better because heads are operated 180° out of phase with each other. One pump head pumps while the other is filling and vice versa (Fritz, & Gjerde, 2000).

The eluent flow rate is usually controlled by the pump motor speed although there are a few pumps that control flow rate by control of the piston stroke distance.

Figure 2.9 shows how the check valve works. On the intake stroke, the piston is withdrawn into the pump head, causing suction. The suction causes the outlet check valve to settle onto its seat while the inlet check valve rises from its seat, allowing eluent to fill the pump head. Then the piston travels back into the pump head on the delivery stroke. The pressure increase seals the inlet check valve and opens the outlet valve, forcing the eluent to flow out of the pump head to the injection valve and through the column. Failure of either of the check valves to sit properly will cause pump head failure and eluent will not be pumped. In most cases, this is due to air trapped in the valve so that the ball cannot sit properly. Flushing or purging the head usually takes care of this problem. Using degassed eluents is also helpful. In few cases, particulate material can prevent sealing of the valve. In these cases, the valve must be cleaned or replaced. The pump manufacturer has instructions on how to perform this operation (Fritz, & Gjerde, 2000).

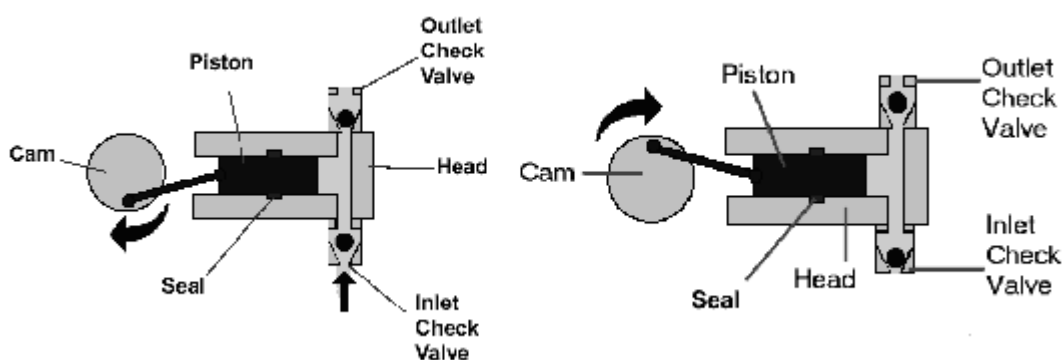


Figure 2.9 Check valve positions during intake and delivery strokes of the pump head piston (taken from <http://www.lcresources.com/resources/getstart/i.htm>)

2.6.3 Pressure

Column inlet pressures can vary from 500 psi up to perhaps a high of 3500 psi, with normal operating pressures around 1500 psi. The pressure limit on an IC is usually 4000 to 5000 psi, depending on the fittings and other hardware used. The eluent backpressure is directly proportional to the eluent flow rate. Although still popular, psi (pounds per square inch) is gradually being replaced by more modern terms for pressure measurement. Namely, 1 bar = 1 atm (atmospheres) = 14.5 psi = 10^5 Pa (Pascal) (Fritz, & Gjerde, 2000).

2.6.4 Injector

The injection system may be manual or automated, but both rely on the injection valve. An injection valve is designed to introduce precise amounts of sample into the sample stream. The variation is usually less than 0.5 % precision from injection to injection. Figure 2.10 schematically represents the valve. It is a 6-port and 2-position device; one position is load and the other is injected. In the load position, the sample from the syringe or auto sampler vial is pushed into the injection loop. The loop may be partially filled (partial loop injection) or completely filled (full loop injection) (Fig. 2.10). Partial loop injection depends on the precision filling of the loop with small known amounts of material. If partial loop injection is used, the loop must not be filled to more than 50 % of the total loop volume or the injection may not be precise. In full loop injection, the sample is pushed completely through the loop. Typical loop sizes are 10-200 μ L. Normally, at least a two-fold amount of sample is used to fill the loop with excess sample from the loop going to waste. At the same time that the sample loop is loaded with sample, the eluent travels in the by-pass channel of the injection valve and to the column. Injection of the sample is accomplished by turning the valve and placing the injection loop into the eluent stream. Usually the flow of the eluent is opposite to that of the loading sample into the loop. The injected sample travels to the head of the column as a slug of fluid. The ions in the sample interact with the column and the separation process is started with the eluent pushing the sample (Fritz, & Gjerde, 2000).

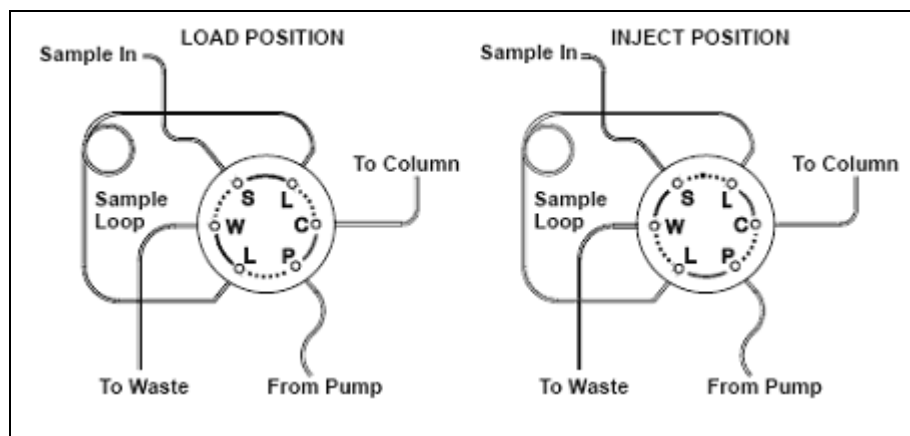


Figure 2.10 Injection valve flow schematics (Courtesy of Dionex Corporation)

2.6.5 Column Oven

The column oven is optional. Most IC separations are not dependent on the use of an oven. Nevertheless, an oven can be quite useful for high-sensitivity work. Conductivity is proportional to temperature. There is about a 2 % change in conductance per °C change in temperature. Conductivity detectors have temperature control, temperature compensation, or both. An oven can help to keep the temperature of the fluid, before the conductivity cell is reached, constant; this can help decrease the detector noise and decrease the detection limit of the instrument (Fritz, & Gjerde, 2000).

2.6.6 IC Column


A typical column used in ion chromatography might be 150 x 4.6 mm although columns as short as 50 mm in length or as long as 250 mm are also used. The column is carefully packed with a spherical anion-exchange resin of rather low exchange capacity and with a particle diameter of 5 or 10 μm . Most anion-exchange resins are functionalized with quaternary ammonium groups, which serve as the sites for the exchange of one anion for another (Fritz, & Gjerde, 2000).

2.6.7 Ion-Exchange Packing


Composition of the stationary phase

- Substrate / Resin carrier
- A spacer group
- A group that carries the separating capacity

SO₃⁻



NR₃⁺



Substrates

- Polystyrene/divinylbenzene
- Polymethacrylate
- Polyalcohol
- Hydroxyethylmethacrylate(HEMA)
- Silicate

Anion exchanger

- Quaternary ammonium groups
- Alkyl amines
- Hydroxy-alkylamines
- Alkyl amines with acrylate type cross linking

Spacer

- Alkyl chain

Cation exchanger

- Sulfonates
- Carboxylates

Figure 2.11 Composition of the stationary phase (taken from http://www.metrohm.com.cn/administrator/resource/upfile/ic_theory_20041011_e.pdf)

Historically, ion-exchange chromatography was performed on small, porous beads formed during emulsion copolymerization of styrene and divinylbenzene. The presence of divinylbenzene (usually —8 %) results in cross-linking, which imparts mechanical stability to the beads. In order to make the polymer active toward ions, acidic or basic functional groups are then bonded chemically to the structure. The most common groups are sulfonic acid and quaternary amines (Skoog, & Leary, 1992).

Table 2.1 Functional groups on typical synthetic ion-exchange materials (taken from http://www.colorado.edu/chemistry/chem5181/Lectures/C5_IC_TLC.pdf)

Species	Functional Groups	Classification
Cation Exchangers		
Sulphonic Acid	- S O ₃ ⁻ H ⁺	Strong
Carboxylic Acid	- C O O ⁻ H ⁺	Weak
Phosphonic Acid	- P O ₃ H H ⁺	Weak
Phosphinic Acid	- P O ₂ H H ⁺	Weak
Phenolic	- O ⁻ H ⁺	Weak
Arsenoic Acid	- A s O ₃ H H ⁺	Weak
Selenoic Acid	- S e O ₃ ⁻ H ⁺	Weak
Anion Exchangers		
Quaternary Amine	- N (CH ₃) ₃ OH	Strong
Quaternary Amine	- N (CH ₃) ₂ (C ₂ H ₅) ⁺ OH ⁻	Strong
Tertiary Amine	- N H (CH ₃) ₂ ⁺ OH ⁻	Weak
Secondary Amine	- N H ₂ (CH ₃) ⁺ OH ⁻	Weak
Primary Amine	- N H ₃ ⁺ OH ⁻	Weak

Anion-exchangers may be polymer-based (commonly polystyrene or polyacrylate) or silica-based. Although many types of anion exchangers are available for ion chromatography, the "strong-base" type with quaternary ammonium functional groups is the most common. These normally come in the chloride form, for example, Solid-N⁺R₃Cl⁻ (Fritz, & Gjerde, 2000).

The alkyl R groups are usually methyl or a methyl with one or two hydroxyethyl groups. -CH₂CH₂OH. The positively charged quaternary ammonium groups are chemically bonded to the solid particles while the chloride groups are able to undergo ion exchange with other anions (Fritz, & Gjerde, 2000).

2.6.7.1 Polymeric Resins

2.6.7.1.1 *Substrate and Cross-Linking.* A variety of polymeric substrates can be used in ion-exchange synthesis, including polymers of esters, amides, and alkyl halides. However, resins based on styrene-divinylbenzene copolymers are probably

the most widely used ion exchangers. The polymer is schematically represented in Fig. 2.12. The resin is made up primarily of polystyrene; however, a small amount of divinylbenzene is added during the polymerization to "cross-link" the resin. This cross-linking confers mechanical stability upon the polymer bead and also dramatically decreases the solubility of the polymer by increasing the molecular weight of the average polymer chain length. Typically, 2 to 25 % weight of the cross-linking compound is used for micro porous resins and up to 55 % weight cross-linking for macro porous resins. In many cases, the resin name will indicate the cross-linking of the material (Fritz, & Gjerde, 2000).

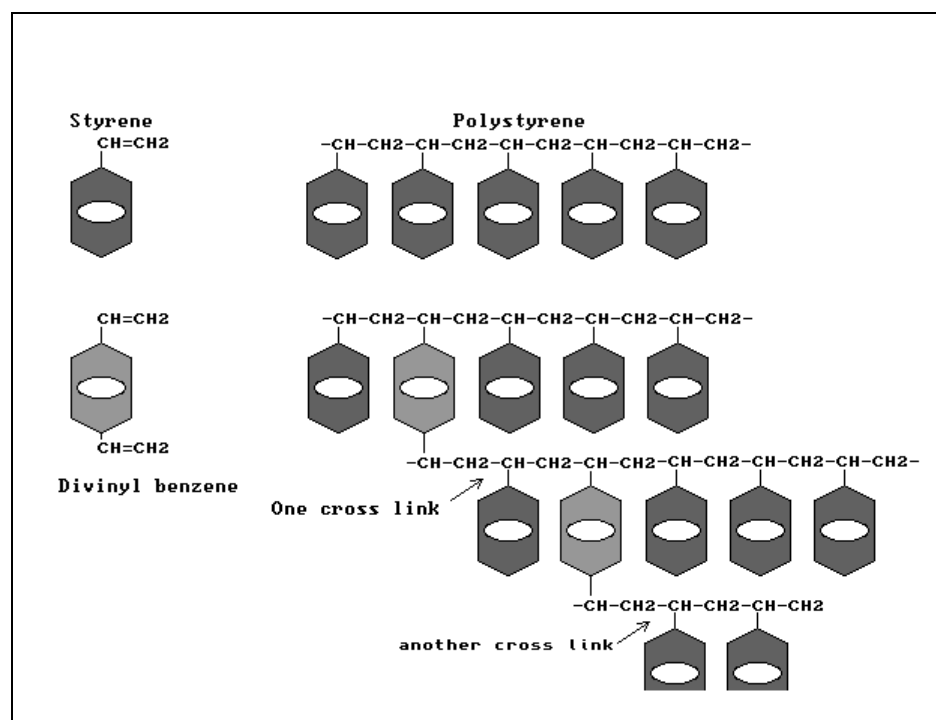
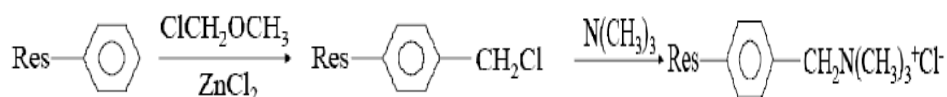


Figure 2.12 Schematic representation of a styrene-divinylbenzene copolymer (taken from <http://www.rpi.edu/dept/chem-eng/Biotech-Environ/IONEX/styrene.html>)

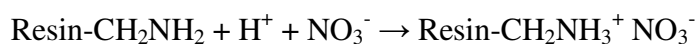
The divinylbenzene "cross-links" the linear chain of the styrene polymer. A high percentage of divinylbenzene produces a more rigid polymer bead (Fritz, & Gjerde, 2000).

2.6.7.1.2 *Chemical Functionalization.* Ion exchangers are created by chemically introducing suitable functional groups into the polymeric matrix. In a few instances, monomers are functionalized first, and then they are polymerized into beads. An attractive feature of the aromatic copolymer used in many ion exchangers is that it can be modified easily by a wide variety of chemical reactions (Fritz, & Gjerde, 2000).

Anion-exchange resins have been made by a two-stage set of reactions. The first step is a Friedel-Crafts reaction to attach the chloromethyl group to the benzene rings of styrene-divinylbenzene copolymer. Then the anion exchanger is formed by reaction of the chloromethylated resin with an amine. The most common type of strong base anion-exchange resin contains a quaternary ammonium functional group, which is obtained by alkylation with trimethylamine (Fritz, & Gjerde, 2000).



In these resins only the anion is mobile and can be exchanged for another anion. Another common strong base anion exchanger is one that contains a hydroxyethyl group in place of a methyl group on the nitrogen. Weak-base anion exchangers are synthesized by reacting the chloromethylated resin with lower substituted amines or with ammonia. Weak-base anion exchange resins cannot function as ion exchangers unless the functional group is protonated:



The protonation depends on the basicity of the functional group and the pH of the solution in which the resin beads are immersed (Fritz, & Gjerde, 2000).

2.6.7.2 Polyacrylate Anion Exchangers

A wide variety of resins based on polyacrylate polymers has been produced for use in chromatography. A type known as HEMA, a macro porous copolymer of 2-hydro-methyl methacrylate and ethylene dimethacrylate has been used extensively in ion chromatography. It is extensively cross-linked to produce a polymeric matrix with high chemical and physical stability. The structure of HEMA is shown in Fig. 2.13 (A). The tertiary carbonyl structure of pivalic acid is one of the most stable and least hydrolyzable esters known, which allows the HEMA stationary phase to be used with a variety of eluents in the pH range 2-12. The excess hydroxyl groups on the HEMA matrix also increase the hydrophilicity of this material, which will be shown later to result in improved peak shapes for polarizable anions. The strong-base anion exchanger of HEMA, shown in Fig. 2.13 (B), is prepared by treating the HEMA precursor with an aqueous solution of trimethylamine (Fritz, & Gjerde, 2000).

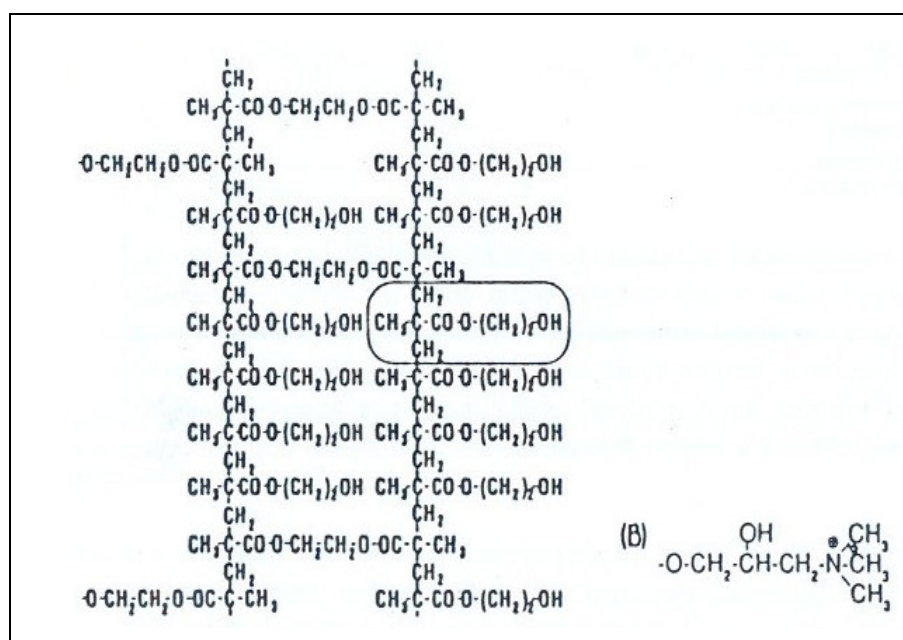


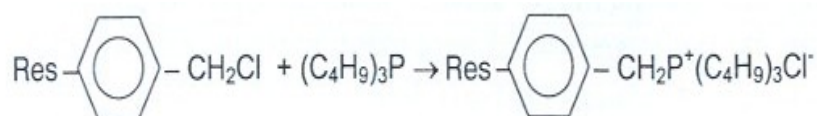
Figure 2.13 Structures of (A) HEMA and (B) strong-base anion exchanger of HEMA (taken from Fritz, & Gjerde, 2000)

A HEMA-based anion exchanger developed by Alltech has been described as a universal stationary phase for the separation of a wide variety of anions (Saari-Nordhaus, Henderson, & Anderson, 1991, 1992).

This anion-exchange resin has been compared to agglomerated pellicular anion exchangers for the separation of anions by chemically suppressed IC. The HEMA-based columns exhibit higher capacities for all anions and particularly for weakly retained anions such as fluoride and formate, which were completely resolved. The HEMA columns could be used for both isocratic and gradient techniques (Fritz, & Gjerde, 2000).

2.6.7.3 Quaternary Phosphonium Resins

An anion exchange resin for IC has been prepared by reaction of a chloromethyl PS-DVB resin with tributylphosphine (TBP).



The TBP resin is quite stable and is suitable for anion chromatography. Warth, Cooper and Fritz (1989) compared the retention times of several anions relative to chloride using columns packed with quaternary ammonium anion exchangers of the conventional trimethyl type (TMA) and tributylamine (TBA), sulfate. The chromatographic separation of traces of chloride from 200 times as much nitrate was possible (Warth, Cooper, & Fritz, 1989). A U.S. Patent was issued for the selective removal of nitrate from drinking water (Lockridge, & Fritz, 1990).

2.6.7.4 Latex Agglomerated Ion Exchangers

Pellicular materials in which the stationary phase is a layer on the outside perimeter of a spherical substrate have been used frequently in liquid chromatography. The relatively thin layer ensures a rapid equilibrium between the

mobile and stationary phases even when the column packing has a relatively large particle size. In their original work on ion chromatography (Small, Stevens, & Bauman, 1975) used a surface-sulfonated material as a pellicular cation exchanger.

Such materials are easy to prepare because sulfonation of a polymer containing benzene rings proceeds from the outside in. Sulfonation for a short period under mild conditions will insert sulfonic acid groups only on or near the outside surface of a spherical resin (Fritz, & Gjerde, 2000).

It was soon discovered that efficient anion exchange resins could be prepared by coating the outside of a surface-sulfonated polymer with a layer of latex particles functionalized with quaternary ammonium groups. The first commercial anion exchangers for ion chromatography (Dionex ASI) consisted of 0.15 μm latex particles coated onto a 25 μm sulfonated substrate. A two-dimensional diagram of this coating is shown in Fig. 2.14 A. The positively charged latex particles are firmly held by electrostatic attraction as shown in Fig. 2.14 B. Each latex particle has several quaternary N^+ groups, so the coated substrate will have many quaternary groups available for ion exchange. Latex agglomerated resins are very stable chemically. Even 4 M sodium hydroxide is unable to cleave the ionic bond between the substrate and the latex bead (Fritz, & Gjerde, 2000).

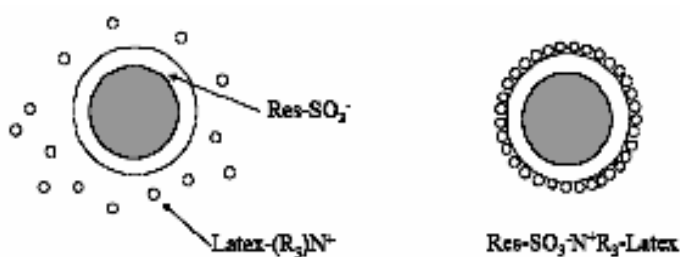


Figure 2.14 A-B Latex agglomerated ion exchangers

Several advantages have been cited for latex coated anion exchangers (Weiss, 1995).

- The substrate provides mechanical stability and gives a moderate backpressure.
- The small size of the latex beads and their location on the outer surface of the substrate ensure fast exchange processes and thus a high chromatographic efficiency.
- Swelling and shrinkage are minimal.

The properties of latex resins can be varied by manipulation of several parameters. Hydrophobic attraction of the exchanger for some anions can be altered by varying the type and cross-linking of the polymeric substrate. The ion-exchange capacity is determined by the substrate particle size, the size of the latex beads, and the degree of latex coverage on the substrate surface. Selectivity for various anions is governed mainly by the type of functional groups attached to the latex bead and by the degree of latex cross-linking (Fritz, & Gjerde, 2000).

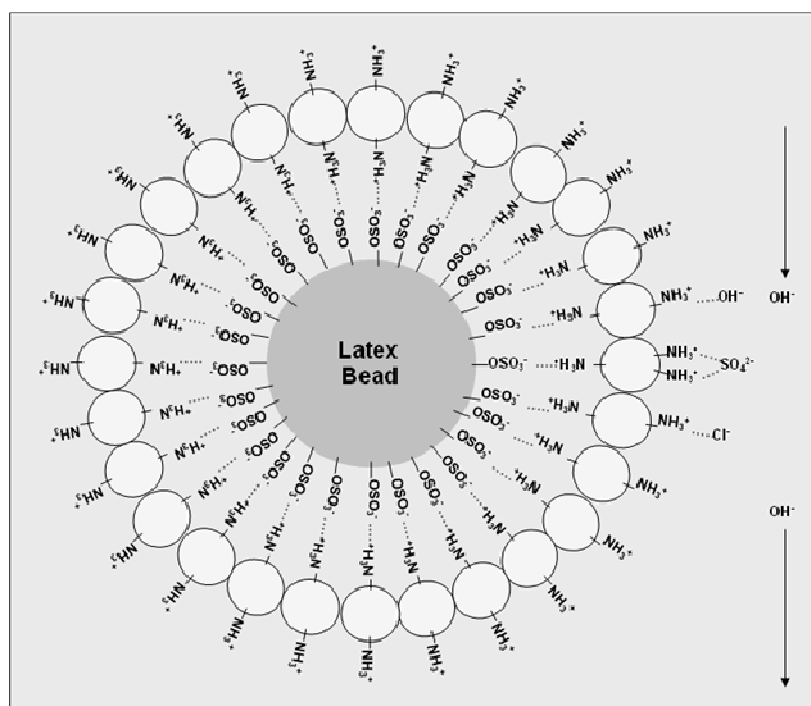


Figure 2.15 Latex agglomerated ion exchangers (taken from <http://faculty.plattsburgh.edu/robert.fuller/437web/Lec5IonChromatography/IonChromatography.ppt#3>)

2.6.7.5 Silica-Based Anion Exchangers

Ion exchangers are available in which an organic material containing a quaternary ammonium functional group is chemically bonded to porous silica spheres. This results in a thin layer of ion-exchange material on the silica surfaces. Vydac IC 302 (Pepper, 1953) is one such resin. This is spherical silica of high mechanical strength with a particle diameter of approximately 15 μm . The particles have a surface area of 86 m^2/g and an average pore diameter of 330 \AA .

Compared to organic polymers, silica-based ion exchangers have the advantages of higher chromatographic efficiency and greater mechanical stability. In general, no problems due to swelling or shrinking are encountered, even if an organic solvent is added to the eluent. A disadvantage of silica materials is their limited stability at lower pH values and especially in alkaline solutions. A fairly narrow pH range of 2 to 8 is recommended (Fritz, & Gjerde, 2000).

2.6.8 Suppressors

2.6.8.1 Fiber Suppressors (Stevens, Davis, & Small, 1981)

The fiber suppressor was the first device based on the use of an ion-exchange membrane. It consisted of a long, hollow fiber made of a semi-permeable ion-exchange material. Column effluent containing zones of separated sample ions passed through the hollow center of the fiber. Here the sodium counter ion was exchanged for H^+ from the membrane. The outside of the hollow fiber was bathed in an acidic solution, allowing for continual replacement of the H^+ as the effluent passed through. The main advantage of this design was that it permitted continuous operation of the IC system. Band broadening in this suppressor was less than with the large packed-bed devices but was still significant. Fiber suppressors were also limited in their ability to suppress flow rates above 2 mL/min or eluents above 5 mM concentration (Fritz, & Gjerde, 2000).

2.6.8.2 Membrane Suppressors (Stillian, 1985)

A flat membrane suppressor from Dionex, known as the Micro-Membrane Suppressor (MMS) had a much higher capacity and lower dead volume than previous devices and was able to operate around the clock with minimal attention. The internal design of the MMS is shown in Fig. 2.16. Two semi-permeable ion-exchange membranes are sandwiched between three sets of ion-exchange screens.

The eluent screen is of fine mesh to promote the suppression reaction while occupying a very low volume. The ion-exchange membranes on either side of this screen define the eluent chamber. There are two ion-exchange regenerant screens that permit tortuous flow of the regenerant solution towards the membranes. These screens provide a reservoir for suppressing ions without having a counter ion present.

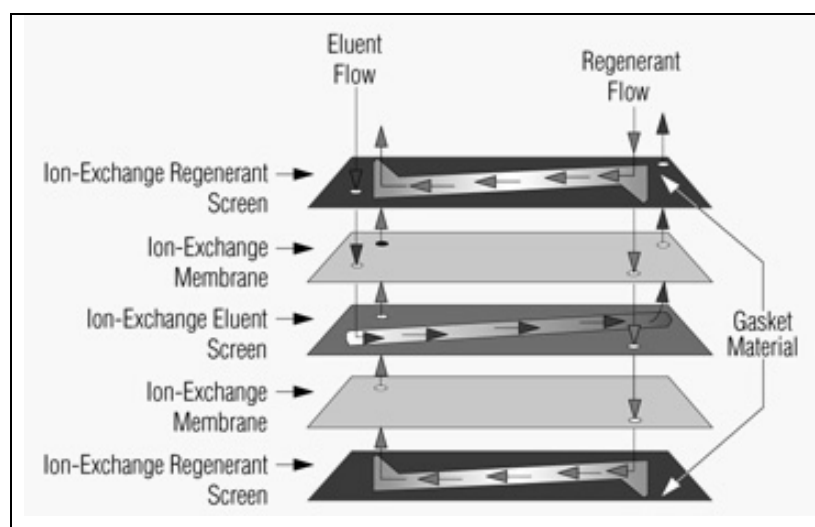


Figure 2.16 Internal design of the micro membrane suppressor (taken from http://www1.dionex.com/enus/columns_accessories/accsup/cons5339.html)

The flow pattern for the anion suppressor is shown in Fig. 2.17. Column effluent flowing through the suppressor exchanges Na^+ for H^+ from the cation exchange membranes, as shown in the middle part of the figure. Since the suppressor is actually a sandwich configuration with fairly broad cation-exchange membranes placed very close together, the exchange reaction proceeds rapidly and there is

adequate exchange capacity to handle eluents of higher concentrations. A mineral acid such as dilute sulfuric acid flows through outer parts of the suppressor to provide continuous regeneration. Regenerant flow is counter-current to the column effluent and at approximately three to ten times the chromatographic flow rate (Fritz, & Gjerde, 2000).

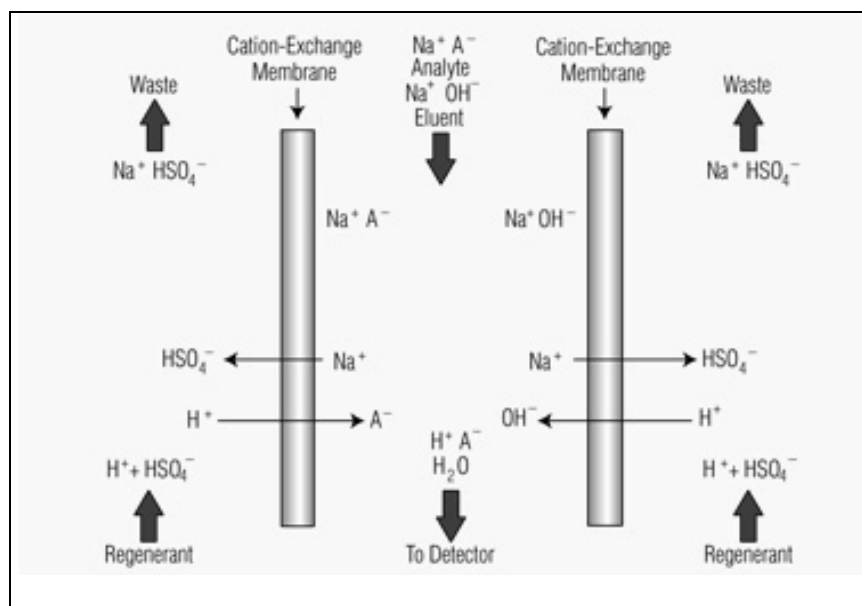


Figure 2.17 Suppression mechanism for the anion micro membrane suppressor (taken from http://www1.dionex.com/enus/columns_accessories/accsup/cons5339.html)

A major drawback of the membrane suppressors was that they required a constant flow of regenerant for continuous suppression. This could consume up to 10 mL/min of regenerant solution to reduce the large volumes of regenerant needed, an accessory for continuous regenerant recycling was introduced by Dionex in 1987. A large ion-exchange cartridge was used to remove the comparatively low concentrations of waste products (Na^+ , etc.) and replace it with fresh regenerant ions (H^+). A pump recirculates the regenerant through the suppressor cartridge. The net effect is that only a small reservoir of regenerant solution is required for effective operation (Fritz, & Gjerde, 2000).

2.6.8.3 Electrolytic Suppressors (Strong, & Dasgupta, 1989)

The ideal way to regenerate a suppressor for IC is to electrolyze water to produce the H^+ or OH^- needed. In this device, a platinum wire-filled tube made of a Nation cation-exchange membrane is inserted into another, larger Nation tube and coiled into a helix. The helical assembly is inserted within an outer jacket packed with granular conductive carbon. An alkaline eluent, for example, NaOH or Na_2CO_3 , flows in the annular channel between the two membranes and pure water flows through the inner membrane and the outer jacket countercurrent to the direction of eluent flow. A DC voltage (3 to 8 V) is applied across the carbon bed and the platinum wire. Sodium ions in the eluent migrate to the cathode compartment resulting in water as the suppressed eluent. Up to 500 $\mu\text{L}/\text{min}$ of sodium hydroxide could be suppressed effectively with a membrane 50 cm in length. The band dispersion was 106 μL for a 20 μL sample.

In 1992 Dionex introduced a commercial electrochemical suppressor called a Self Regeneration Suppressor, or SRS (Henshall, Rabin, Statler, & Stilian, 1992). The internal design is similar to the membrane suppressor, but the regenerating ion (H^+ for anion chromatography) is produced by electrolysis of water. This allows the use of very low flow rates for regenerant water and avoids the use of independent chemical feed needed for earlier suppression devices (Fritz, & Gjerde, 2000).

The SRS ULTRA II includes two regenerant compartments and one eluent compartment separated by ion Exchange membranes. Regenerant flow channels and an eluent flow channel are defined by the membrane. The eluent flow counters current to the regenerant. Electrodes are placed along the length of the regenerant channels. When an electrical potential is applied across the electrodes, water from the regenerant channels is electrolyzed, supplying regenerant hydronium ions (H_3O^+) in the ASRS ULTRA II for the neutralization reaction (Dionex, 2007).

The membrane allows hydronium ions to pass into the eluent chamber resulting in the conversion of the electrolyte of the eluent to a weakly ionized form. Eluent

counter ions (cations in anion exchange) are simultaneously passed into the regenerant chamber to maintain charge balance. The eluent suppression process is illustrated for anion exchange in Figure 2.18 (Dionex, 2007).

As shown in Figure 2.18, the water regenerant undergoes electrolysis to form hydrogen gas and hydroxide ions in the cathode chamber while oxygen gas and hydronium ions are formed in the anode chamber. Cation Exchange membranes allow hydronium ions to move from the anode chamber into the eluent chamber to neutralize hydroxide. Sodium ions in the eluent, attracted by the electrical potential applied to the cathode, move across the membrane into the cathode chamber to maintain electric neutrality with the hydroxide ions at the electrode. When using an eluent generator, the eluent is potassium hydroxide using a KOH cartridge (Dionex, 2007).

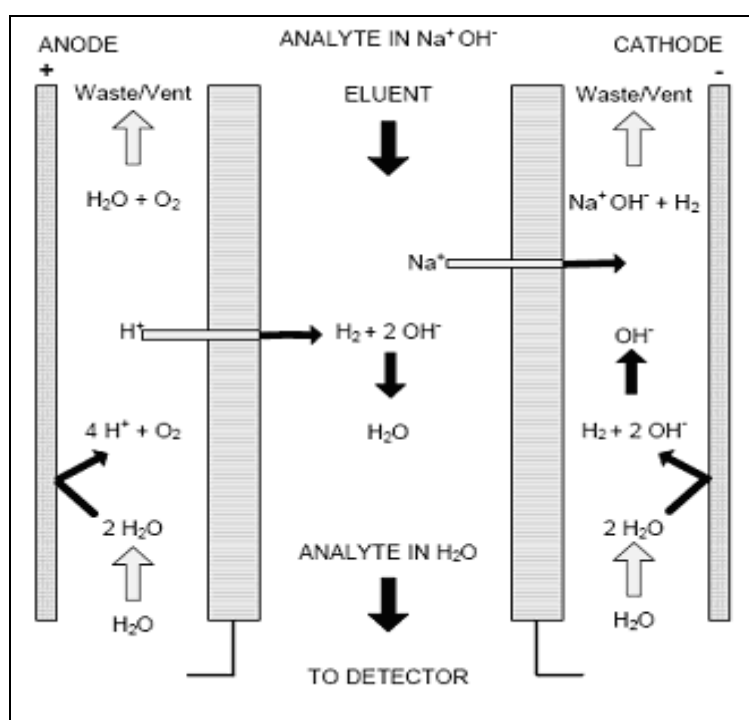
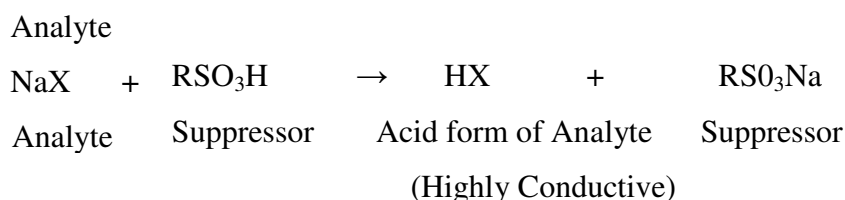
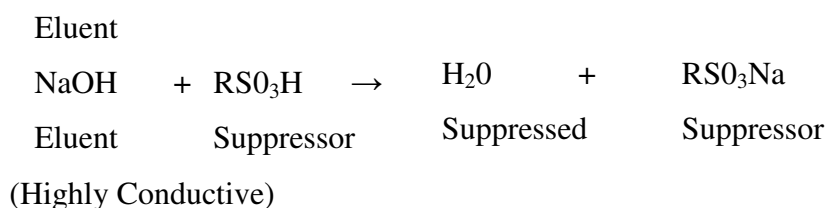


Figure 2.18 Mechanism of suppression for the Anion Self - Regenerating Suppressor (Courtesy of Dionex Corporation)

2.6.8.3.1. Suppressed Anion Chromatography. Chemical suppression provides a simple, yet elegant way to reduce the background conductance of the eluent and at the same time to enhance the conductance of sample ions. In its original form, a

second ion-exchange-column was placed between the separator column and the conductivity cell. For anion analysis a basic anion was used in the eluent and a large. H^+ -form cation exchange column was used as the second "stripper" column (Small, Stevens, & Bauman, 1975)

The reactions for suppressed anion chromatography are as follows:

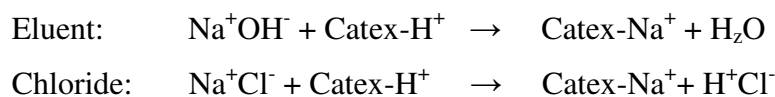


The basic eluent (OH^-) is neutralized by H^+ from the cation exchanger of the suppressor to form water. A sample zone passing through the suppressor is converted from the sodium as the counter ion (Na^+OH^-) to the more highly conducting hydrogen counter ion (H^+X^-) (Fritz, & Gjerde, 2000).

For example;

Example of Suppressed Conductivity Detection

ÖRNEK = 0.1mM NaCl ELÜENT = 1 mM NaOH



C_E = Eluent concentration (mM)

C_S = Sample concentration (mM)

h = Equivalent conductance of X ($\mu\text{S}/\text{mM}$)

GE = Background conductance of eluent,

$$GE = (\lambda H^+ + \lambda X^-) \times C_E$$

GS = Conductance in the sample band,

$$GS = (\lambda H^+ + \lambda X^-) \times C_E + (\lambda C^+ + \lambda X^-) \times C_S$$

ΔG S-E = Sample signal

$$GE = 0$$

$$GS = (\lambda Na^+ + \lambda OH^-) \times C_E + (\lambda H^+ + \lambda Cl^-) \times C_S$$

$$GS = (50 + 198) \times 0 + (350 + 76) \times 0.1 = 42.6 \mu S$$

$$GS = \Delta G = GS - GE$$

$$\Delta G = 42.6 - 0 = 42.6 \mu S$$

2.6.8.3.2 Non-Suppressed Anion Chromatography. Non-suppressed ion chromatography employs a conventional liquid chromatographic system with a conductivity detector cell connected directly to the outlet end of an ion-exchange separation column. No suppressor unit is required. The successful development of this method was made possible by three principal innovations:

- (1) The use of an anion- or cation-exchange resin of very low capacity (initially 0.007 to 0.04 m equiv/g).
- (2) An eluent with a low ionic concentration and hence a low conductivity.
- (3) An eluting ion in the eluent that has a significantly lower equivalent conductance than the analyte ions (Fritz, & Gjerde, 2000).

For example;

The basis for direct conductivity detection is that the highly conductive OH⁻ (equivalent conductance = 198 S cm² equiv⁻¹) in the eluent is partially replaced by an anion of lower conductance when a sample zone passes through the detector. The equivalent conductance of Cl⁻ and Br⁻ is 76[S*cm²/equiv] and 78[S*cm²/equiv] respectively.

$$Cl^- (76[S*cm^2/equiv]) < OH^- (198[S*cm^2/equiv])$$

$$Br^- (78[S*cm^2/equiv]) < OH^- (198[S*cm^2/equiv])$$

The decrease in conductance on an equivalent basis can be calculated as follows:

Background: $\text{Na}^+ + \text{OH}^- = 50 + 198 = 248 \text{ [S}\cdot\text{cm}^2/\text{equiv}]$

Sample Peaks: $\text{Na}^+ + \text{Cl}^- = 50 + 76 = 126 \text{ [S}\cdot\text{cm}^2/\text{equiv}]$; a decrease of 122

$\text{Na}^+ + \text{Br}^- = 50 + 78 = 128 \text{ [S}\cdot\text{cm}^2/\text{equiv}]$; a decrease of 120

SAMPLE = 0.1mM NaCl ELUENT = 1 mM NaOH

$$\text{GE} = (\lambda\text{Na}^+ + \lambda\text{OH}^-) \times \text{C}_E$$

$$\text{GE} = (50 + 198) \times 1 = 248 \mu\text{S}$$

$$\text{GS} = (\lambda \text{Na}^+ + \lambda \text{OH}^-) \times \text{C}_E + (\lambda \text{Na}^+ + \lambda \text{Cl}^-) \times \text{C}_S$$

$$\text{GS} = (50 + 198) \times 0.9 + (50 + 76) \times 0.1 = 235.8 \mu\text{S}$$

$$\Delta\text{G} = \text{GS} - \text{GE}$$

$$\Delta\text{G} = 235.8 - 248 = -12.2 \mu\text{S}$$

The change in conductivity is actually slightly greater with non-suppressed conductivity. However, the noise is much higher in the non-suppressed detection mode (Fritz, & Gjerde, 2000).

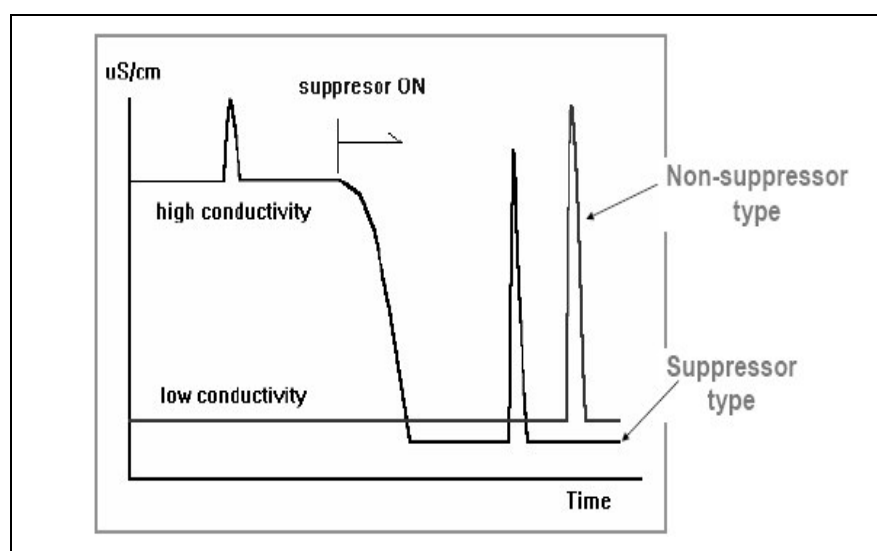


Figure 2.19 The differences between suppressed and non-suppressed type (taken from http://www.thairohs.org/index.php?option=com_docman&task=doc_view&gid=68&PHPSESSID=26f0d608883bf42c165507d213ec5ace)

2.6.9 Detectors

Several types of detectors used in ion chromatographic analysis along with a brief description. In IC, the detector must be able to "pick out or see" sample ions in the presence of the eluent ions. There are several methods that can be employed to make this possible. One is to choose a detector that will response only to the sample ions of interest, but not the eluent ions. Another method is to use indirect detection. This is where the eluent has a background signal and the presence of samples ions cause a decrease in eluent ions through a replacement process. The detector looks for the absence of eluent ions when the sample ion peak elutes and a decreasing signal is detected (Fritz, & Gjerde, 2000).

2.6.9.1 Conductivity Detectors

Conductivity is the ability of a solution containing a salt to conduct electricity across two electrodes. The ability of the solution to conduct is directly proportional to the salt content and the mobility of the individual anions and cations. As the ionic character of a molecule is increased, the conductivity increases. Small, mobile ions conduct quite readily and to a much greater extent than large bulky ions. For example, hydroxide anion is small and mobile and will conduct much better than propionate anion which larger and bulkier. The relative conductances of ions are shown in Table 2.2 (Fritz, & Gjerde, 2000).

Table 2.2 Limiting equivalent ionic conductances in aqueous solution at 25 °G Units: ohm⁻¹ cm² equiv⁻¹

Anions	r	Cations	r
OH ⁻	198	H ⁺	350
F ⁻	54	Li ⁺	39
Cl ⁻	76	Na ⁺	50
Br ⁻	78	K ⁺	74
I ⁻	77	NH ₄ ⁺	73
NO ₃ ⁻	71	Mg ²⁺	53
HCO ₃ ⁻	45	Ca ²⁺	60
Formate	55	Sr ²⁺	59
Acetate	41	Ba ²⁺	64
Propionate	36	Zn ²⁺	53
Benzoate	32	Hg ²⁺	53
SCN ⁻	66	Cu ²⁺	55
SO ₄ ²⁻	80	Pb ²⁺	71
CO ₃ ²⁻	72	Co ²⁺	53
C ₂ O ₄ ²⁻	74	Fe ³⁺	68
CrO ₄ ²⁻	85	La ³⁺	70
PO ₄ ³⁻	69	Ce ³⁺	70
Fe(CN) ₆ ³⁻	101	CH ₃ HN ₃ ⁺	58
Fe(CN) ₆ ⁴⁻	111	N(Et) ₄ ⁺	33

Molecular substances such as solvents (water and methanol) and solutions of non-ionized organic acids do not conduct electricity and are not detected by conductivity. The portion of a weak acid that does ionize results in a contribution to the conductivity signal. The ionic form of the weak acid depends on pH. A weak acid with a pKa larger than about six cannot be detected with suppressed conductivity detection because all anions are converted to the acid form by the suppressor. Because of high sensitivity and reduced background noise, the most common form of conductivity detection is with the use of suppressors. The advantage of this detection method is simplicity in instrument design and operation and the ability to detect salts

of weak acids. There is a number of IC users who employ non-suppressed, direct or indirect conductivity detection where the separation column is connected directly to the conductivity cell (Fritz, & Gjerde, 2000).

2.6.9.2 Ultraviolet-Visible Detectors

There are several reasons why a spectrophotometric detector is a useful detector for monitoring ion-exchange separations. It is selective, yet its selectivity can be changed simply by changing the wavelength monitored by the detector. Versatility of the detector can be increased by adding a color-forming reagent to the eluent or the column effluent. The fundamental law under which ultraviolet-visible (UV-VIS) detectors operate is the Lambert-Beer law. It can be stated in the following form:

$$A = \epsilon b C \quad (2.7)$$

A is the absorbance of a species of concentration C, and with an absorptivity ϵ , in a cell of length b. Concentration is usually in molar concentration and the path length is measured in cm. The term (molar) absorptivity has units that are the inverse of the C and ϵ units. This leaves a dimensionless; it is usually described in terms of absorbance units. A detector set to a certain sensitivity.

The Lambert-Beer equation is useful for choosing conditions for the separation and detection of ions. The eluent ions should have a low absorptivity and the sample ions should have reasonably high absorptivity. In a special case of indirect detection, this should be reversed. In this case, the eluent has an absorption signal and the sample is detected by a decrease of the background signal (Fritz, & Gjerde, 2000).

If ion absorptivity for a particular wavelength is unknown, it can be measured with a spectrophotometer and ion solution of known concentration.

The discussion of UV-VIS detectors for use in ion chromatography is divided into two parts: (a) the direct monitoring of column effluents and (b) post-column derivatization with subsequent spectrophotometric measurement (Fritz, & Gjerde, 2000).

a. Direct Spectrophotometric Measurement: Alkali metal ions are not detected by UV. However, many anions do absorb at lower wavelengths. The 190 to 210 nm range can be used for the detection of azide, chloride, bromide, bromate, iodide, iodate, nitrite, nitrate, sulfite, sulfide, and selenite. Other work has shown that the 210 to 220 nm range is useful for detecting trithionate, tetrathionate, and pentathionate down to the low nanogram levels. The usefulness of direct UV detection can be considered to be limited because sulfate is not detected by UV, and chloride, phosphate and others are difficult to detect. The absorbance of metal chloride complexes in the ultraviolet spectral region has been used extensively to automatically detect metal ions in liquid chromatography (Seymour, Sickafoose, & Fritz, 1971; Seymour, & Fritz, 1973; Goodkin, & Fritz, 1974; Goodkin, Seymour, & Fritz, 1975).

Another technique is indirect detection. In this method, the eluent absorbs strongly in the visible or ultraviolet spectral region. A wavelength is selected where the (usually aromatic) eluent absorbs but the sample ions do not absorb (Denkert, HacEzell, Schill, & Sjogren, 1981; Small, & Miller, 1982; Cochrane, & Hillman, 1982).

Briefly, because an ion-exchange process is involved, a sample ion can only be eluted by displacement of the eluent ion. This results in a decrease in the signal when a sample ion peak is eluted. Indirect UV detection is generally used only in cases where the separation and detection conditions have been carefully worked out and where a high quality UV detector is available. Temperature control of the column is recommended to control the baseline noise (Fritz, & Gjerde, 2000).

b. Post-Column Derivatization: The post-column method of derivatization of column fractions has been well established from older ion-exchange separations. An appropriate reaction is performed on each fraction to determine the metal ion concentration in that fraction. The automatic addition of a color-forming reagent to an ion-exchange column effluent and analysis by flow-through cell detection is more recent. However, many of the color-forming reagents and buffers used in ion chromatography are the same as those used in the classical fraction method determinations (Fritz, & Gjerde, 2000).

2.6.9.3 *Electrochemical Detectors*

Electrochemical detectors are sometimes divided into the groups of potentiometric, amperometric and conductometric detectors, that is, according to the three parameters of electric measurements. Potentiometric detectors measure voltage, amperometric measure current and conductometric measure resistance.

Conductometric detectors respond to all ions, but the other detectors respond only to certain electroactive ions (Fritz, & Gjerde, 2000).

The potentiometric detector operates on the same principles as ion-selective electrodes. An indicating electrode measures a change in the potential in the presence of certain sample ions. Hershcovitz, Yarnitsky, & Schmuckler (1982), explored the use of potentiometric-type detectors for ion chromatography.

Amperometric detectors are some of the most selective and sensitive detectors used to monitor ion chromatography separations. They are selective because they operate on the principles of oxidation or reduction of substances at an electrode. The potential needed to induce electrolysis differs for each ion (Fritz, & Gjerde, 2000).

Other advantages of electrochemical detection include a wide range of detector response (four to five orders of magnitude) and small cell dead volumes (as low as 1 μL). The detectors are simple, inexpensive, and rugged. Their main disadvantage is that they are sometimes difficult to use. Detectors are sensitive to the eluent flow rate

and pH (Fritz, & Gjerde, 2000).

2.6.9.4 Refractive Index Detection

Extensive work has been performed with refractive index (R_i) detection for ion chromatography (Chrompack, 1981; Buytenhuys, 1981; Haddad, & Heckenberg, 1982).

The refractive index detector can be considered to be a universal detector because any salt (or acid or base) added to water will cause a change in refractive index of the solvent. The differences in refractive index can be measured as the sample ions pass through the detector window replacing some of the eluent ions and changing the refractive index. Depending on the relative change, the peak may be increasing or decreasing. The detector has been used for both anion and cation separations with good results (Fritz, & Gjerde, 2000).

The refraction index of solution increases with the molecular weight (and concentration) of the solute dissolved in the solution. Organic ions usually cause a greater change than inorganic ions in the refractive index of a solution.

Refractive index detection allows extremely wide latitude in the selection of the eluent type, eluent pH and the ionic strength. In principle, refractive index detection can be substituted for conductance or UV absorption detection in many separations (Fritz, & Gjerde, 2000).

2.6.9.5 Other Detectors

Many other detectors have been used to monitor ion chromatography separations. Most of these detectors have been used only in special cases. Flame photometric detection (Freed, 1975; Downey, & Hieftje, 1983) has been used to detect alkali, alkaline earth, and some rare earth metals. Atomic absorption (AA) detectors

(Woolson, & Aharonson, 1980; Ricci, Shepard, Colovos, & Hester, 1981; Grabinski, 1981) have been used for arsenite, arsenate, monomethyl arsenate, dimethyl arsenate and p-aminophenoarsenate separations. Detectors of this type can be extremely sensitive detecting arsenic down to 10 ng/mL.

Research developing environmental methods might consider the use of AA detection. Perhaps some of the more interesting are detectors that use inductively coupled plasma (ICP) as an energy source and either atomic emission (AE) or mass spectrometry (MS) as the detector. ICP-AE and ICP-MS are well-developed analytical tools. One of the major advantages of these techniques is that mixture of metals can be analyzed without the need for separation. Thus, workers who use these instruments normally do not think about their use as detectors. However, ICP-AE and ICP-MS cannot determine the oxidation or chemical state of a particular metal ion. Some samples are quite important from a toxicological and environmental standpoint since the toxicity of a metal may depend on its oxidation state (Yoshida, & Haraguchi, 1984).

2.7 Experimental Method and Instrumentation

An ion chromatography method for the simultaneous determination of common anions (Fluoride, Chloride, Nitrite, Bromide, Nitrate, Phosphate, and Sulfate) in real-ground water samples has been employed using an anion-exchange column and the suppressed conductivity detector.

2.7.1 Instrument

All systems and components for ionic analysis were from Dionex (Sunnyvale, CA, USA). The hardware used for these analyses consisted of an ICS-1000 ion chromatograph equipped with an isocratic pump, a conductivity detector, a self-regenerating suppressor (ASRS ultra II 4mm), an AS40 auto sampler and a column heater. Eluent flow rates were set at 1 mL/min with an injection volume of 25 μ L. An Ion Pac® AG9-HC (50mm \times 4mm I.D.) guard column and an Ion Pac® AS9-HC

Analytical (250mm×4mm I.D) analytical column were used to separate the anions. The current of the suppressor was set at 45 mA to give a background conductivity of 25.5-26.5 μ s. The complete operating conditions and the composition of the eluent used by the ion chromatography system during the chromatographic runs were summarized in Table 2.3.

Table2.3 Operating conditions

IC	
Ion-Chromatographic Unit	Dionex ICS-1000 IC
Pump	GP50 Gradient Pump
Guard Column	IonPac® AG9-HC Guard, 50mm×4mm I.D
Column	IonPac® AS9-HC Analytical, 250mm×4mm I.D
Column Temperature	30 °C
Suppressor	ASRS Ultra II 4mm
Suppressor Current	45 mA
Eluent	9mM NaCO ₃
Flow-Rate	1 mL/min
Detector	Dionex DS6 Heated Conductivity Cell
Cell Temperature	35 °C
Injection Volume	25 μ L
Run Time	30 min
Background Conductance	\approx 25.5-26.5mS
Back Pressure	\approx 2000 psi
Data Management	Chromeleon® 6.5 Chromatography Workstation
Auto Sampler	AS-40

2.7.2 Reagents

Deionized water, generated by a Milli-Q deionized water unit that had a resistance better than 18.2 M Ω cm, was used for the preparation of all the solutions. Certified reference anion standard solution of Dionex (Fluoride 20 mg/L, Chloride 30mg/L, Nitrite 100mg/L, Bromide 100 mg/L, Nitrate 100mg/L, Phosphate 150 mg/L, Sulfate 150mg/L) were used throughout the study. All chemicals were of analytical reagent grade unless otherwise specified.

2.7.3 Preparation of the Solutions

All the solutions were prepared with deionized water (Milli-Q, USA). The standard solutions of seven anions (as sodium salts) were prepared daily by serial dilution of certified reference anion standard solution of Dionex. NaCO₃ (0.5 M) was obtained from DIONEX and used for the mobile phase. The mobile phase was prepared daily before use. For preparing 9 mM eluent, 18 mL NaCO₃ added to the volumetric flask and finally diluted to 1000 mL by water.

2.7.4 Pretreatment of Samples

The method was applied to the determination of anions in real ground water samples. The ground water samples were taken from Pamukkale Antique Pool, Denizli, Turkey. To avoid accidental contamination of the samples, the samples were collected to polyethylene collectors on daily basis. Then they were filtered with Pionex/Millipore/Sartorius through a filter with a pore diameter 0.45 µm to polyethylene bottles at 25 °C. In laboratory conditions prior to injection samples were kept under refrigeration at 4 °C.

2.8 Results and Discussion

2.8.1 Analysis of Seven Anion Standards

The anion standards were analyzed with ion exchange chromatography method employing guard (AG9 HC (4x50 mm)) and analytical columns (AS9 HC (4x250 mm)) of DIONEX with alkyl-quaternary ammonium functional groups, respectively.

Characteristics of the analytical and guard columns were given below.

Table 2.4 IonPac AS9-HC/AG9-HC packing specifications (taken from http://www1.dionex.com/en-us/webdocs/4347_31267-07_Manual,IP,AS9-HC_V28.pdf)

Column	Particle Diameter μm	Substrate X-linking %	Column Capacity $\mu\text{eq}/\text{column}$	Functional Group	Hydrophobicity
AS9-HC 4 x 250 mm	9.0	55	190	Alkyl/Alkanol quaternary ammonium	Medium-low
AG9-HC 4 x 50 mm	9.0	55	6	Alkyl/Alkanol quaternary ammonium	Medium-low

Three different concentration levels of the employed standards were shown in Table 2.5

Table 2.5 Three different concentration levels of the employed standards

Peak Name	Amount Std.1 (ppm)	Amount Std.2 (ppm)	Amount Std.3 (ppm)
Fluoride	1.72	6.72	20.1
Chloride	2.57	10.09	30.2
Nitrite	8.46	33.24	99.4
Bromide	8.60	33.78	101
Nitrate	8.68	34.11	102
Phosphate	12.86	50.50	151
Sulfate	12.77	50.16	150

Optimum conditions: mobile phase; 9 mM of Sodium Carbonate, 1 mL/ min flow rate, 1950 – 2050 psi column pressure, 30 °C of column temperature, 35 °C of detector temperature, 45 mA of suppressor current.

Retention times of standards were measured between 3.8–19.3 min. under optimized working conditions. The peaks of the standards were sharp, symmetrical,

well shaped, Gaussian type and well separated. The resolution throughout the chromatogram was satisfactory.

The chromatogram of the anion standards were shown in Figure 2.20

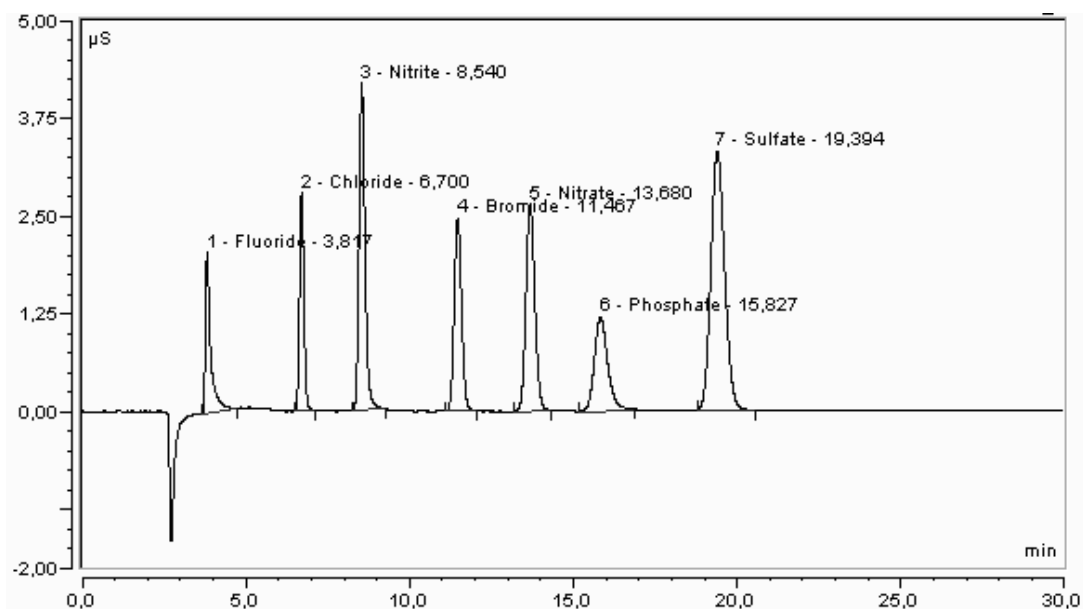


Figure 2.20 IC chromatogram of the standards (Fluoride, Chloride, Nitrite, Bromide, Nitrate, Phosphate, and Sulfate) acquired at optimum working conditions

The calibration plot of each standard consists of six different concentration points. In all cases, the quadratic fit was employed for the acquired data since it has been statistically significant.

Calibration plots of seven anion standards were shown in Figure 2.21.

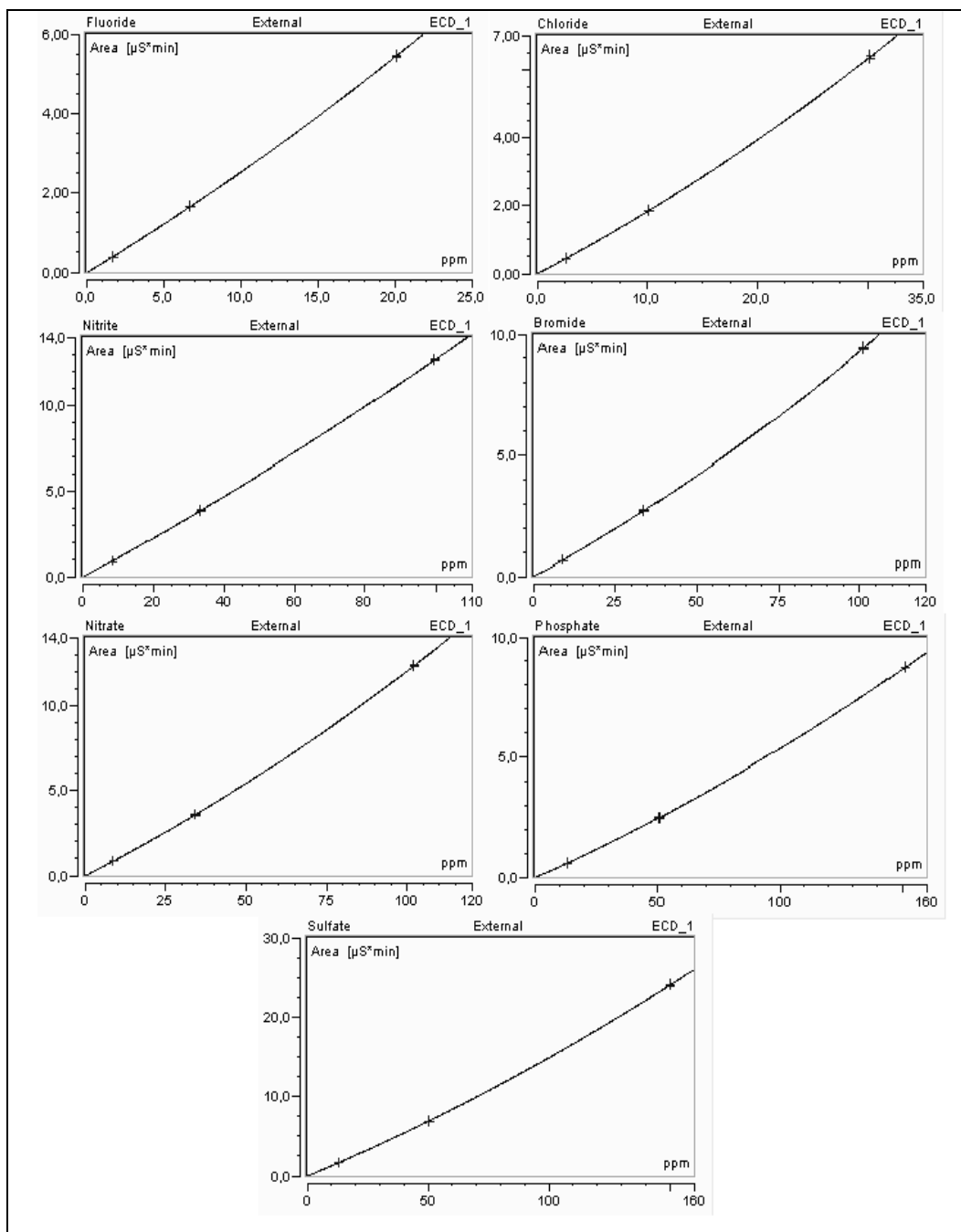


Figure 2.21 Calibration curves of standards

Table 2.6 shows regression coefficient and relative standard deviation values of the calibration plots of 7 different anion standards.” 0QOff” represents quadratic and originated fit.

Table2.6 Shows regression coefficient and relative standard deviation values of the calibration plots of 7 different anion standards

Peak Name	Cal. Type	Points	Rel. Std. Dev. %	Coeff. Det. %
F ⁻	0QOff	6	0.8983	99.9946
Cl ⁻	0QOff	6	0.9895	99.9936
NO ₂ ⁻	0QOff	6	0.7041	99.9966
Br ⁻	0QOff	6	0.6999	99.9968
NO ₃ ⁻	0QOff	6	0.5592	99.9980
PO ₄ ³⁻	0QOff	6	0.5200	99.9983
SO ₄ ²⁻	0QOff	6	0.3937	99.9990
AVE:		6	0.6807	99.9967

Table 2.7 Six different concentrations of anions employed for the calibration plot in (ppm), Peak Area ($\mu\text{s} \cdot \text{min}$) and Peak Height (μs)

	F ⁻	Cl ⁻	NO ₂ ⁻	Br ⁻	NO ₃ ⁻	PO ₄ ³⁻	SO ₄ ²⁻
Concentration (ppm)	1.6826	2.5476	8.1919	8.5552	8.5783	12.6955	12.6325
	1.6297	2.5478	8.2919	8.5588	8.5705	12.3369	12.7044
	6.7177	10.1069	33.2204	33.6401	34.0352	50.3407	50.0483
	6.7627	10.1080	33.4118	33.9430	34.2594	50.8699	50.3475
	20.0280	30.0619	99.1128	100.6975	101.7633	150.888	149.7670
	20.1691	30.3368	99.6756	101.3003	102.2316	151.0973	150.2283
Peak Area ($\mu\text{s} \cdot \text{min}$)	0.3818	0.4354	0.8988	0.6429	0.8318	0.5652	1.6157
	0.3691	0.4355	0.9103	0.6432	0.8310	0.5483	1.6252
	1.6415	1.8486	3.8745	2.7004	3.5510	2.4656	6.8767
	1.6531	1.8488	3.8980	2.7267	3.5763	2.4940	6.9213
	5.4225	6.3260	12.5946	9.3654	12.2815	8.7065	23.9622
	5.4661	6.3953	12.6746	9.4330	12.3494	8.7213	24.0516
Peak Height (μs)	2.0512	2.7905	4.1880	2.4695	2.6475	1.1982	3.3113
	2.0824	2.7955	4.2035	2.4713	2.6478	1.1933	3.3131
	10.4010	11.8495	18.2291	10.6471	11.4093	5.5167	14.3613
	10.4843	11.8577	18.3080	10.6682	11.4235	5.5378	14.3937
	38.3069	38.0525	58.1488	37.6121	38.6774	20.4546	49.6913
	38.5565	38.1696	58.4135	37.6738	38.7469	20.5094	49.7761

Table 2.8 reveals retention time, peak area, relative peak area, peak width, peak height, asymmetry, resolution and plate number values for six different calibration points.

From Table 2.8 it can be concluded that retention times of seven anion standards are in correlation for six different concentration points.

The peak area of each anion standard was increased as concentration rose as expected.

Peak asymmetry (EP) is a factor regarding with peak symmetry and its value should be around 10 % of the peak height. A peak asymmetry value of 1-1.05 points out excellent peak symmetry. Where the asymmetry values between 1.2 -2 are acceptable, the higher ones are being unacceptable. Except that of fluoride, all of the measured asymmetry values were acceptable. However, the asymmetry values of low concentrations of fluoride exhibited a little bit deviation from the acceptable numbers.

The resolution of a column provides a quantitative measure of its ability to separate two analyte. A resolution value of 1.5 means essentially complete separation of peaks whereas a resolution of 0.75 does not. The resolution values were calculated with respect to SO_4^{2-} and were found to be 12.25, 6.49, 7.98, 4.9, 3.55 and 4.8 for F^- , Cl^- , NO_2^- , Br^- , NO_3^- and PO_4^{3-} respectively. From Table 2.8 it can be concluded that the resolution performance of the column was very satisfactory.

The efficiency of chromatographic columns increases as the number of plates (N) becomes greater and the plate height becomes smaller. Efficiencies in terms of plate numbers can vary from a few hundred to several hundred thousand. Plate number of $N > 2000$ is a desirable value. In our case number of plates are 4450, 12134, 11037, 12473, 12188, 7799 and 10079 for F^- , Cl^- , NO_2^- , Br^- , NO_3^- , PO_4^{3-} and SO_4^{2-} respectively which are quite good for all calibration points (See Table 2.8).

Table 2.8 Retention time(min), peak area($\mu\text{S}\cdot\text{min}$), relative peak area(%), peak width(min), peak height(μS), asymmetry(EP), resolution and plate number(EP) values for six different calibration points for six different calibration points.

First point of calibration

Peak Name	Ret. Time (min)	Area ($\mu\text{S}\cdot\text{min}$)	Rel. Area %	Peak Width (min)	Height (μS)	Asym. (EP)	Resol.	Plates (N)
F ⁻	3.817	0.3818	7.11	0.23	2.051	2.52	12.25	4450
Cl ⁻	6.700	0.4354	8.11	0.25	2.790	1.14	6.49	12134
NO ₂ ⁻	8.540	0.8988	16.73	0.33	4.188	1.23	7.98	11037
Br ⁻	11.467	0.6429	11.97	0.41	2.470	1.11	4.90	12473
NO ₃ ⁻	13.680	0.8318	15.48	0.50	2.647	1.10	3.55	12188
PO ₄ ³⁻	15.827	0.5652	10.52	0.72	1.198	1.22	4.80	7799
SO ₄ ²⁻	19.394	1.6157	30.08	0.78	3.311	1.13	n.a.	10079

Second point of calibration

Peak Name	Ret. Time (min)	Area ($\mu\text{S}\cdot\text{min}$)	Rel. Area %	Peak Width (min)	Height (μS)	Asym. (EP)	Resol.	Plates (N)
F ⁻	3.813	0.3691	6.88	0.23	2.082	2.43	12.31	4543
Cl ⁻	6.700	0.4355	8.12	0.25	2.795	1.12	6.46	12077
NO ₂ ⁻	8.537	0.9103	16.98	0.33	4.203	1.25	7.98	10933
Br ⁻	11.467	0.6432	11.99	0.41	2.471	1.09	4.89	12524
NO ₃ ⁻	13.677	0.8310	15.50	0.50	2.648	1.11	3.56	12112
PO ₄ ³⁻	15.823	0.5483	10.22	0.73	1.193	1.17	4.81	7863
SO ₄ ²⁻	19.397	1.6252	30.31	0.78	3.313	1.11	n.a.	10031

Third point of calibration

Peak Name	Ret. Time (min)	Area ($\mu\text{S}\cdot\text{min}$)	Rel. Area %	Peak Width (min)	Height (μS)	Asym. (EP)	Resol.	Plates (N)
F ⁻	3.807	1.6415	7.11	0.20	10.401	2.24	12.99	5949
Cl ⁻	6.697	1.8486	8.00	0.24	11.850	1.17	6.59	12292
NO ₂ ⁻	8.537	3.8745	16.77	0.32	18.229	1.23	8.15	11504
Br ⁻	11.450	2.7004	11.69	0.40	10.647	1.13	4.93	13208
NO ₃ ⁻	13.630	3.5510	15.37	0.49	11.409	1.20	3.69	12481
PO ₄ ³⁻	15.790	2.4656	10.67	0.69	5.517	1.20	4.94	8498
SO ₄ ²⁻	19.333	6.8767	29.77	0.76	14.361	1.18	n.a.	10520

Fourth point of calibration

Peak Name	Ret. Time (min)	Area ($\mu\text{S}\cdot\text{min}$)	Rel. Area %	Peak Width (min)	Height (μS)	Asym. (EP)	Resol.	Plates (N)
F ⁻	3.810	1.6531	7.10	0.20	10.484	2.19	13.00	5994
Cl ⁻	6.697	1.8488	7.94	0.24	11.858	1.18	6.58	12292
NO ₂ ⁻	8.537	3.8980	16.75	0.32	18.308	1.23	8.13	11463
Br ⁻	11.450	2.7267	11.72	0.40	10.668	1.14	4.92	13152
NO ₃ ⁻	13.630	3.5763	15.37	0.49	11.424	1.21	3.69	12423
PO ₄ ³⁻	15.790	2.4940	10.72	0.69	5.538	1.22	4.93	8491
SO ₄ ²⁻	19.337	6.9213	29.74	0.76	14.394	1.18	n.a.	10468

Fifth point of calibration

Peak Name	Ret. Time (min)	Area ($\mu\text{S}\cdot\text{min}$)	Rel. Area %	Peak Width (min)	Height (μS)	Asym. (EP)	Resol.	Plates (N)
F ⁻	3.810	5.4225	6.88	0.19	38.307	1.76	12.98	6666
Cl ⁻	6.713	6.3260	8.03	0.26	38.052	1.07	6.21	10483
NO ₂ ⁻	8.540	12.5946	15.98	0.33	58.149	1.19	8.03	10847
Br ⁻	11.410	9.3654	11.88	0.39	37.612	1.21	4.78	13794
NO ₃ ⁻	13.520	12.2815	15.58	0.50	38.677	1.43	3.86	11836
PO ₄ ³⁻	15.733	8.7065	11.05	0.66	20.455	1.20	4.92	9292
SO ₄ ²⁻	19.197	23.9622	30.40	0.76	49.691	1.33	n.a.	10210

Sixth point of calibration

Peak Name	Ret. Time (min)	Area ($\mu\text{S}\cdot\text{min}$)	Rel. Area %	Peak Width (min)	Height (μS)	Asym. (EP)	Resol.	Plates (N)
F ⁻	3.810	5.4661	6.91	0.19	38.557	1.73	12.94	6647
Cl ⁻	6.714	6.3953	8.09	0.26	38.170	1.06	6.19	10438
NO ₂ ⁻	8.540	12.6746	16.03	0.33	58.413	1.18	8.00	10791
Br ⁻	11.410	9.4330	11.93	0.39	37.674	1.20	4.77	13674
NO ₃ ⁻	13.524	12.3494	15.61	0.50	38.747	1.41	3.85	11775
PO ₄ ³⁻	15.737	8.7213	11.03	0.66	20.509	1.19	4.91	9272
SO ₄ ²⁻	19.200	24.0516	30.41	0.76	49.776	1.33	n.a.	10198

2.8.2 Method Validation Studies and Accuracy

The precision and accuracy of the method were tested at three different concentration levels for each standard. Table 2.9 shows concentrations of seven different anion standards in ppm.

Table 2.9 Three different concentration levels for the standards

Standard Name	I. Concentration (ppm)	II. Concentration. (ppm)	III. Concentration (ppm)
Fluoride	1.67	6.67	20
Chloride	2.50	10.00	30
Nitrite	8.33	33.33	100
Bromide	8.33	33.33	100
Nitrate	8.33	33.33	100
Phosphate	12.50	50.00	150
Sulfate	12.50	50.00	150

Table 2.10 shows real retention times, experimentally measured average retention times, relative retention times, standard deviation and relative standard deviations of the seven anion standards. For three different concentration points, double injections were performed. Therefore, the retention times were extracted from six

measurements for each standard. Relative retention times were measured with respect to Br⁻. The calculation of relative retention time (RRT) for F⁻ is as follows. RRT values of other standards were calculated similarly.

$$\text{RRT} = \frac{t_{\text{standard}}}{t_{\text{reference}}}$$

$$\text{RRT} = \frac{3.790}{11.450}$$

$$\text{RRT} = 0.3331$$

RRT: Relative Retention Time, t standard: Real retention time of standard, t reference: Real retention time of standards which used as a reference

Table 2.10 Retention time (min), average retention time, standard deviation (SD, min, n=3), relative standard deviation (%RSD) and relative retention time of the employed anion standards.

Peak Name	Ret. Time (min)	Ave. Retention time	SD (min) (n=3)	% RSD	Rel. Ret. Time (RRT)
Fluoride	3.790	3.8112	0.0034	0.09	0.3331
Chloride	6.700	6.7035	0.0079	0.12	0.5859
Nitrite	8.550	8.5385	0.0016	0.02	0.7462
Bromide	11.450	11.4423	0.0262	0.23	1.0000
Nitrate	13.600	13.6102	0.0717	0.53	1.1895
Phosphate	15.800	15.7833	0.0406	0.26	1.3794
Sulfate	19.200	19.3097	0.0903	0.47	1.6876

Precision can be determined by replicating a measurement. In this work, precision of the retention times was evaluated with six replicate measurements for each standard. Average retention times were found to be 3.8112, 6.7035, 8.5385, 11.4423, 13.6102, 15.7833 and 19.3097 min. for fluoride, chloride, nitrite, bromide, nitrate, phosphate and sulfate respectively. Their standard deviations were in the range of 0.0034 – 0.0903 min. which is less than 0.5 %.

Accuracy

The accuracy of an analytical method is one of the key features of validation. A few alternative methods have been proposed for the assessment of the accuracy which is the use of certified reference materials, the comparison of the proposed method with a reference one and the use of recovery assays on samples (Gonzalez, Herrador, & Agustin, 1998). The average recovery should be in the range of 99–101 %.

In this work, recovery studies were performed by adding standards in to the geothermal groundwater samples and drinking water. For groundwater samples recovery tests was performed between two successive months. Additionally, the accuracy was also defined as the difference between the calculated amount and the specified amount for the selected certified reference standard and expressed as RSD%.

The groundwater samples were treated with different concentrations of certified reference standards, which were diluted in the ratio of 1:8, 1:6 and 1:4.

2.8.2.1 Recovery Studies with Real Ground Water Samples

Table 2.11, 2.12 and 2.13 shows % recovery values of seven different anions for two different months and three different dilution ratios. The column “Found” in Table 2.11 is the average of three-injections. Amounts of the added certified reference standards were kept in the range of calibration limits.

In real groundwater samples, the deviations in recovery values (%) were less than 10 %, except that of fluoride. However, in fluoride the deviations may extend to 17 %. This can be attributed to the complexation tendency of fluoride with metal cations.

Drinking water samples exhibited excellent recovery values with respect to groundwater samples. This can be referred to the rich heavy metal content of groundwater samples, which is a strongly possible reason for interferences.

Table 2.11 Anion concentrations, recovery, relative standard deviation and % recovery values for groundwater samples collected from Sarıkız in April 29, 2008 and May 29, 2008 respectively. Certified reference standards were diluted 1:8 with pure water.

29-04-2008

Ion	Real Conc. (ppm)	Found (ppm)	Added (ppm)	Recovery (ppm)	RSD (%) (n =3)	Recovery (%)
Fluoride	0.4744	2.7015	2.5207	2.2271	11.6476	88.3524
Chloride	22.8911	26.8476	3.7873	3.9565	-4.4676	104.4676
Nitrite	-	11.8386	12.4655	11.8386	5.0291	94.9709
Bromide	-	12.6517	12.6662	12.6517	0.1145	99.8855
Nitrate	0.8016	13.1111	12.7916	12.3095	3.7689	96.2311
Phosphate	-	18.2173	18.9365	18.2173	3.7980	96.2020
Sulfate	93.0210	111.6837	18.8111	18.6627	0.7889	99.2111

29-05-08

Ion	Real Conc. (ppm)	Found (ppm)	Added (ppm)	Recovery (ppm)	RSD (%) (n =3)	Recovery (%)
Fluoride	0.7962	2.8721	2.5115	2.0759	17.3442	82.6558
Chloride	20.1622	24.3620	3.7734	4.1998	-11.3002	111.3002
Nitrite	-	11.7158	12.4199	11.7158	5.6691	94.3309
Bromide	-	12.5266	12.6198	12.5266	0.7385	99.2615
Nitrate	-	12.9546	12.7448	12.9546	-1.6462	101.6462
Phosphate	-	18.1395	18.8672	18.1395	3.8570	96.1430
Sulfate	89.2852	109.5140	18.7423	20.2288	-7.9313	107.9313

Table 2.12 Anion concentrations, recovery, relative standard deviation and % recovery values for groundwater samples collected from Sarıkız in April 29, 2008 and May 29, 2008 respectively. Certified reference standards were diluted 1:6 with pure water.

29-04-08

Ion	Real Conc. (ppm)	Found (ppm)	Added (ppm)	Recovery (ppm)	RSD (%) (n =3)	Recovery (%)
Fluoride	0.4744	3.4237	3.3734	2.9493	12.5719	87.4281
Chloride	22.8911	28.2686	5.0685	5.3775	-6.0965	106.0965
Nitrite	-	15.7784	16.6825	15.7784	5.4195	94.5805
Bromide	-	16.9659	16.9511	16.9659	-0.0873	100.0873
Nitrate	0.8016	17.3505	17.1189	16.5489	3.3297	96.6703
Phosphate	-	24.4142	25.3427	24.4142	3.6638	96.3362
Sulfate	93.0210	118.5228	25.1749	25.5018	-1.2985	101.2985

29-05-08

Ion	Real Conc. (ppm)	Found (ppm)	Added (ppm)	Recovery (ppm)	RSD (%) (n =3)	Recovery (%)
Fluoride	0.7962	3.6227	3.3651	2.8265	16.0055	83.9945
Chloride	20.1622	25.4217	4.988	5.2595	-5.4431	105.4431
Nitrite	-	15.6203	16.4173	15.6203	4.8546	95.1454
Bromide	-	16.7664	16.6816	16.7664	-0.5083	100.5083
Nitrate	-	17.2096	16.8467	17.2096	-2.1541	102.1541
Phosphate	-	24.7894	24.9398	24.7894	0.6031	99.3969
Sulfate	89.2852	115.9925	24.7746	26.7073	-7.8011	107.8011

Table 2.13 Anion concentrations, recovery, relative standard deviation and % recovery values for groundwater samples collected from Sarıkız in April 29, 2008 and May 29, 2008 respectively. Certified reference standards were diluted 1:4 with pure water.

29-04-08

Ion	Real Conc. (ppm)	Found (ppm)	Added (ppm)	Recovery (ppm)	RSD (%) (n =3)	Recovery (%)
Fluoride	0.4744	5.0824	5.0314	4.6080	8.4152	91.5848
Chloride	22.8911	30.7702	7.5596	7.8791	-4.2264	104.2264
Nitrite	-	23.4273	24.8817	23.4273	5.8453	94.1547
Bromide	-	25.4306	25.2822	25.4306	-0.5870	100.5870
Nitrate	0.8016	25.7960	25.5325	24.9944	2.1075	97.8925
Phosphate	-	36.2190	37.7981	36.2190	4.1777	95.8223
Sulfate	93.0210	131.6331	37.5478	38.6121	-2.8345	102.8345

29-05-08

Ion	Real Conc. (ppm)	Found (ppm)	Added (ppm)	Recovery (ppm)	RSD (%) (n =3)	Recovery (%)
Fluoride	0.7962	5.0870	4.9775	4.2908	13.7961	86.2039
Chloride	20.1622	27.5724	7.4786	7.4102	0.9146	99.0854
Nitrite	-	23.0036	24.6152	23.0036	6.5472	93.4528
Bromide	-	25.1190	25.0114	25.1190	-0.4302	100.4302
Nitrate	-	25.5267	25.2590	25.5267	-1.0598	101.0598
Phosphate	-	36.9145	37.3933	36.9145	1.2804	98.7196
Sulfate	89.2852	129.0739	37.1457	39.7887	-7.1152	107.1152

Table 2.14 Anion concentrations, recovery, relative standard deviation and % recovery values for two parallel drinking water samples. Certified reference standards were diluted 1:6 with pure water.

Sample 1

Ion	Real Conc. (ppm)	RSD (%)	Found (ppm)	Added (ppm)	Recovery (ppm)	Recovery (%)
Fluoride	-	-0.0178	3.3678	3.3672	3.3678	100.0178
Chloride	0.4549	4.4118	5.2909	5.0592	4.836	95.5882
Nitrite	-	1.7391	16.3623	16.6519	16.3623	98.2609
Bromide	-	-0.3534	16.9797	16.9199	16.9797	100.3534
Nitrate	1.0025	1.5743	17.821	17.0875	16.8185	98.4257
Phosphate	-	-1.9552	25.7907	25.2961	25.7907	101.9552
Sulfate	2.8253	2.4410	27.3405	25.1286	24.5152	97.5590

Sample 2

Ion	Real Conc. (ppm)	RSD (%)	Found (ppm)	Added (ppm)	Recovery (ppm)	Recovery (%)
Fluoride	-	0.0059	3.368	3.3682	3.368	100.0059
Chloride	0.4549	3.6300	5.3318	5.0606	4.8769	103.7667
Nitrite	-	1.2361	16.4507	16.6566	16.4507	101.2516
Bromide	-	-1.4570	17.1713	16.9247	17.1713	98.5639
Nitrate	1.0025	0.8624	17.9473	17.0922	16.9448	100.8699
Phosphate	-	-2.2831	25.8809	25.3032	25.8809	97.7679
Sulfate	2.8253	1.6972	27.5344	25.1357	24.7091	101.7265

2.8.2.2 Statistical Assessment of Recovery Results of Groundwater Samples

The recovery results acquired with three different concentrations of standards were compared statistically in 95 % confidence level. For this purpose, pooled standard deviations, experimental difference ($|\bar{x}_1 - \bar{x}_2|$) and computed values were calculated for groundwater samples of Sarıkız location. Calculations made for fluoride are as follows.

$$S_{\text{pooled}} = \sqrt{\frac{\sum_{i=1}^n (x_i - \bar{x})^2 + \sum_{j=1}^n (x_j - \bar{x})^2}{N_1 + N_2 - 2}}$$

$$S_{\text{pooled}} = \sqrt{\frac{(-0,0064)^2 + (0,0415)^2 + (-0,0351)^2 + (-0,0147)^2 + (-0,0136)^2 + (-0,0283)^2}{3 + 3 - 2}}$$

$$S_{\text{pooled}} = 0.0324$$

S_{pooled} : Pooled standard deviation, x_i : any measurement value, \bar{x} : mean value of first group of measurements, N_1 and N_2 : number of replicated analysis.

For 95 % confidence level $t=2.78$; and if

$$|\bar{x}_1 - \bar{x}_2| < t * S_{\text{pooled}} * \sqrt{\frac{N_1 + N_2}{N_1 * N_2}}$$

The data were collected is identical. In our case;

$$|5.0824 - 5.0870| < 2.78 * 0.0324 * \sqrt{\frac{3+3}{3*3}}$$

$$0.0046 < 0.0735$$

Therefore; the experimental difference is smaller than the computed value and no significant difference between the means has been demonstrated at 95 % confidence level for fluoride measurements.

In all cases for chloride and sulfate the experimental difference ($|\bar{x}_1 - \bar{x}_2|$) has been found greater than the computed value which means a significant difference between the measurements performed at different dates.

These differences can be attributed to the precipitate formation tendencies of these two anions with metal cations at high concentrations.

Table 2.15 Statistical evaluation of groundwater samples of Sarıkız location. The results were acquired with 1:4 diluted standards. First and second measurements were performed at April 29, 2008 and May 29, 2008 respectively.

Ion	1 st Measurement (Ave.) (ppm)	2 nd Measurement (Ave.) (ppm)	S _{pooled}	$ \text{1st - 2nd} $ Measurement (Ave.) (ppm)	t*S _{pooled} * $\sqrt{(N1+N2)/}$ (N1*N2)	Statistical Results
F ⁻	5.0824	5.0870	0.0324	0.0046	0.0735	NO DIFFERENCE
Cl ⁻	30.7702	27.5724	0.0453	3.1978	0.1027	DIFFERENT
NO ₂ ⁻	23.4273	23.0036	0.1904	0.4237	0.4321	NO DIFFERENCE
Br ⁻	25.4306	25.1190	0.1278	0.3116	0.2901	DIFFERENT
NO ₃ ⁻	25.7960	25.5267	0.1876	0.2692	0.4257	NO DIFFERENCE
PO ₄ ³⁻	36.2190	36.9145	0.9339	0.6955	2.1199	NO DIFFERENCE
SO ₄ ²⁻	131.6331	129.0739	0.0988	2.5592	0.2242	DIFFERENT

Table 2.16 Statistical evaluation of groundwater samples of Sarıkız location. The results were acquired with 1:6 diluted standards. First and second measurements were performed at April 29, 2008 and May 29, 2008 respectively.

Ion	1 st Measurement (Ave.) (ppm)	2 nd Measurement (Ave.) (ppm)	S _{pooled}	$ \text{1st - 2nd} $ Measurement (Ave.) (ppm)	t*S _{pooled} * $\sqrt{(N1+N2)/}$ (N1*N2)	Statistical Results
F ⁻	3.4237	3.6227	0.1443	0.1990	0.3275	NO DIFFERENCE
Cl ⁻	28.2687	25.4217	0.0720	2.8469	0.1634	DIFFERENT
NO ₂ ⁻	15.7784	15.6203	0.1680	0.1581	0.3813	NO DIFFERENCE
Br ⁻	16.9659	16.7664	0.1063	0.1995	0.2412	NO DIFFERENCE
NO ₃ ⁻	17.3503	17.2097	0.0912	0.1406	0.2071	NO DIFFERENCE
PO ₄ ³⁻	24.4142	24.7894	0.4085	0.3752	0.9272	NO DIFFERENCE
SO ₄ ²⁻	118.5228	115.9925	0.1844	2.5303	0.4187	DIFFERENT

Table 2.17 Statistical evaluation of groundwater samples of Sarıkız location. The results were acquired with 1:8 diluted standards. First and second measurements were performed at April 29, 2008 and May 29, 2008 respectively.

Ion	1 st Measurement (Ave.) (ppm)	2 nd Measurement (Ave.) (ppm)	S _{pooled}	1 st - 2 nd Measurement (Ave.) (ppm)	t*S _{pooled} *√(N1+N2)/(N1*N2)	Statistical Results
F ⁻	2.7015	2.8721	0.0711	0.1706	0.1978	DIFFERENT
Cl ⁻	26.8476	24.3620	0.0686	2.4856	0.1558	DIFFERENT
NO ₂ ⁻	11.8386	11.7158	0.1672	0.1229	0.3794	NO DIFFERENCE
Br ⁻	12.6517	12.5266	0.0784	0.1251	0.1779	NO DIFFERENCE
NO ₃ ⁻	13.1111	12.9546	0.0713	0.1565	0.1618	NO DIFFERENCE
PO ₄ ³⁻	18.2173	18.1395	0.3622	0.0778	0.8222	NO DIFFERENCE
SO ₄ ²⁻	111.6837	109.5143	0.1095	2.1694	0.2485	DIFFERENT

2.8.3 Reproducibility

Precision was also assessed as the percentage relative standard deviation (%RSD) of both repeatability (within-day) and reproducibility (between-day and different concentrations) for groundwater samples from Sarıkız location.

Standard deviation (SD) and relative standard deviation (RSD) calculations of Sulfate; as a representative example; were shown below.

$$SD = \sqrt{\frac{\sum (x_{ave} - x_i)^2}{N - 1}}$$

$$SD = \sqrt{\frac{0.001232}{6 - 1}}$$

$$SD = 0.0157$$

$$\text{RSD} = \frac{S.D.}{x_{av.}} \times 100$$

$$\text{RSD} = \frac{0.0157}{3.6929} \times 100$$

$$\text{RSD} = \% 0.4246$$

Where N is the number of measurements, RSD is relative standard deviation, SD is standard deviation and X_{ave} is average of peak area. Calculations for other anions were performed similarly.

2.8.3.1 Reproducibility of Replicate Injections

The certified reference standard solutions were diluted 1: 6 with ultra pure water and used as test material. After 12 injections the peak areas were integrated, standard deviation and relative standard deviation of peak areas were calculated. For a satisfactory reproducibility, the relative standard deviation should be less than 1 %. Except that of fluoride, RSD values of six anions were found to be less than 1 % for 12 replicate measurements.

Table 2.18 Average, SD and RSD values of seven anions for 12 measurements.

N=12	Area $\mu\text{S} \cdot \text{min}$ Fluoride	Area $\mu\text{S} \cdot \text{min}$ Chloride	Area $\mu\text{S} \cdot \text{min}$ Nitrite	Area $\mu\text{S} \cdot \text{min}$ Bromide	Area $\mu\text{S} \cdot \text{min}$ Nitrate	Area $\mu\text{S} \cdot \text{min}$ Phosphate	Area $\mu\text{S} \cdot \text{min}$ Sulfate
I. Inj.	0.8639	0.9757	2.1211	1.4437	1.8965	1.3799	3.6936
II. Inj.	0.8679	0.9769	2.1049	1.4624	1.8957	1.3613	3.6746
III. Inj.	0.8693	0.9782	2.1172	1.4520	1.8813	1.3503	3.6577
IV. Inj.	0.8718	0.9762	2.1177	1.4534	1.8980	1.3811	3.6805
V. Inj.	0.8848	0.9747	2.1220	1.4686	1.8931	1.3776	3.6965
VI. Inj.	0.8973	0.9734	2.1079	1.4703	1.8984	1.3511	3.6988
VII. Inj.	0.8628	0.9772	2.1163	1.4524	1.8859	1.3611	3.6962
VIII. Inj.	0.8925	0.9779	2.1259	1.4662	1.8807	1.3656	3.6924
IX .Inj.	0.8985	0.9796	2.1251	1.4792	1.9022	1.3514	3.6956
X Inj.	0.8678	0.9834	2.1253	1.4719	1.8886	1.3839	3.7118
XI. Inj.	0.8904	0.9863	2.1246	1.4751	1.9044	1.3856	3.7035
XII. Inj.	0.8886	0.9891	2.1280	1.4570	1.9117	1.3757	3.7139
AVERAGE	0.8796	0.9791	2.1197	1.4627	1.8947	1.3687	3.6929
S.D	0.0136	0.0048	0.0073	0.0109	0.0093	0.0135	0.0157
% R.S.D.	1.5456	0.4899	0.3423	0.7478	0.4933	0.9836	0.4246

2.8.3.2 Reproducibility Studies of Intraday

Three different concentrations of two parallel standards were injected three times to the instrument within the same day. Concentrations were calculated from earlier calibration graphs. SD and RSD values were extracted from these data. The expected RSD values within intraday should be less than 2 % according to the statements of international organizations like ISO 9000, EPA (Environmental Protection Agency), FDA (Federal Drug Administration) and 17025 and EN (European Norms) 45001.

For dilution ratio of 1:4, RSD values were excellent, however, for the dilution ratio of 1:6 and 1:8 the RSD values were found to be a little bit excess for fluoride and phosphate.

Table 2.19 reveals average, SD and RSD values of seven anions for 6 replicate measurements of two parallel samples measured within the same day.

Table 2.19 Average, SD and RSD values of 7 anions for six replicate measurements of two parallel samples measured within the same day.

1:4 dilution

N=6	Amount ppm Fluoride	Amount ppm Chloride	Amount ppm Nitrite	Amount ppm Bromide	Amount ppm Nitrate	Amount ppm Phosphate	Amount ppm Sulfate
Exp. Conc.	5.1662	8.7364	24.9687	25.3768	25.6988	38.1020	37.8160
	5.1980	8.6950	25.1679	25.4575	25.8112	38.1790	37.9238
	5.1667	8.7002	25.2345	25.5671	25.6904	38.2697	37.7540
	5.1676	8.6597	25.2545	25.6981	25.5926	38.6921	37.8929
	5.2051	8.6683	25.2961	25.6690	25.5328	38.4152	37.9256
	5.1379	8.7205	25.2668	25.7645	25.8321	38.7680	37.8336
Average	5.1736	8.6967	25.1981	25.5888	25.6930	38.4043	37.8577
S.D	0.0245	0.0294	0.1203	0.1496	0.1176	0.2740	0.0683
%R.S.D	0.4735	0.3385	0.4774	0.5846	0.4576	0.7136	0.1803
Teo.Conc.	5.0283	7.5549	24.8663	25.2666	25.5167	37.7748	37.5246

1:6 dilution

N=6	Amount ppm Fluoride	Amount ppm Chloride	Amount ppm Nitrite	Amount ppm Bromide	Amount ppm Nitrate	Amount ppm Phosphate	Amount ppm Sulfate
Exp. Conc.	3.7349	5.3518	17.5042	18.0535	18.2008	27.2572	26.6597
	3.7602	5.3671	17.6527	17.9898	18.2150	27.9067	26.5312
	3.7402	5.3677	17.6713	18.0680	18.4233	28.2939	26.8530
	3.6818	5.3484	17.6558	18.0119	18.1155	28.2788	26.7575
	3.6794	5.3653	17.7674	17.9789	18.1711	27.7846	26.7235
	3.5306	5.3558	17.7002	18.0746	18.3371	28.1202	26.6924
Average	3.6879	5.3594	17.6586	18.0294	18.2438	27.9402	26.7029
S.D	0.0837	0.0084	0.0867	0.0413	0.1143	0.3909	0.1071
%R.S.D	2.2695	0.1572	0.4912	0.2292	0.6266	1.3990	0.4012
Teo.Conc.	3.3575	5.0446	16.6038	16.8710	17.0381	25.2230	25.0560

1:8 dilution

N=6	Amount ppm Fluoride	Amount ppm Chloride	Amount ppm Nitrite	Amount ppm Bromide	Amount ppm Nitrate	Amount ppm Phosphate	Amount ppm Sulfate
Exp. Conc.	2.4962	3.9616	12.7169	13.1815	13.3062	20.8202	19.7703
	2.5114	3.9531	12.9041	13.2374	13.3026	21.2667	19.8330
	2.5265	3.9454	12.8010	13.2529	13.3240	19.7986	19.6529
	2.7548	3.9421	12.9719	13.2763	13.3590	20.3175	19.6164
	2.7473	3.9558	12.8133	13.2358	13.3613	20.9767	19.7725
	2.7680	3.9401	12.9892	13.3045	13.4041	20.3254	19.5685
Average	2.6340	3.9497	12.8661	13.2481	13.3429	20.5842	19.7023
S.D	0.1349	0.0085	0.1068	0.0417	0.0392	0.5349	0.1043
%R.S.D	5.1206	0.2145	0.8304	0.3149	0.2936	2.5988	0.5292
Teo.Conc.	2.4936	3.7466	12.3316	12.5301	12.6541	18.7331	18.6090

2.8.3.3 Reproducibility Studies between Months

Three different concentrations of two parallel standards were injected three times to the instrument at two different dates after a period of one month. Concentrations were calculated from earlier calibration graphs. SD and RSD values were extracted from these data. The expected RSD should be less than 2%.

Table 2.20 Average, SD and RSD values of seven anions for two sets of measurements of two parallel samples measured after a period of one month.

1:4 dilution

n = 12	Amount ppm Fluoride	Amount ppm Chloride	Amount ppm Nitrite	Amount ppm Bromide	Amount ppm Nitrate	Amount ppm Phosphate	Amount ppm Sulfate
Exp. Conc. (May)	5.1662	8.7364	24.9687	25.3768	25.6988	38.1020	37.8160
	5.1980	8.6950	25.1679	25.4575	25.8112	38.1790	37.9238
	5.1667	8.7002	25.2345	25.5671	25.6904	38.2697	37.7540
	5.1676	8.6597	25.2545	25.6981	25.5926	38.6921	37.8929
	5.2051	8.6683	25.2961	25.6690	25.5328	38.4152	37.9256
	5.1379	8.7205	25.2668	25.7645	25.8321	38.7680	37.8336
Exp. Conc. (June)	5.2721	7.7729	24.8450	26.1917	26.3405	39.8070	38.6930
	5.2132	7.7724	24.9534	26.0091	26.3086	39.9675	38.6733
	5.2558	7.7778	24.9474	26.0195	26.3439	39.1059	38.6491
	5.2305	7.7991	24.9462	26.1603	26.3749	39.8053	38.6369
	5.1851	7.8065	24.9389	26.1646	26.3477	39.7278	38.6527
	5.1930	7.7711	24.9967	26.2085	26.4063	39.9922	38.7189
Average	5.1993	8.2400	25.0680	25.8572	26.0233	39.0693	38.2642
S.D	0.0392	0.4775	0.1618	0.3038	0.3547	0.7512	0.4276
%R.S.D	0.7532	5.7952	0.6454	1.1748	1.3631	1.9228	1.1174

1:6 dilution

n = 12	Amount ppm Fluoride	Amount ppm Chloride	Amount ppm Nitrite	Amount ppm Bromide	Amount ppm Nitrate	Amount ppm Phosphate	Amount ppm Sulfate
Exp. Conc. (May)	3.7349	5.3518	17.5042	18.0535	18.2008	27.2572	26.6597
	3.7602	5.3671	17.6527	17.9898	18.2150	27.9067	26.5312
	3.7402	5.3677	17.6713	18.0680	18.4233	28.2939	26.8530
	3.6818	5.3484	17.6558	18.0119	18.1155	28.2788	26.7575
	3.6794	5.3653	17.7674	17.9789	18.1711	27.7846	26.7235
	3.5306	5.3558	17.7002	18.0746	18.3371	28.1202	26.6924
Exp. Conc. (June)	3.1094	4.9518	16.1227	16.9565	17.1198	25.9883	25.1963
	3.1054	4.9381	16.1867	17.0208	17.1481	25.9616	25.1082
	3.2794	4.9399	16.1358	16.9218	17.1798	25.9848	25.0448
	3.4139	4.9217	16.1444	17.1065	17.1352	26.1756	25.1731
	3.4394	4.9147	16.1323	16.9064	17.2733	26.3203	25.2193
	3.3857	4.9097	16.1998	17.0167	17.0786	26.2787	25.1722
Average	3.4884	5.1443	16.9061	17.5088	17.6998	27.0292	25.9276
S.D	0.2386	0.2249	0.7884	0.5469	0.5751	0.9933	0.8141
%R.S.D	6.8398	4.3722	4.6635	3.1234	3.2494	3.6748	3.1400

1:8 dilution

n = 12	Amount ppm Fluoride	Amount ppm Chloride	Amount ppm Nitrite	Amount ppm Bromide	Amount ppm Nitrate	Amount ppm Phosphate	Amount ppm Sulfate
Exp. Conc. (May)	2.4962	3.9616	12.7169	13.1815	13.3062	20.8202	19.7703
	2.5114	3.9531	12.9041	13.2374	13.3026	21.2667	19.8330
	2.5265	3.9454	12.8010	13.2529	13.3240	19.7986	19.6529
	2.7548	3.9421	12.9719	13.2763	13.3590	20.3175	19.6164
	2.7473	3.9558	12.8133	13.2358	13.3613	20.9767	19.7725
	2.7680	3.9401	12.9892	13.3045	13.4041	20.3254	19.5685
Exp. Conc. (June)	2.3126	3.7198	12.1741	12.8385	12.8991	19.8011	18.9601
	2.8079	3.7134	12.1675	12.7591	12.7866	19.4339	18.8541
	2.5214	3.7343	12.1713	12.9424	12.8084	19.6960	18.9050
	2.6540	3.7427	12.1258	12.8343	12.8238	19.8100	18.9139
	2.7154	3.7146	12.0839	12.7587	12.8556	19.6841	18.9447
	2.6529	3.6949	12.0814	12.8169	12.7775	19.6658	18.9800
Average	2.6224	3.8348	12.5000	13.0365	13.0840	20.1330	19.3143
S.D	0.1486	0.1206	0.3901	0.2273	0.2734	0.6005	0.4124
%R.S.D	5.6671	3.1461	3.1211	1.7439	2.0895	2.9825	2.1353

From Table 2.20 it can be concluded that the RSD values of groundwater samples measured two successive months were slightly deviated from the expected value; 2%; for dilution ratio of 1:4; except that of chloride, the RSD values of the anions were found to be within the expected values. The deviations were more pronounced for the dilution ratio of 1:6 and 1:8.

2.8.4 Analysis of Groundwater Samples of Pamukkale Location with Ion Chromatography

In this work, seven anions (Fluoride, Chloride, Nitride, Bromide, Nitrate, Phosphate, and Sulfate) in geothermal water samples, that were collected daily during eight months (June 2007- January 2008) from Denizli Pamukkale Antique Pool, were tested and analyzed with ion chromatographic method. Fluoride, chloride and sulfate were found to be major ions in Pamukkale geothermal water samples. Nitrite and Nitrate were under limit of detection (LOD) of the instrument. Bromide and Phosphate concentrations were found to be zero.

Table 2.21, 2.22 and 2.23 reveal retention time (min), peak area ($\mu\text{S}\cdot\text{min}$) and peak height (μS) values of fluoride, chloride and sulfate of geothermal water samples of Pamukkale Antique Pool, respectively.

For 26 consecutive measurements, the average value of fluoride concentration was found to be 1.4750 ppm. SD and RSD of the measurements were calculated as 0.1146 ppm and 7.7706 % respectively.

Average concentrations of chloride and sulfate were found to be 13.7169 ppm and 662.8689 ppm respectively. Sulfate measurements were performed after 1:4 dilution.

SD and RSD of chloride were 0.4373 ppm and 3.1881 % respectively. SD and RSD values of Sulfate were 6.8312 ppm and 1.0305 %. Among them, fluoride measurements resulted with the highest SD and RSD. In case of chloride and sulfate SD and RSD values were satisfactory (See Table 2.21, 2.22 and 2.23).

Table 2.21 Retention time (min), peak area ($\mu\text{S}\cdot\text{min}$) and peak height (μS) values for fluoride in geothermal water samples of Pamukkale Antique Pool, Denizli.

Sample Date	Ret. Time (min) Fluoride	Area ($\mu\text{S}\cdot\text{min}$) Fluoride	Height (μS) Fluoride	Amount (ppm) Fluoride
28.03.2008	3.817	0.3776	2.0193	1.4907
29.03.2008	3.817	0.3776	2.0196	1.4905
30.03.2008	3.820	0.4073	2.1255	1.6178
31.03.2008	3.824	0.4142	2.1877	1.6469
01.04.2008	3.824	0.4212	2.1925	1.6768
02.04.2008	3.820	0.3678	1.9933	1.4485
03.04.2008	3.817	0.3792	2.0443	1.4977
04.04.2008	3.824	0.4147	2.1966	1.6494
05.04.2008	3.820	0.3776	2.0281	1.4906
06.04.2008	3.817	0.3072	1.6535	1.1883
07.04.2008	3.820	0.3767	2.0152	1.4870
08.04.2008	3.820	0.3788	2.0222	1.4957
09.04.2008	3.820	0.3775	2.0130	1.4901
10.04.2008	3.817	0.3430	1.8424	1.3424
11.04.2008	3.820	0.3754	1.9913	1.4813
12.04.2008	3.820	0.3707	1.9821	1.4612
13.04.2008	3.820	0.3817	2.0141	1.5083
16.04.2008	3.817	0.3095	1.6488	1.1984
18.04.2008	3.820	0.3750	1.9871	1.4793
21.04.2008	3.820	0.3716	1.9684	1.4651
22.04.2008	3.820	0.3893	1.9756	1.5409
24.04.2008	3.820	0.3770	1.9814	1.4882
26.04.2008	3.820	0.3398	1.7903	1.3285
27.04.2008	3.823	0.3745	1.9591	1.4775
28.04.2008	3.827	0.3693	1.9503	1.4550
30.04.2008	3.817	0.3689	1.8980	1.4535
AVERAGE	3.8200	0.3740	1.9808	1.4750
S.D	0.0026	0.0267	0.1343	0.1146
%R.S.D	0.0681	7.1512	6.7807	7.7706

Table 2.22 Retention time (min), peak area ($\mu\text{S}\cdot\text{min}$) and peak height (μS) values for chloride in geothermal water samples of Pamukkale Antique Pool, Denizli.

Sample Date	Ret. Time (min) Chloride	Area ($\mu\text{S}\cdot\text{min}$) Chloride	Height (μS) Chloride	Amount (ppm) Chloride
28.03.2008	6.730	2.4767	16.3615	13.2245
29.03.2008	6.730	2.4841	16.2845	13.2606
30.03.2008	6.754	2.6186	17.1206	13.9114
31.03.2008	6.770	2.5665	16.7304	13.6599
01.04.2008	6.780	2.6058	16.8733	13.8495
02.04.2008	6.780	2.5003	16.1574	13.3395
03.04.2008	6.797	2.5901	16.6883	13.7737
04.04.2008	6.804	2.5812	16.5984	13.7307
05.04.2008	6.800	2.5239	16.1483	13.4538
06.04.2008	6.783	2.4527	15.6364	13.1079
07.04.2008	6.814	2.5052	16.0908	13.3631
08.04.2008	6.817	2.5512	16.2445	13.5861
09.04.2008	6.800	2.5686	16.4731	13.6703
10.04.2008	6.773	2.5332	16.3199	13.4988
11.04.2008	6.783	2.5306	16.3113	13.4861
12.04.2008	6.783	2.5689	16.5861	13.6714
13.04.2008	6.784	2.7664	17.9364	14.6198
16.04.2008	6.764	2.4955	16.1154	13.3158
18.04.2008	6.787	2.5970	16.5922	13.8070
21.04.2008	6.794	2.6655	17.1072	14.1369
22.04.2008	6.787	2.5528	16.2602	13.5938
24.04.2008	6.797	2.7692	17.8702	14.6332
26.04.2008	6.770	2.5456	16.4166	13.5588
27.04.2008	6.803	2.6000	16.6632	13.8215
28.04.2008	6.803	2.5690	16.4033	13.6719
30.04.2008	6.790	2.8239	16.7417	14.8938
AVERAGE	6.7837	2.5786	16.5666	13.7169
S.D	0.0217	0.0909	0.5096	0.4373
% R.S.D	0.3202	3.5245	3.0764	3.1881

Table 2.23 Retention time (min), peak area ($\mu\text{S}\cdot\text{min}$) and peak height (μS) values for Sulfate in geothermal water samples of Pamukkale Antique Pool, Denizli.

Sample Date	Ret. Time (min) Sulfate	Area ($\mu\text{S}\cdot\text{min}$) Sulfate	Height (μS) Sulfate	Amount (ppm) Sulfate
28.03.2008	19.184	27.1966	55.4924	664.6229
29.03.2008	19.180	27.3298	55.9092	667.2713
30.03.2008	19.183	27.4250	56.0175	669.1629
31.03.2008	19.177	27.1307	55.5960	663.3124
01.04.2008	19.180	26.8444	55.0579	657.6013
02.04.2008	19.177	26.8015	54.8688	656.7456
03.04.2008	19.184	26.9283	55.1906	659.2780
04.04.2008	18.770	27.3537	57.1736	667.7464
05.04.2008	18.774	27.2041	57.1105	664.7724
06.04.2008	18.774	27.3795	57.4263	668.2587
07.04.2008	18.780	26.7803	56.2762	656.3209
08.04.2008	18.774	27.0167	56.7713	661.0401
09.04.2008	18.777	27.3939	57.4950	668.5450
10.04.2008	18.770	27.3738	57.5101	668.1454
11.04.2008	18.774	27.0875	56.9294	662.4519
12.04.2008	18.777	26.6343	55.9419	653.4005
13.04.2008	18.764	27.5732	57.8287	672.1026
16.04.2008	18.763	27.4806	57.6252	670.2667
18.04.2008	18.760	26.4730	55.6946	650.1679
21.04.2008	18.764	26.4726	55.5934	650.1589
22.04.2008	18.764	26.8215	56.2949	657.1452
24.04.2008	18.767	26.9835	56.6088	660.3787
26.04.2008	18.764	26.7793	56.2585	656.3001
27.04.2008	18.760	27.2748	57.2654	666.1799
28.04.2008	18.764	27.2612	57.0078	665.9085
30.04.2008	18.760	27.8363	57.8724	677.3078
AVERAGE	18.8794	27.1091	56.4929	662.8689
S.D	0.1866	0.3429	0.9061	6.8312
% R.S.D	0.9883	1.2649	1.6039	1.0305

Fluoride, chloride and sulfate concentrations were monitored during 8 months. Table 2.24 shows the gathered measurement results of SD and RSD on bases of months from June 2007 to January 2008. The statistical evaluation was performed by employing all of the acquired data. The questionable values did not sorted out employing either Q or T_n tests.

Except that of value of July 2007 and January 2008, fluoride measurements exhibited parallel RSD results. Fluctuations observed in July 2007 and January 2008 can be attributed to the fluoride ion content of the groundwater of Pamukkale, which is quite low and is around or below the bottom of the detection range of the instrument.

SD and RSD values of chloride and sulfate are in acceptable range for 220 data acquired during 8 months.

Table 2.25 reveals gathered measurements results of 8 months of averages SD and RSD values of F^- , Cl^- and SO_4^{2-} .

Table 2.24 Concentrations in ppm, SD (ppm) and RSD% values of F⁻, Cl⁻ and SO₄²⁻ on bases of month from June 2007 to January 2008

		F ⁻				Cl ⁻				SO ₄ ²⁻			
		Ret. Time min	Area μS*min	Height μS	Amount ppm	Ret. Time min	Area μS*min	Height μS	Amount ppm	Ret. Time min	Area μS*min	Height μS	Amount ppm
June 07	AVE.	3.7526	0.4137	2.0573	1.6934	6.2149	2.3480	9.9278	13.3563	17.1123	26.8384	44.5999	709.2889
	S.D	0.0018	0.0468	0.1023	0.2093	0.0136	0.1022	0.1937	0.5484	0.0480	0.5979	1.7921	13.3949
	% R.S.D	0.0490	11.3211	4.9745	12.3612	0.2183	4.3518	1.9509	4.1057	0.2802	2.2279	4.0181	1.8885
July 07	AVE.	3.7524	0.4079	1.8843	1.6659	6.2104	2.1709	9.0567	12.2291	16.7507	26.2316	46.4857	688.6910
	S.D	0.0110	0.0921	0.2525	0.4071	0.0748	0.1362	0.7941	0.8564	0.4210	1.7453	1.2992	47.1355
	% R.S.D	0.2927	22.5822	13.3999	24.4397	1.2051	6.2721	8.7684	7.0031	2.5134	6.6533	2.7948	6.8442
August 07	AVE.	3.7758	0.3473	1.6946	1.3323	6.2009	2.0193	8.0375	11.0334	16.1363	24.4221	45.9277	638.0955
	S.D	0.0417	0.0076	0.0715	0.1000	0.0377	0.1529	0.3073	0.6832	0.2590	1.0863	2.3975	23.4764
	% R.S.D	1.1041	2.1904	4.2180	7.5023	0.6087	7.5716	3.8239	6.1918	1.6048	4.4482	5.2201	3.6791

		F ⁻				Cl ⁻				SO ₄ ²⁻			
		Ret. Time min	Area μS*min	Height μS	Amount ppm	Ret. Time min	Area μS*min	Height μS	Amount ppm	Ret. Time min	Area μS*min	Height μS	Amount ppm
Sept. 07	AVE.	3.7349	0.3285	1.4578	1.2672	6.0832	2.0401	7.7865	11.6263	15.2647	25.0888	46.5652	661.7266
	S.D	0.1513	0.0328	0.1708	0.1655	0.2758	0.0757	0.2915	1.4530	0.6617	1.0277	2.2536	33.3234
	% R.S.D	4.0517	9.9887	11.7184	13.0575	4.5333	3.7096	3.7434	12.4977	4.3349	4.0964	4.8397	5.0358
Oct. 07	AVE.	3.5171	0.3059	1.2459	1.4659	5.7215	2.1091	7.9756	13.6292	13.8164	25.2024	45.0374	686.9971
	S.D	0.0049	0.0353	0.1057	0.1699	0.0245	0.1129	0.1766	0.6400	0.4350	0.4385	0.7952	9.3512
	% R.S.D	0.1389	11.5518	8.4871	11.5899	0.4279	5.3524	2.2143	4.6954	3.1488	1.7399	1.7657	1.3612
Nov. 07	AVE.	3.5254	0.4450	1.6631	2.1303	5.8684	2.1413	7.3218	13.9072	14.6932	24.1707	38.1360	668.2975
	S.D	0.0178	0.0562	0.1664	0.2653	0.0596	0.1030	0.2947	0.7865	0.3560	1.0732	2.0883	33.1500
	% R.S.D	0.5053	12.6211	10.0060	12.4551	1.0152	4.8081	4.0250	5.6553	2.4232	4.4400	5.4760	4.9604
Dec. 07	AVE.	3.6124	0.4396	1.5735	2.0696	6.1415	2.0978	7.6152	15.4163	16.7499	26.0155	38.8582	784.0046
	S.D	0.0059	0.0536	0.1218	0.3346	0.0263	0.0828	0.4455	1.9377	1.3458	1.3652	6.5922	58.3482
	% R.S.D	0.1647	12.1982	7.7375	16.1655	0.4282	3.9475	5.8499	12.5689	8.0349	5.2474	16.9647	7.4423
Jan. 08	AVE.	3.6060	0.4115	1.2081	1.3371	6.16312	2.21299	7.6962	10.8164	20.2895	28.6744	54.7876	641.2816
	S.D	0.0624	0.1380	0.3235	0.5190	0.25964	0.17272	3.5048	0.8806	0.3490	0.8710	2.5972	18.1374
	% R.S.D	1.7293	33.5289	26.7771	38.8176	4.2128	7.8046	45.5391	8.1411	1.7202	3.0377	4.7405	2.8283

Table 2.25 Gathered measurements results of 8 months of averages SD and RSD values of F⁻, Cl⁻ and SO₄²⁻.

DATE	F ⁻				Cl ⁻				SO ₄ ²⁻			
	Ret. Time min	Area μS*min	Height μS	Amount ppm	Ret. Time min	Area μS*min	Height μS	Amount ppm	Ret. Time min	Area μS*min	Height μS	Amount ppm
June 07	3.7526	0.4137	2.0573	1.6934	6.2149	2.3480	9.9278	13.3563	17.1123	26.8384	44.5999	709.2889
July 07	3.7524	0.4079	1.8843	1.6659	6.2104	2.1709	9.0567	12.2291	16.7507	26.2316	46.4857	688.6910
Agust07	3.7758	0.3473	1.6946	1.3323	6.2009	2.0193	8.0375	11.0334	16.1363	24.4221	45.9277	638.0955
Sept. 07	3.7349	0.3285	1.4578	1.2672	6.0832	2.0401	7.7865	11.6263	15.2647	25.0888	46.5652	661.7266
Oct. 07	3.5171	0.3059	1.2459	1.4659	5.7215	2.1091	7.9756	13.6292	13.8164	25.2024	45.0374	686.9971
Nov.07	3.5254	0.4450	1.6631	2.1303	5.8684	2.1413	7.3218	13.9072	14.6932	24.1707	38.1360	668.2975
Dec. 07	3.6124	0.4396	1.5735	2.0696	6.1415	2.0978	7.6152	15.4163	16.7499	26.0155	38.8582	784.0046
Jan. 08	3.6060	0.4115	1.2081	1.3371	6.1631	2.2130	7.6962	10.8164	20.2895	28.6744	54.7876	641.2816
AVE.	3.6596	0.3874	1.5981	1.6202	6.0755	2.1424	8.1772	12.7518	16.3516	25.8305	45.0497	684.7979
S.D.	0.1068	0.0527	0.2934	0.3340	0.1827	0.1047	0.8726	1.5950	1.9570	1.4630	5.1588	46.8144
% R.S.D	2.9187	13.6020	18.3613	20.6173	3.0072	4.8886	10.6709	12.5082	11.9683	5.6637	11.4514	6.8362

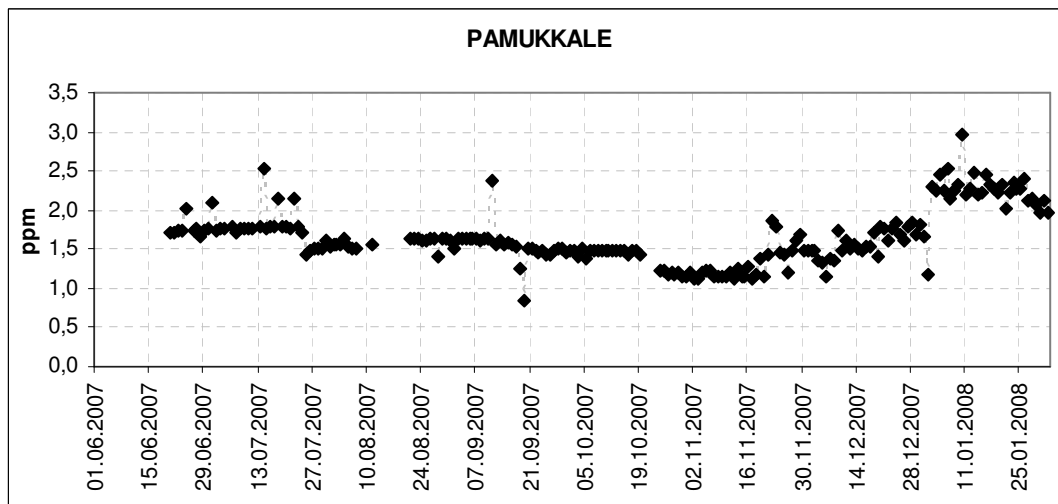


Figure 2.22 Variation of fluoride concentration of groundwater samples of Pamukkale Antique Pool from June 2007 to January 2008

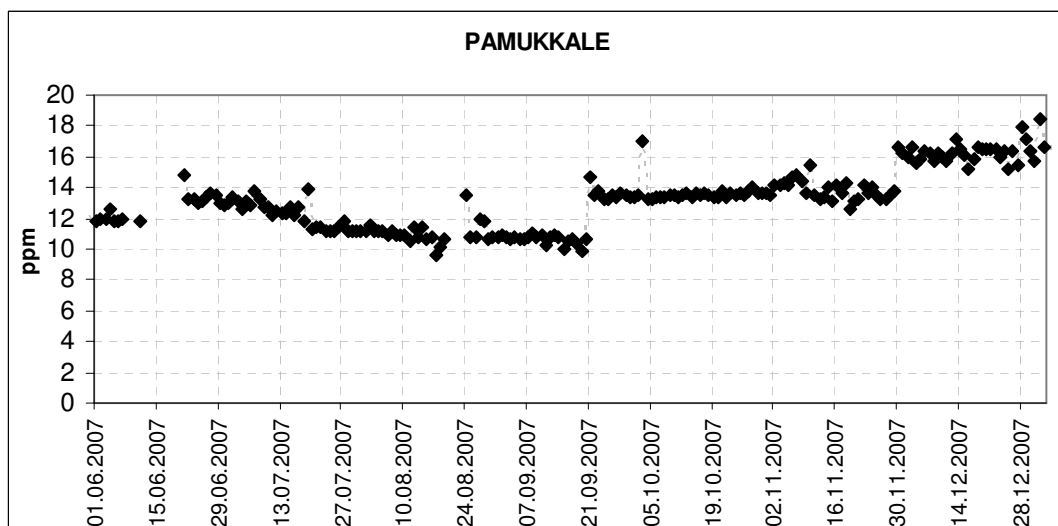


Figure 2.23 Variation of chloride concentration of groundwater samples of Pamukkale Antique Pool from June 2007 to January 2008

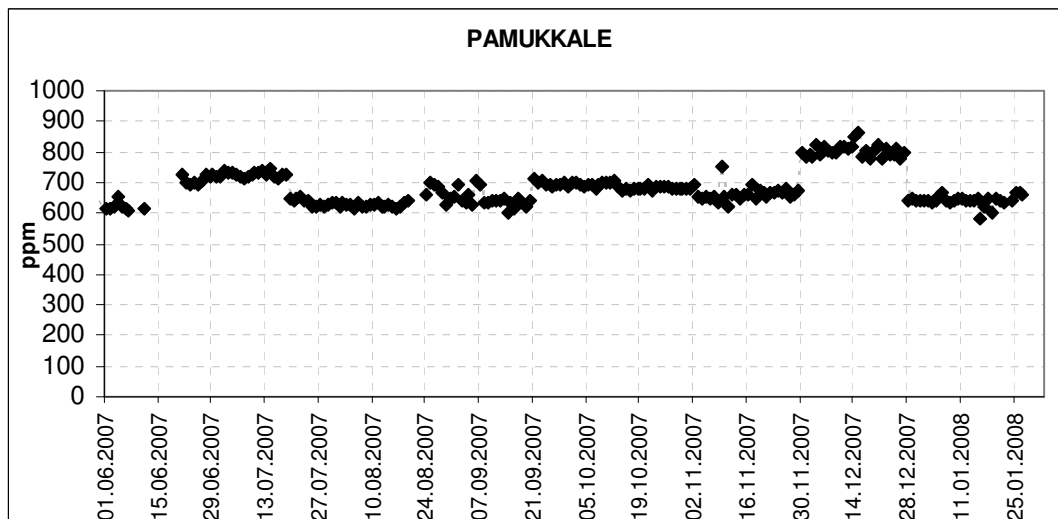


Figure 2.24 Variation of Sulfate concentration of groundwater samples of Pamukkale Antique Pool from June 2007 to January 2008.

Figure 2.22, 2.23 and 2.24 reveal gathered anion concentration measurement results of 8 months of averages on bases of days. The fluctuations observed in the above mentioned figures can be attributed to the seasonal changes of the ion concentrations. It also should be noted that the deviated values were kept among the recorded values.

CHAPTER THREE

INTRODUCTION

In this part, absorption and emission based tests of groundwater samples were performed employing UV-Visible Spectroscopy and Fluorescence Spectroscopy techniques for bicarbonate (HCO_3^-) analysis together with the classical titrimetric method.

For this purpose, three different molecular pH probes N, N'-bis (4-dimethylaminobenzylidene) benzene-1, 4-diamine (Y-10), 4-[4-(dimethylamino) phenylmethylene] amino acetophenone (Y-11) and 4-(4-(dimethylamino) phenyl)methyleneamino benzonitrile (Y-13) were employed for measurement of low concentrations of HCO_3^- . Absorption based spectral data, photostability and acidity constant (pK_a) of the pH probes were determined in ionic liquid media, PVC and/or in conventional solvents. Solutions of NaHCO_3 were used as standards. The working range for the detection of HCO_3^- was between 4×10^{-5} – 4×10^{-1} mol l^{-1} . Performances of the probes were also tested for real - groundwater samples.

3.1 UV-Vis spectrophotometric Method

Ultraviolet and visible spectrometers have been in general use for the last 35 years and over this period have become the most important analytical instrument in the modern day laboratory. In many applications, other techniques could be employed but UV-Visible spectrometry has been the most intensively used one due to its simplicity, versatility, speed, accuracy and cost-effectiveness (taken from <http://www.molecularinfo.com/MTM/UV.pdf>).

3.2 Basic Principles of UV-Vis Spectrophotometric Method

3.2.1 The electromagnetic spectrum

Ultraviolet (UV) and visible radiation comprise only a small part of the electromagnetic spectrum, which includes such other forms of radiation as radio, infrared (IR), cosmic, and X rays (Owen, 2000).

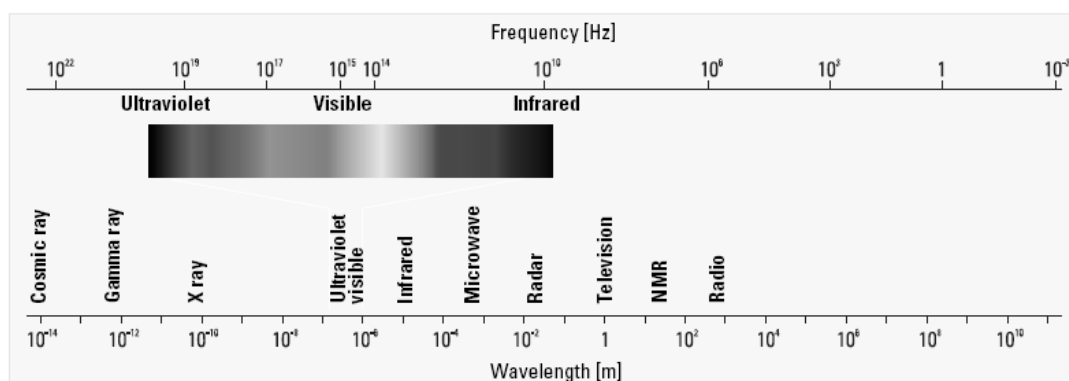


Figure 3.1 The electromagnetic spectrum (taken from https://www.ucursos.cl/medicina/2007/2/TM1BIOQ22/1/material_docente/objeto/144797%20-)

The energy associated with electromagnetic radiation is defined by the following equation:

$$E = h \nu \quad (3.1)$$

where E is energy (in joules), h is Planck's constant (6.62×10^{-34} Js), and ν is frequency (in seconds) (Owen, 2000).

3.2.2 Wavelength and Frequency

Electromagnetic radiation can be considered a combination of alternating electric and magnetic fields that travel through space with a wave motion. Because radiation acts as a wave, it can be classified in terms of either wavelength or frequency, which is related by the following equation:

$$\nu = c / \lambda \quad (3.2)$$

where ν is frequency (in seconds), c is the speed of light ($3 \times 10^8 \text{ ms}^{-1}$), and λ is wavelength (in meters) (Owen, 2000).

In UV-visible spectroscopy, wavelength usually is expressed in nanometers ($1 \text{ nm} = 10^{-9} \text{ m}$). It follows from the above equations that radiation with shorter wavelength has higher energy. In UV visible spectroscopy, the low-wavelength UV light has the highest energy (Owen, 2000).

3.2.3 Transmittance and Absorbance

When light passes through or is reflected from a sample, the amount of light absorbed is the difference between the incident radiation (I_0) and the transmitted radiation (I). The amount of light absorbed is expressed as either transmittance or absorbance. Transmittance usually is given in terms of a fraction of 1 or as a percentage and is defined as follows

$$T = I / I_0 \quad \text{or} \quad \%T = (I / I_0) \times 100 \quad (3.3)$$

Absorbance is defined as follows:

$$A = -\log T \quad (3.4)$$

For most applications, absorbance values are used since the relationship between absorbance and both concentration and path length normally is linear (Owen, 2000).

3.2.4 Theory of UV-visible Spectra

When radiation interacts with matter, a number of processes can occur, including reflection, scattering, absorbance, fluorescence/phosphorescence (absorption and reemission), and photochemical reaction (absorbance and bond breaking). In general, when measuring UV-visible spectra, we want only absorbance to occur (Owen, 2000).

Because light is a form of energy, absorption of light by matter causes the energy content of the molecules (or atoms) to increase. The total potential energy of a molecule generally is represented as the sum of its electronic, vibrational, and rotational energies:

$$E_{\text{total}} = E_{\text{electronic}} + E_{\text{vibrational}} + E_{\text{rotational}}$$

The amount of energy a molecule possesses in each form is not a continuum but a series of discrete levels or states. The differences in energy among the different states are in the order:

$$E_{\text{electronic}} > E_{\text{vibrational}} > E_{\text{rotational}}$$

In some molecules and atoms, photons of UV and visible light have enough energy to cause transitions between the different electronic energy levels. The wavelength of light absorbed is that having the energy required to move an electron from a lower energy level to a higher energy level (Owen, 2000).

.

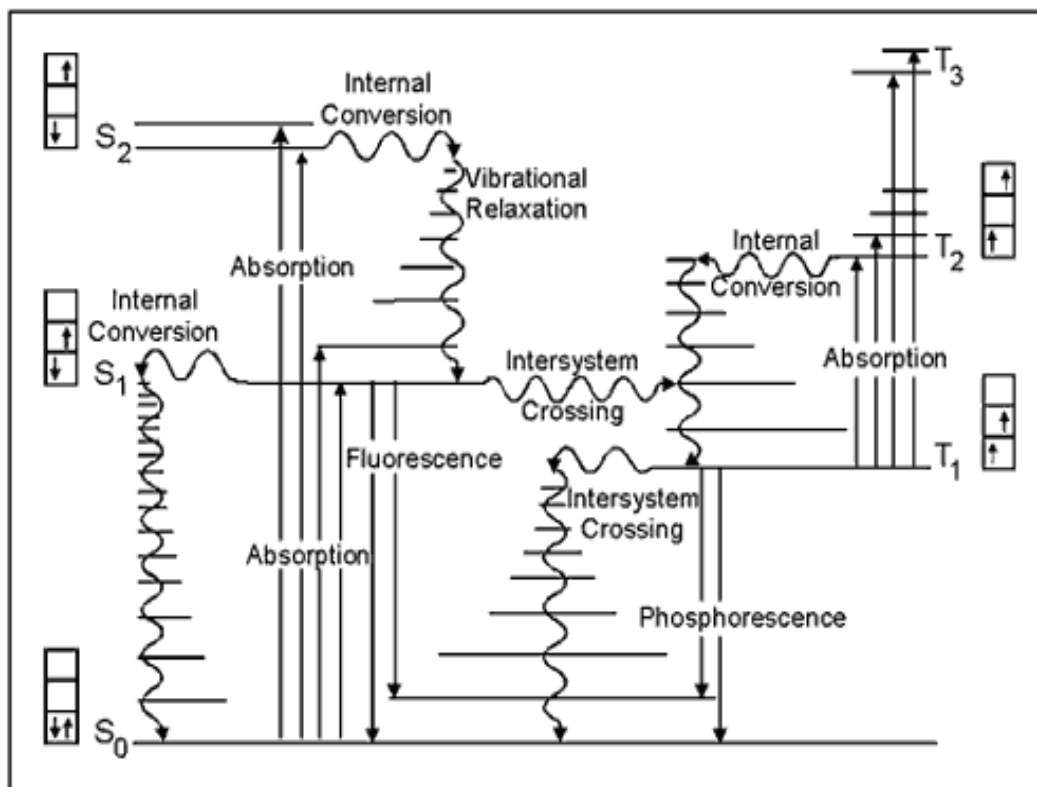


Figure 3.2 Electronic transitions and UV-visible spectra in molecules (taken from <http://www.photobiology.info/graphics/photochem13.gif>)

3.2.5 Luminescence

3.2.5.1 Mechanism of Luminescence (Lakowicz, 1993; Parker, 1968; Schmidt, 1994)

Luminescence means emission of light by electronically excited atoms or molecules. Electronic excitation requires the supply of energy. Various kinds of luminescence, such as electroluminescence, chemiluminescence, thermoluminescence and photoluminescence, are known and called by the source from which energy is derived. In the case of photoluminescence (fluorescence and phosphorescence), the energy is provided by the absorption of infrared, visible or ultra-violet light.

According to the Boltzmann distribution, at room temperature the valance electrons are in the lowest vibration level ($v=0$) of the ground electronic state. A

transition of these electrons from the ground state (level 0 of S_0) to higher energy levels takes place on absorption (a) of light. The Franck-Condon principle states that there is approximately no change in nuclear position and spin orientation, because absorption of light occurs in about 10^{-15} s. Therefore, the electronic transition is represented by a vertical line.

Molecules excited to an upper vibrational level of any excited state rapidly lose their excess of vibrational energy by collision with solvent molecules, and falls to the lowest vibrational level. Molecules in the upper excited states (S_2 , S_3 ,...) relax by internal conversion (IC), radiation less to the lowest excited singlet state (S_1) within 10^{-12} s. Transition from this level to the vibration levels of the ground state can take place by emitting photons (f). A portion of the excited molecules may return to the ground state by other mechanisms, such as electron transfer, collision, intersystem crossing (ICS), internal conversion or chemical reaction.

Fluorescence emission occurs spontaneously, again in accordance with the Franck-Condon principle, if the radiation less transition lifetime is sufficiently long. The radiative lifetime of fluorescence lies between 10^{-9} s for spin allowed transitions ($\pi \rightarrow \pi$) to 10^{-6} for less probable transitions ($\pi \rightarrow n$). Molecules in the lowest excited state (S_1) can also undergo conversion to the first triplet state (T_1) by intersystem crossing (ISC).

This process requires a time of the same order of magnitude as fluorescence radiation lifetime and therefore competes with fluorescence. Although radiative transitions between states of different multiplicity are spin forbidden, these transitions do take place with low probability compared with singlet-singlet, or triplet-triplet transitions. Emission from the first triplet state (T_1) to the ground state is termed phosphorescence, and usually shifted to higher wavelengths than fluorescence. The radiation lifetime for this transition is about 10^{-2} to 10^{+2} s.

3.2.6. Experimental Method and Instrumentation

3.2.6.1 Reagents

All solvents used in this thesis were of analytical grade and purchased from Merck, Johnson and Mathey, Acros, Fluka and Riedel. Solvents for the spectroscopic studies were used without further purification. The ionic liquids were obtained from Merck and Fluka. Tetrabutylammonium hydroxide for titration (in nonaqueous medium) was standard 0.1 M solution in isopropanol/methanol (0.1 N) from Fluka. The solution was concentrated to 1 M with vacuum evaporator before use for the titrations in ethanol (EtOH). The sodium bicarbonate in powder form was puriss from Riedel (99-100 %).

The polymer polyvinyl chloride (PVC) was high molecular weight and obtained from Fluka. The plasticiser, dioctyl phtalate (DOP) was 99 % from Aldrich. The additive potassium tetrakis (4-chlorophenyl) borate was selectophore, 98 % from Fluka. The pH and dissolved CO₂ sensitive dyes; N, N'-bis(4 dimethylaminobenzylidene) benzene (Y-10) 1, 4 -diamine, 4-[4-(dimethylamino) phenylmethylene] amino acetophenone (Y-11) and 4-(4-(dimethylamino)phenyl)methyleneamino benzonitrile (Y-13) were obtained from associated Prof. Dr. Yavuz ERGÜN and were synthesized in our laboratories. Chemical structures of the employed indicator dyes were shown in Figure 3.3.

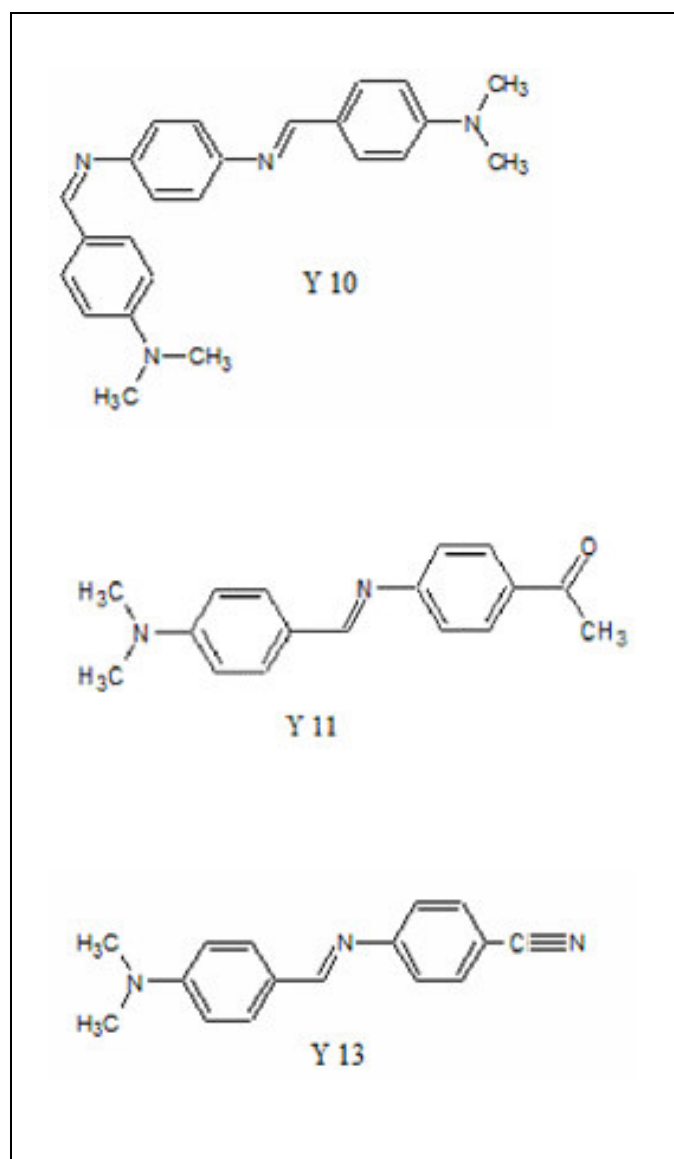


Figure 3.3 Chemical structures of the employed indicator dyes

The standard metal solutions were prepared from their 0.1 M stock solutions by using the metal salts of $\text{Cu}(\text{NO}_3)_2$, $\text{Co}(\text{NO}_3)_2$, $\text{NiCl}_2 \cdot 6\text{H}_2\text{O}$, $\text{Pb}(\text{NO}_3)_2$, $\text{Hg}_2(\text{NO}_3)_2$, $\text{Hg}(\text{NO}_3)_2$, CrCl_3 , CdCl_2 , $\text{Fe}(\text{NO}_3)_3$, ammonium-iron(II) sulphate.hexahydrate, $\text{Al}(\text{SO}_4)_3 \cdot 16\text{H}_2\text{O}$.

In the HCO_3^- sensing studies standard solutions were prepared freshly from 1 mol L^{-1} NaHCO_3 stock solution before the measurements

Absorption spectra were recorded using a Shimadzu 1601 UV-Visible spectrophotometer. Steady state fluorescence emission and excitation spectra were measured using Varian Cary Eclipse Spectrofluorometer with a xenon flash lamp as the light source.

3.2.6.2 Preparation of the Buffer Solutions

Deionised water, generated by a Milli-Q deionised water unit, which had a resistance better than $18.2 \text{ M}\Omega\text{cm}$, was used for the preparation of all the solutions.

Preparation of 0.005 M acetic acid / acetate buffer

0.1 gr acetic acid (%35) and 0.26 gr sodium acetate were dissolved in 950 mL ultra pure water. The solution was titrated to pH 5.0 at the lab temperature of 20°C either with 0.1 M HNO_3 or 0.1 M NaOH as needed. The resulting solution was made up to 1000 ml with ultra pure water in a volumetric flask. The buffer solutions in the range of pH 3.0-7.0 were prepared by the same way by adjusting to the desired pH.

Preparation of 0.005/0.01 M NaH_2PO_4 / Na_2HPO_4 buffer

0.36 gr NaH_2PO_4 and 0.57 gr Na_2HPO_4 were dissolved in 950 mL ultra pure water. The solution was titrated to pH 7.0 at the lab temperature of 20°C either with 0.1 M HNO_3 or 0.1 M NaOH as needed. The resulting solution was made up to 1000 ml with ultra pure water in a volumetric flask. The buffer solutions in the range of pH 7.0-9.0 were prepared by the same way by adjusting to the desired pH.

3.2.6.3 Construction of the Sensing Films

Depending on the analyte type the sensing cocktails were prepared either with PVC, or in ionic liquid media.

PVC cocktail preparation (Seiler, & Simon, 1992; Bakker, & Simon, 1992; Lerchi, Bakker, Rusterholz, & Simon, 1992)

The membranes were prepared to contain the dye, 33 % PVC (High molecular weight), 66 % plasticizer (Diethyl phthalate, DOP) by weight and the additive potassium tetrakis-(4-chlorophenyl) borate (PTCPB). The chemical structures of PVC, DOP and PTCPB were shown in Figure 3.5. The mixture was dissolved in the solvent of tetrahydrofuran (THF) and mixed by several hours by the help of a magnetic stirrer.

The resulting cocktail was spread on a 125 μm polyester support (Mylar from Du Pont) and dried in a desiccator, which was saturated with the solvent vapour. The polyester support was optically fully transparent, ion impermeable and exhibited good adhesion to PVC. The most important function of the polyester was to act as a mechanical support because the thin silicon films were impossible to handle. Once dried, the film was insoluble in water and could be cut into pieces of appropriate size. The approximate thickness of the film was 5 μm . Film thicknesses were measured using Tencor Alpha Step 500 Profilometer. The films were kept in a desiccator in the dark. This way, the photostability of the membrane was ensured and the damage from the ambient air of the laboratory was avoided. For absorbance and steady state fluorescence measurements each sensing film was cut to 1.2 cm width and 2.5 cm length and fixed diagonally into the sample cuvette (Figure 3.4) and the absorption or emission spectra were recorded. For fiber optical and flow system measurements, each sensing film was cut to 1 cm width and 1 cm length and fixed into the flow cell shown in Figure 3.4.

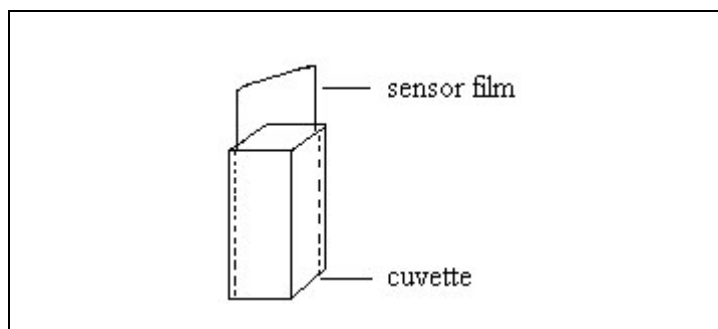


Figure 3.4 The placement of the sensor film in the sample cuvette.

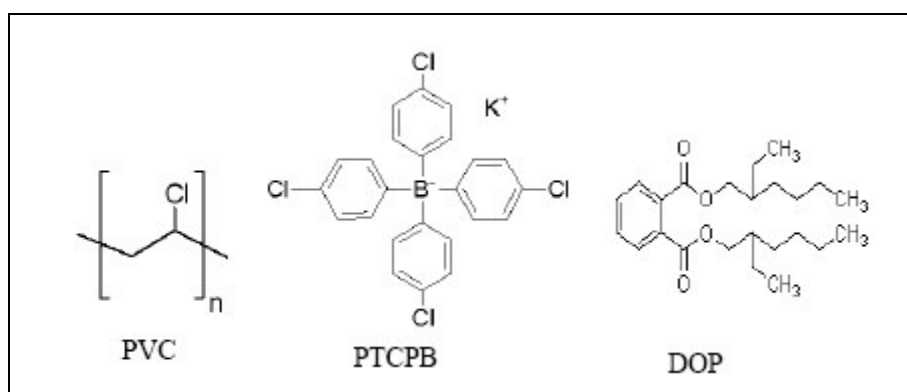


Figure 3.5 Structures of PVC, PTCPB and DOP

3.2.6.4. Preparation of Ionic Liquid Media

In this study, a new and very stable matrix material; water-miscible room temperature ionic liquid (RTIL) was employed. The indicator dyes Y 10, Y 11 and Y 13 have also been studied in RTIL.

3.3 Absorption Based Spectral Characterization of the Employed Indicator Dyes

For spectral characterization, three different indicator dyes N,N'-bis(4-dimethylaminobenzylidene)benzene-1,4-diamine (Y-10), 4-[4-(dimethylamino)phenylmethylene] amino acetophenone (Y-11) and 4-(4-(dimethylamino)phenyl)methyleneamino benzonitrile (Y-13) were studied in the different solvents of ethanol (EtOH), dichloromethane (DCM), tetrahydrofurane (THF) and Toluene/Ethanol (To: EtOH) mixture (80:20)), in solid matrix of PVC and in Ionic Liquid media. Maximum absorption wavelength (λ_{abs}) and molar extinction coefficients (ϵ) of the indicators were determined with Uv-Vis spectrophotometer in all of the employed matrices.

Table 3.1 reveals UV/Vis spectra related data of Y 10, Y 11 and Y 13 in the solvents of EtOH, DCM, THF and Toluene/Ethanol mixture (80:20), in solid matrix of PVC and Ionic Liquid media.

Table 3.1: UV/Vis spectra related data of Y 10, Y 11 and Y 13 in the solvents of EtOH, DCM, THF and Toluene/Ethanol mixture (80:20), in solid matrix of PVC and Ionic Liquid media (Y 10 1×10^{-5} M; Y 11 1×10^{-5} M; Y 13 1×10^{-5} M)

Compound	Solvent/Matrix	n (refractive index)	λ^1_{abs}	λ^2_{abs}	ϵ_{max} (λ^1_{abs})	ϵ_{max} (λ^2_{abs})
Y10	EtOH	1.3590	390	--	24700	--
Y10	DCM	1.4241	391	--	35000	--
Y10	THF	1.4070	390	--	29000	--
Y10	To: EtOH	1.4694	392	--	56100	--
Y10	PVC	1.5200	500	390	49067	--
Y10	IL	--	495	--	71058	--
Y11	EtOH	1.3590	379	--	45100	--
Y11	DCM	1.4241	377	--	46700	--
Y11	THF	1.4070	373	--	41000	--
Y11	To: EtOH	1.4694	379	--	51600	--
Y11	PVC	1.5200	460	375	137444	--
Y11	IL	--	470	--	85561	--
Y13	EtOH	1.3590	376	--	36000	--
Y13	DCM	1.4241	375	--	46000	--
Y13	THF	1.4070	372	--	42800	--
Y13	To: EtOH	1.4694	376	--	31200	--
Y13	PVC	1.5200	470	375	99337	--
Y13	IL	--	460	--	68000	--

Figure 3.7, 3.8 and 3.9 show UV-Vis spectra of the studied indicator dyes (Y 10, Y 11 and Y 13) in four different solvents (EtOH, DCM, THF and Toluene/Ethanol mixture (80:20)).

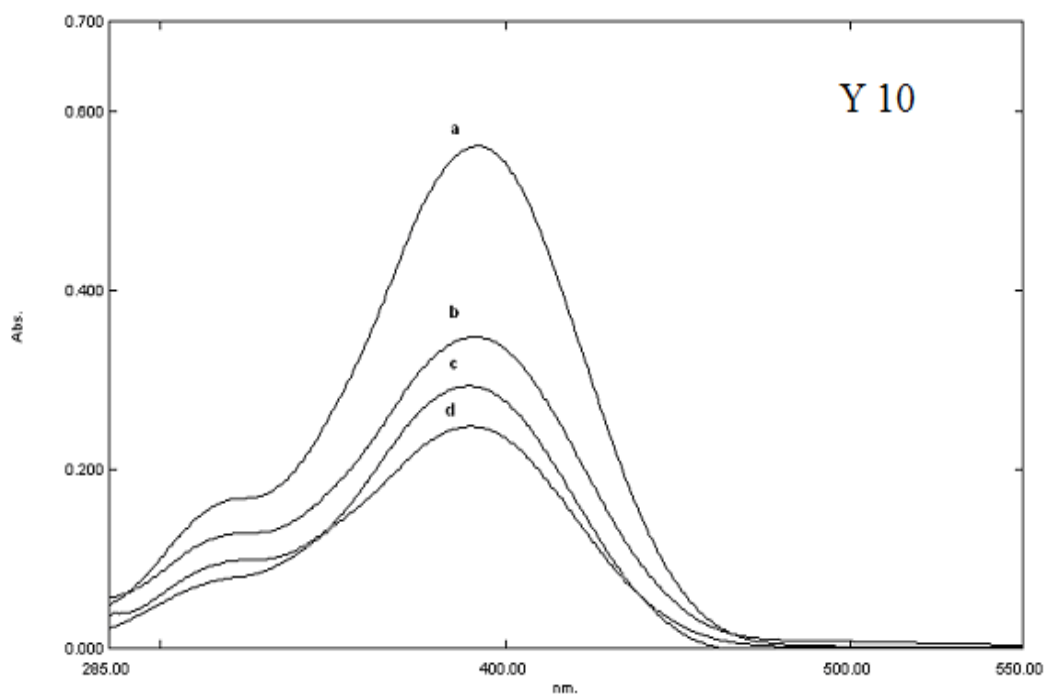


Figure 3.7 UV/Vis spectra of Y 10 in the solvents of EtOH, DCM, THF and Toluene/Ethanol mixture (80:20) (a) To: EtOH (b) DCM (c) THF (d) EtOH

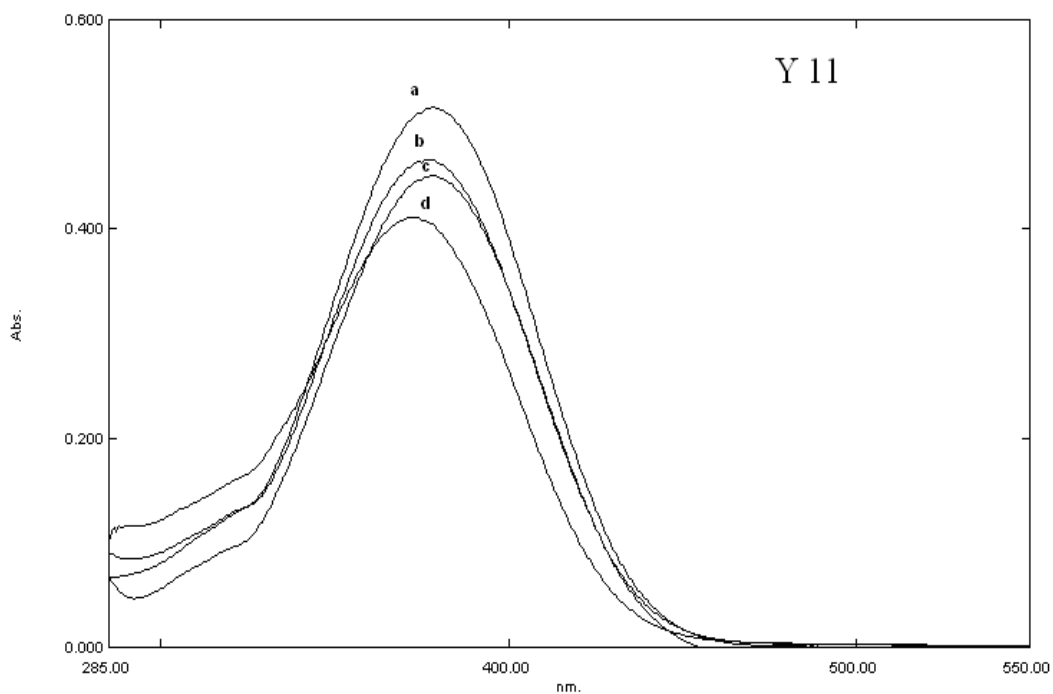


Figure 3.8 UV/Vis spectra of Y 11 in the solvents of EtOH, DCM, THF and Toluene/Ethanol mixture (80:20) (a) To: EtOH (b) DCM (c) EtOH (d) THF

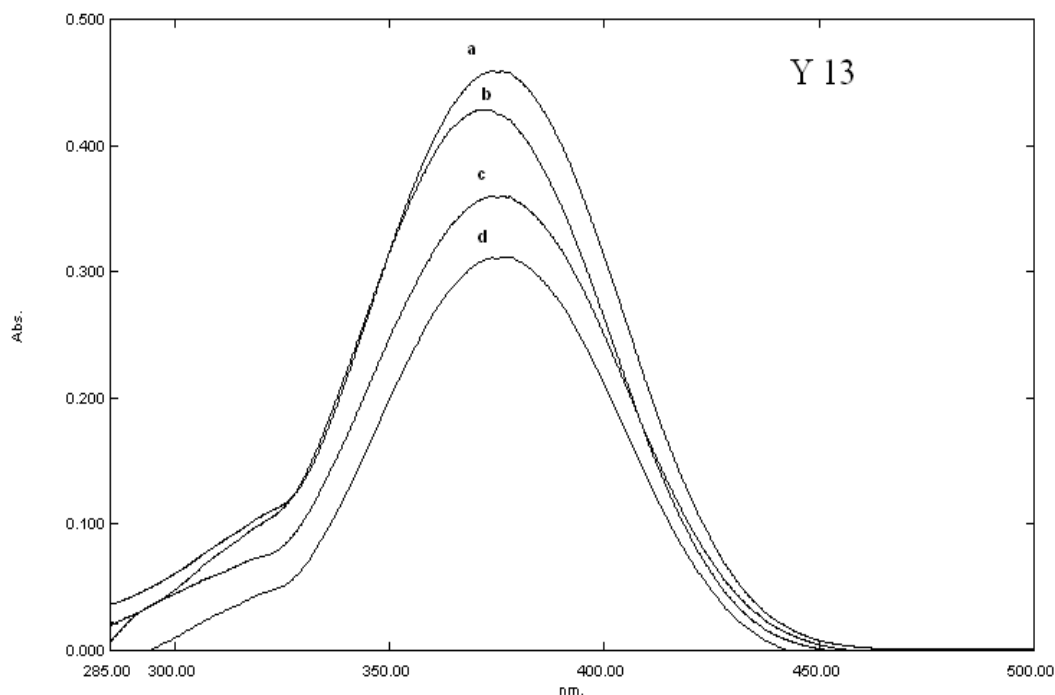


Figure 3.9 UV/Vis spectra of Y 13 in the solvents of EtOH, DCM, THF and Toluene/Ethanol mixture (80:20) (a) DCM (b) THF (c) EtOH (d) To: EtOH

3.3.1 *pKa* Calculations of Y 10, Y 11 and Y 13 in the Solvent of EtOH

The knowledge of dissociation constant (pK_a) of the employed indicator dyes (Y 10, Y 11 and Y 13) is of fundamental importance in order to provide information on chemical reactivity range of them. Therefore, to evaluate the availability of Y 10, Y 11 and Y 13 for HCO_3^- sensing purposes, the acidity constants were determined. Indicators with pK_a values between 6.8 and 10.0 are essential for sensitive determinations of HCO_3^- . For this purpose, the pK_a values of Y 10, Y 11 and Y 13 were determined in EtOH and PVC.

pH induced absorption characteristics of Y 10, Y 11 and Y 13 were monitored after addition of 1 M TBAOH solution in EtOH.

Y 10, Y 11 and Y 13 exhibited a pH dependent response between pH 6.0–10.0, pH 7.0–10.0, and pH 5.5–9.5 in the direction of a signal increase respectively. The signal intensities of Y 10, Y 11 and Y 13 were monitored at 390 nm, 379 nm and 376 nm from absorption spectrum, respectively.

Figure 3.10, 3.11 and 3.12 reveal pH dependent UV-Vis spectra of Y 10, Y 11 and Y 13 in EtOH respectively.

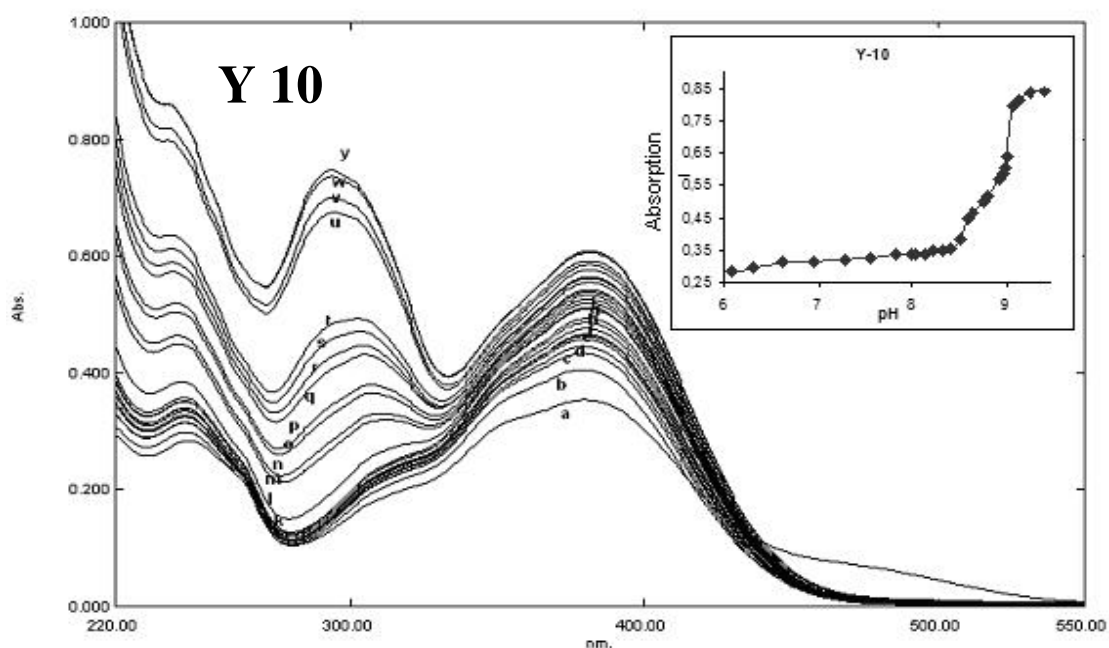


Figure 3.10 pH induced absorption characteristics and sigmoidal calibration curve of Y 10 in EtOH at 390 nm in the pH range of 6.07 and 9.4 (pH =(a) 6.07, (b) 6.31, (c) 6.62, (d) 6.96, (e) 7.28, (f) 7.56, (g) 7.83, (h) 8.00, (i) 8.05, (j) 8.13, (k) 8.23, (l) 8.33, (m) 8.41, (n) 8.51, (o) 8.60, (p) 8.65, (q) 8.75, (r) 8.80, (s) 8.92, (t) 8.98, (u) 8.99, (v) 9.00, (w) 9.07, (x) 9.14, (y) 9.25, (z) 9.4)

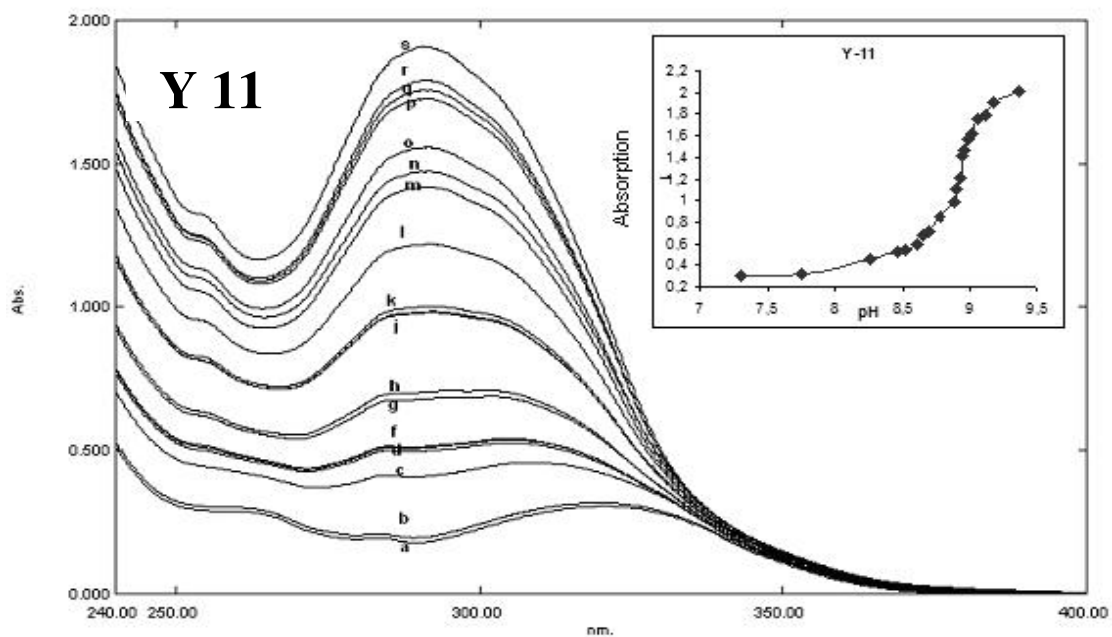


Figure 3.11 pH induced absorption characteristics and sigmoidal calibration curve of Y 11 in EtOH at 379 nm in the pH range of 7.3 and 9.26 (pH = (a)7.3, (b) 7.75, (c) 8.25, (d) 8.46, (e) 8.53, (f) 8.66, (g) 8.7, (h) 8.78, (i) 8.88, (j) 8.93, (k) 8.95, (l) 8.99, (m) 9.01, (n) 9.06, (o) 9.11, (p) 9.18, (q) 9.26)

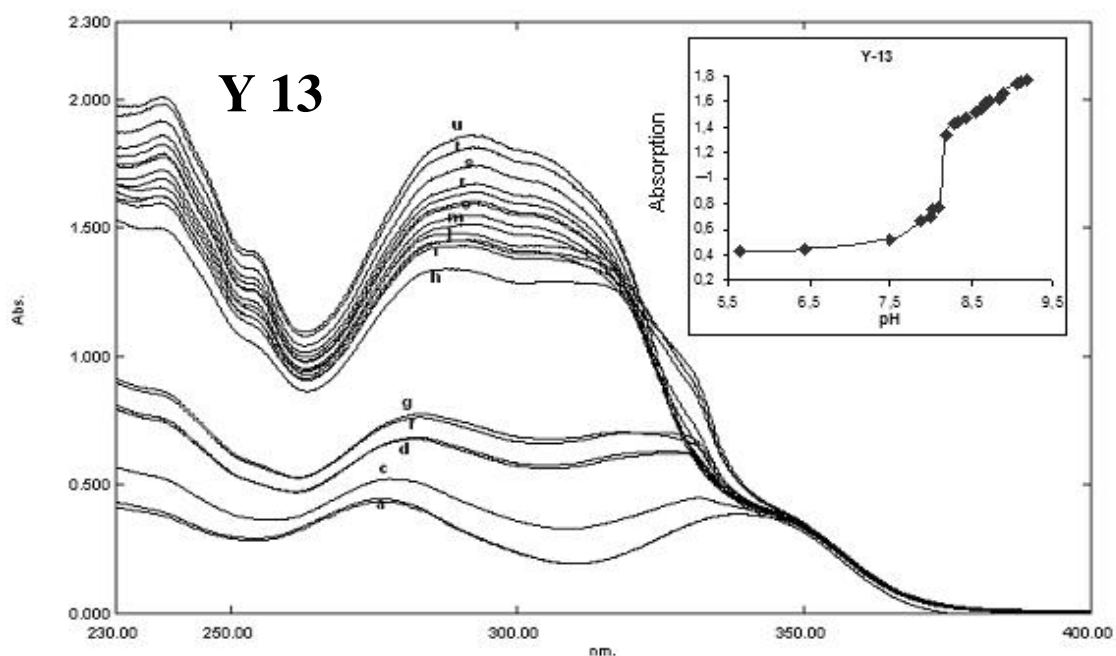


Figure 3.12 pH induced absorption characteristics and sigmoidal calibration curve of Y 13 in EtOH at 376 nm in the pH range of 5.65 and 9.18 (pH = (a) 5.65, (b) 6.45, (c) 7.5, (d) 7.88, (e) 7.98, (f) 8.03, (g) 8.1, (h) 8.18, (i) 8.3, (j) 8.32, (k) 8.33, (l) 8.44, (m) 8.54, (n) 8.64, (o) 8.68, (p) 8.73, (q) 8.83, (r) 8.89, (s) 9.06, (t) 9.1, (u) 9.18)

3.3.2 pKa Calculations of Y 10, Y 11 and Y 13 in PVC Matrix

In order to calculate the pKa values of the PVC doped indicator dyes the thin films of Y 10, Y 11 and Y 13 were exposed to buffered solutions at different pH values.

The sensor membranes reversibly responded in the alkaline region of the pH scale. The relative signal changes of absorption spectra of Y 10, Y 11 and Y 13 were monitored after addition of certain concentrations of buffered solutions. Y 10, Y 11 and Y 13 exhibited the best response to pH between pH 8.5–12.0, pH 7.5–12.0, pH 7.5–12.0, respectively

Figure 3.13, 3.14 and 3.15 reveal pH dependent absorption characteristics and sigmoidal calibration curves of PVC doped Y 10, Y 11 and Y 13 in the pH range of 8.50–12.00, pH 7.5–12.0 and pH 7.5–12.0 respectively.

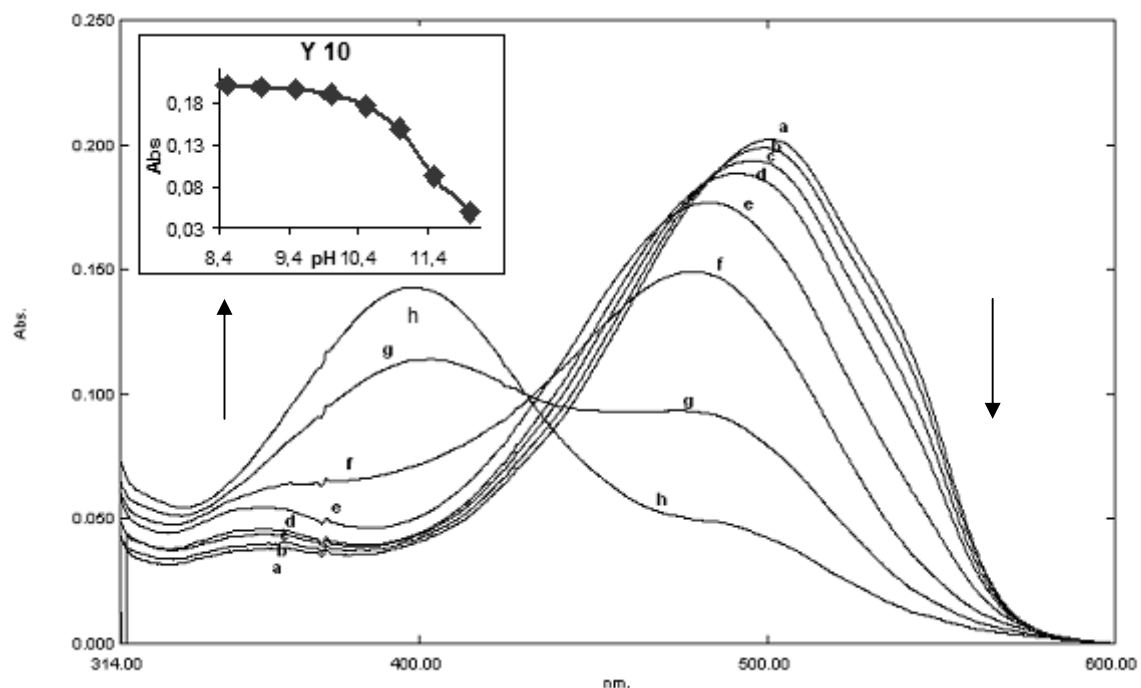


Figure 3.13 pH induced absorption spectra and sigmoidal calibration curve of PVC doped Y 10 in the pH range of 8.50–12.00. pH: a) 8.50, b) 9.00, c) 9.50, d) 10.00, e) 10.50, f) 11.00, g) 11.50, h) 12.00

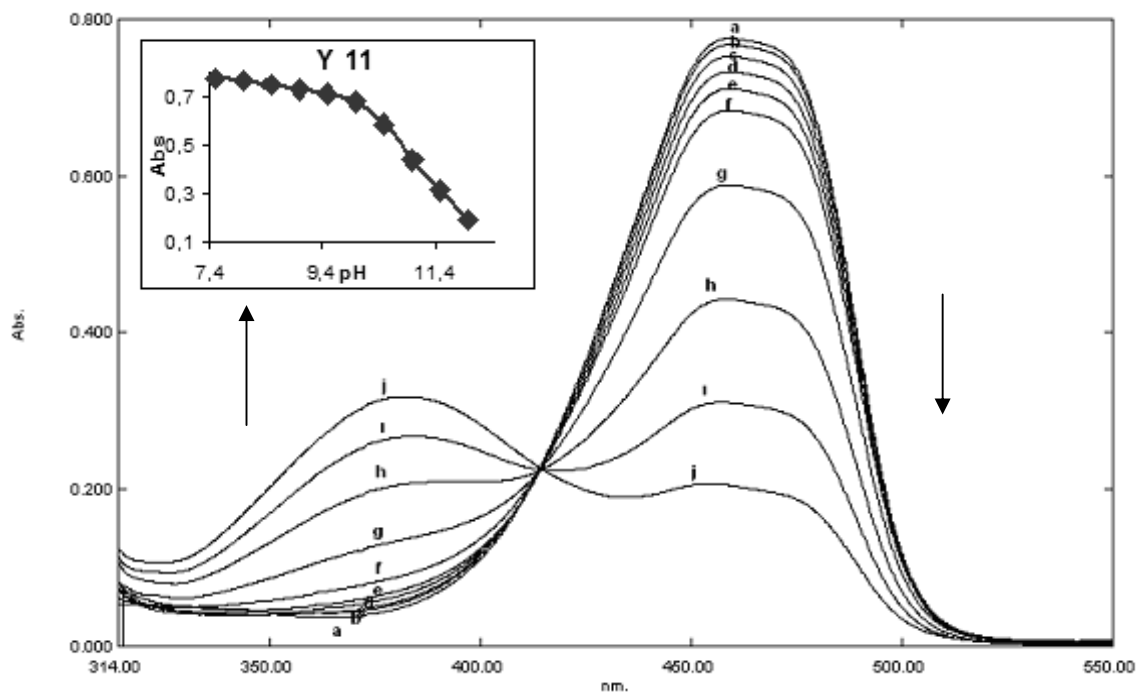


Figure 3.14 pH induced absorption spectra and sigmoidal calibration curve of PVC doped Y 11 in the pH range of 7.50-12.00. pH: a) 7.50, b) 8.00, c) 8.50, d) 9.00, e) 9.50, f) 10.00, g) 10.50, h) 11.00, i) 11.50, j) 12.00

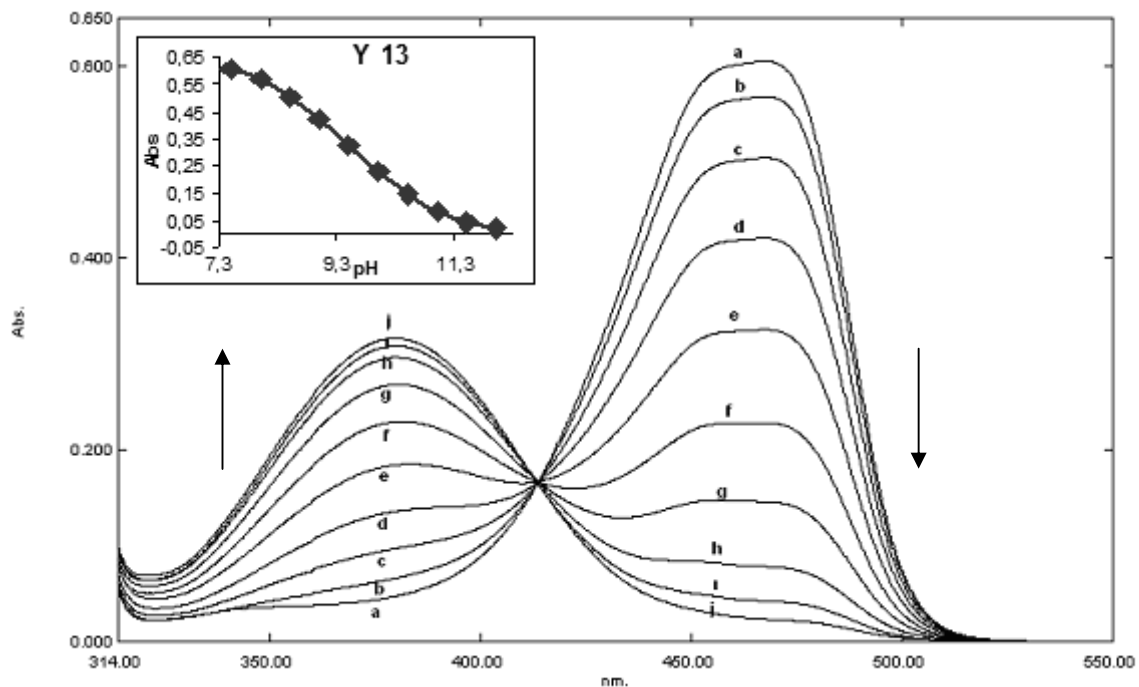


Figure 3.15 pH induced absorption spectra and sigmoidal calibration curve of PVC doped Y 13 in the pH range of 7.50-12.00. pH: a) 7.50, b) 8.00, c) 8.50, d) 9.00, e) 9.50, f) 10.00, g) 10.50, h) 11.00, i) 11.50, j) 12.00

pK_a values of Y 10, Y 11 and Y 13 were found to be 10.9, 10.7 and 9.50 from the inflection points of the insert plots of Fig.3.6, 3.7 and 3.8 respectively. The pK_a values were also calculated as 10.7, 10.5 and 9.30 by using non-linear fitting algorithm of Gauss–Newton–Marquardt equation (Oter, 2007);

$$pK_a = pH + \log \left[\frac{(I_x - I_b)}{(I_a - I_x)} \right]$$

where I_a and I_b are the absorption intensities of acidic and basic forms and I_x is the intensity at a pH near to the pK_a. The calculated pK_a values reveal that the Y 10, Y 11 and Y 13 dyes can be used as chromophore HCO₃⁻ indicators.

3.4 Emission Based HCO₃⁻ Tests of the PVC Doped Indicator Dyes

Emission and excitation spectra of Y 10, Y 11 and Y 13 were recorded with Fluorescence spectrophotometer.

The emission based relative signal changes of Y 10, Y 11 and Y 13 were shown in Figure 3.16, 3.17 and 3.18 the pH range of 7.0–12.0; 7.5–12.0; 7.5–12.0, respectively.

Emission based test results exhibited similar behavior to the absorption-based ones. When the above-mentioned Gauss–Newton–Marquardt algorithm was employed to the emission based spectral data the pK_a values of 10.6, 10.4 and 9.3 were found for Y 10, Y 11 and Y 13 respectively.

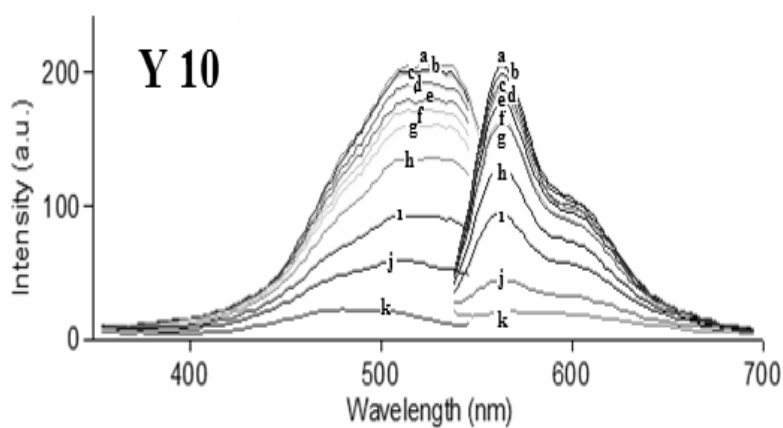


Figure 3.16 pH induced emission characteristics PVC doped Y 10 in the pH range of 7.00-12.00. pH: a) 7.00, b) 7.50, c) 8.00, d) 8.50, e) 9.00, f) 9.50, g) 10.00, h) 10.50, i) 11.00, j) 11.50, k) 12.00

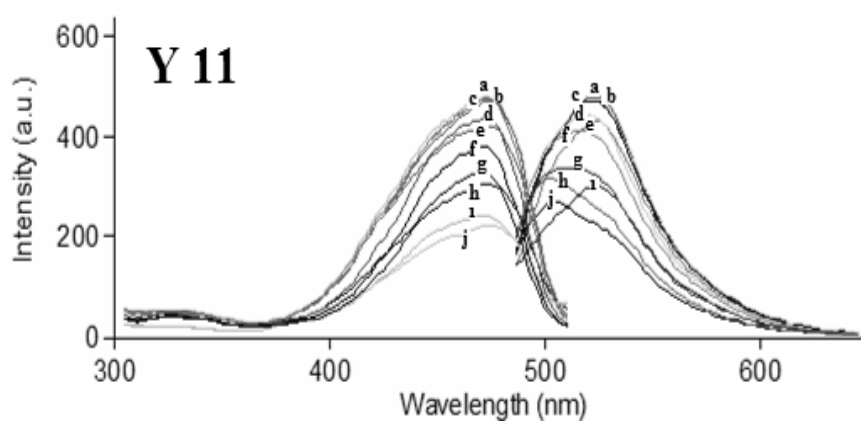


Figure 3.17 pH induced emission characteristics PVC doped Y 11 in the pH range of 7.50-12.00. pH: a) 7.50, b) 8.00, c) 8.50, d) 9.00, e) 9.50, f) 10.00, g) 10.50, h) 11.00, i) 11.50, j) 12.00

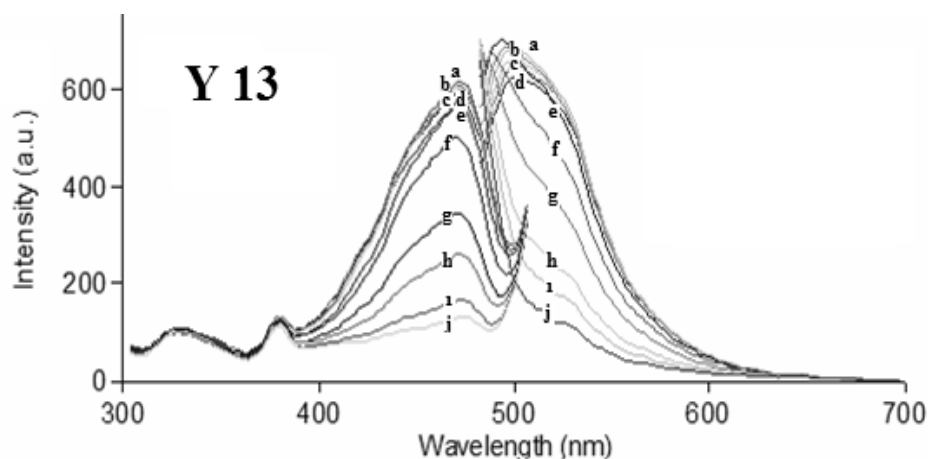


Figure 3.18 pH induced emission characteristics PVC doped Y 13 in the pH range of 7.50-12.00. pH: a) 7.50, b) 8.00, c) 8.50, d) 9.00, e) 9.50, f) 10.00, g) 10.50, h) 11.00, i) 11.50, j) 12.00

3.4.1 Calibration Graph of PVC Doped Y 10, Y 11 and Y 13 Dyes for HCO_3^-

Absorption based HCO_3^- response of immobilized Y10, Y 11 and Y 13 dyes were recorded after exposure to different concentrations of HCO_3^- solutions. All of the employed dyes exhibited an increasing response in signal intensity in the concentration range of 4×10^{-8} - 4×10^{-4} M.

Figure 3.19, 3.21 and 3.23 show the absorption-based response of the PVC doped employed dyes to HCO_3^- solutions.

Standard solutions were prepared freshly from 1 mol L^{-1} NaHCO_3 stock solution before the measurements. CO_2 -free standard solutions were prepared with doubly distilled water after boiling and bubbling with nitrogen; they were stored in closed containers. Micro liter volumes of (10 μL) of standard solutions of NaHCO_3 were added to the sensing agent-containing cuvette, mixed and the changes in absorption intensity caused by addition of different concentrations of HCO_3^- were measured. All the experiments were performed at room temperature (25 $^\circ\text{C}$).

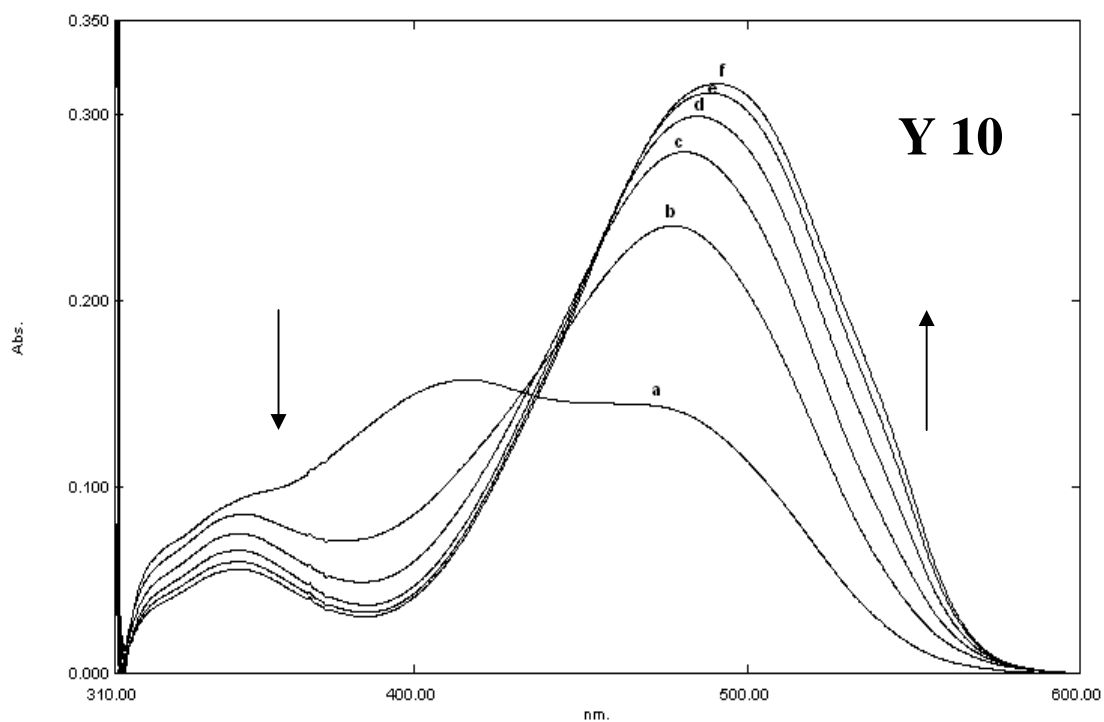


Figure 3.19 Absorption based spectra of PVC doped Y 10 (a)Blank (pure water); (b) 4×10^{-8} M; (c) 4×10^{-7} M; (d) 4×10^{-6} M; (e) 4×10^{-5} M; (f) 4×10^{-4} M

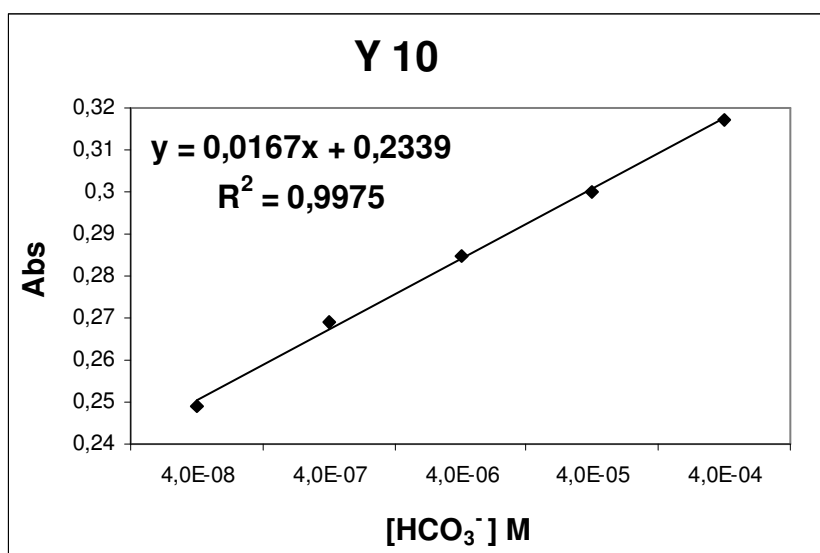


Figure 3.20 Absorption based calibration plot of PVC doped Y 10 for HCO_3^- test solutions.

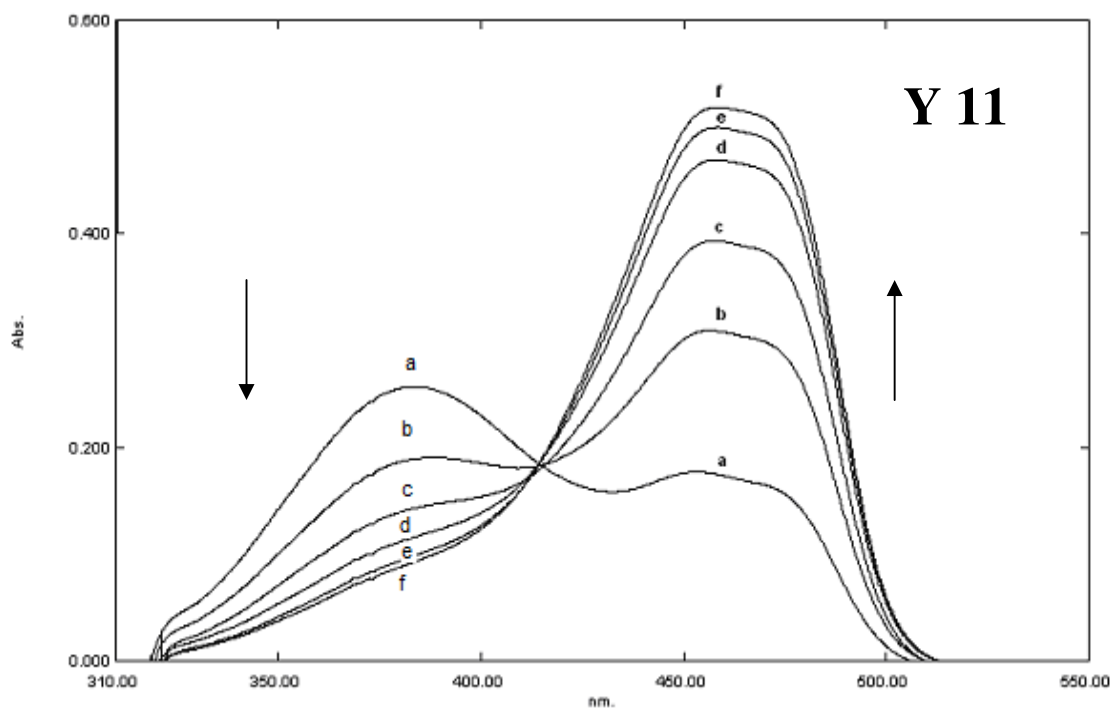


Figure 3.21 Absorption based spectra of PVC doped Y 11 (a)Blank (pure water); (b) 4×10^{-8} M; (c) 4×10^{-7} M; (d) 4×10^{-6} M; (e) 4×10^{-5} M; (f) 4×10^{-4} M

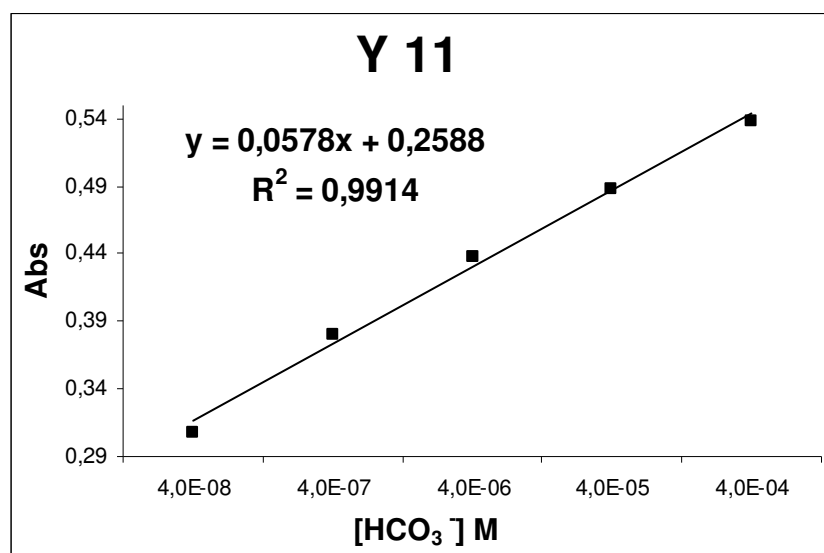


Figure 3.22 Absorption based calibration plot of PVC doped Y 11 for HCO_3^- test solutions.

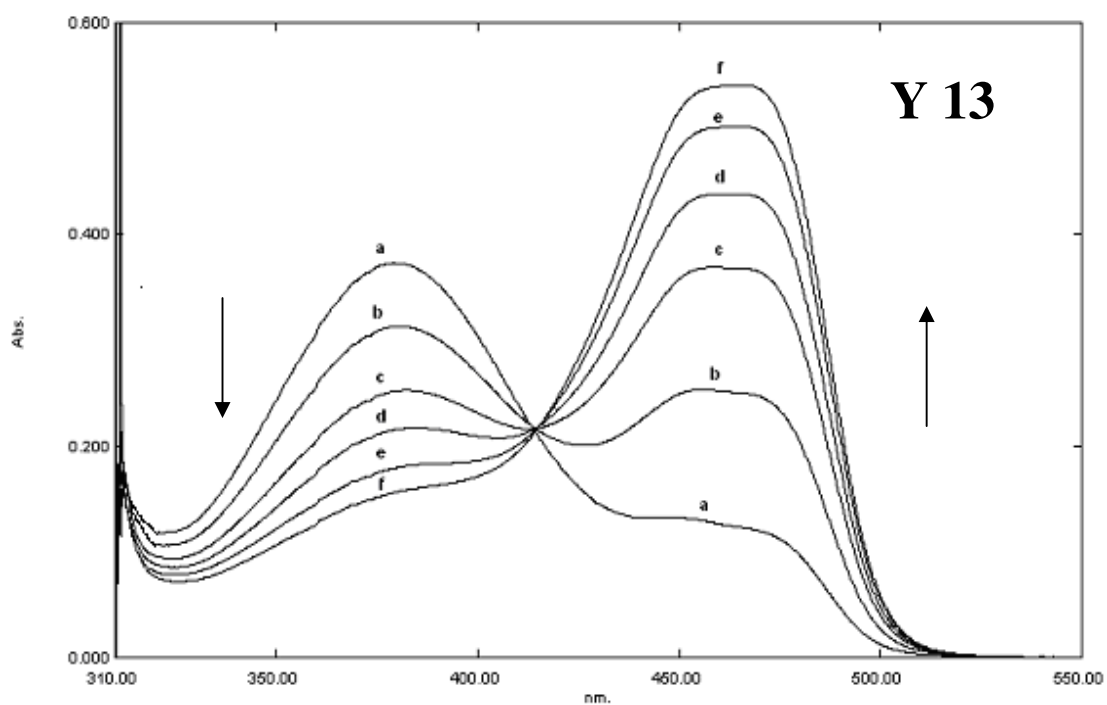


Figure 3.23 Absorption based spectra of PVC doped Y 13 (a)Blank (pure water); (b) 4×10^{-8} M; (c) 4×10^{-7} M; (d) 4×10^{-6} M; (e) 4×10^{-5} M; (f) 4×10^{-4} M

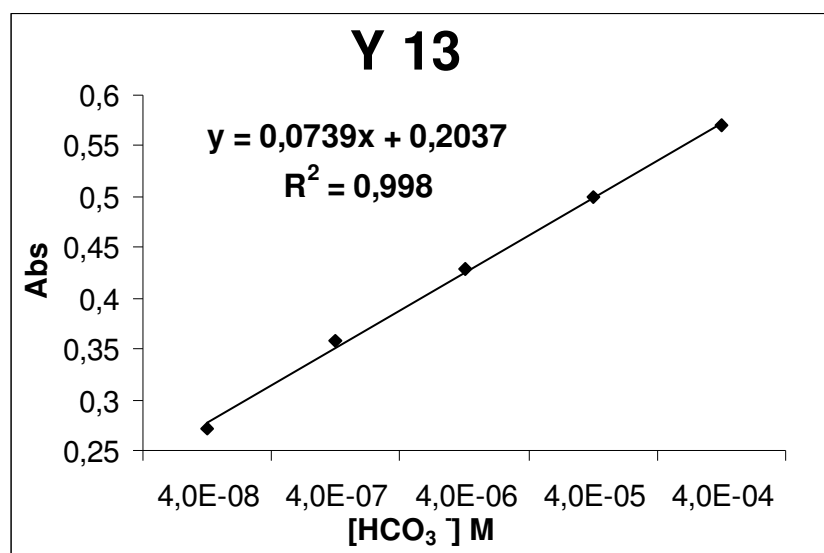


Figure 3.24 Absorption based calibration plot of PVC doped Y 13 for HCO_3^- test solutions

3.4.2 HCO_3^- Analysis in Real-Groundwater Samples

After calibration studies real groundwater samples were tested in the same experimental setup. The recorded absorption intensities of the groundwater samples were employed to the calibration equations. Solution of the calibration equations was yielded the HCO_3^- concentration of the groundwater samples. HCO_3^- concentration of the groundwater samples was also determined with potentiometric and classical indicator based titrimetric method.

Potentiometric titration plot of the employed HCO_3^- containing groundwater sample is given in Figure 3.25 and 3.26. The plots were drawn titrant volume (mL standardized 0.1 M HCl) versus pH and/or potential (mV).

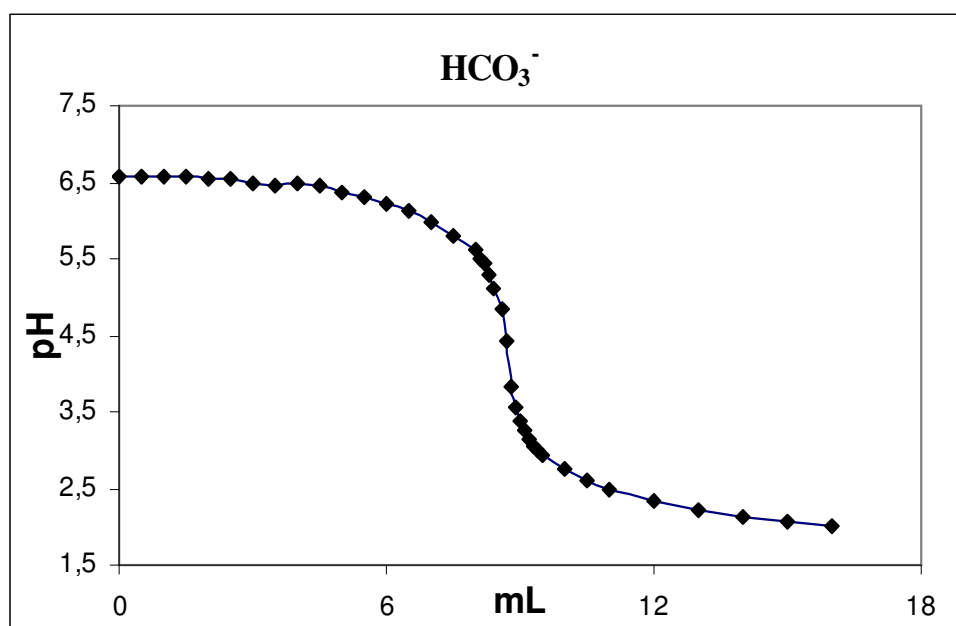


Figure 3.25 Potentiometric titration plot of Pamukkale Antique Pool groundwater sample. (mL titrant volume/ pH)

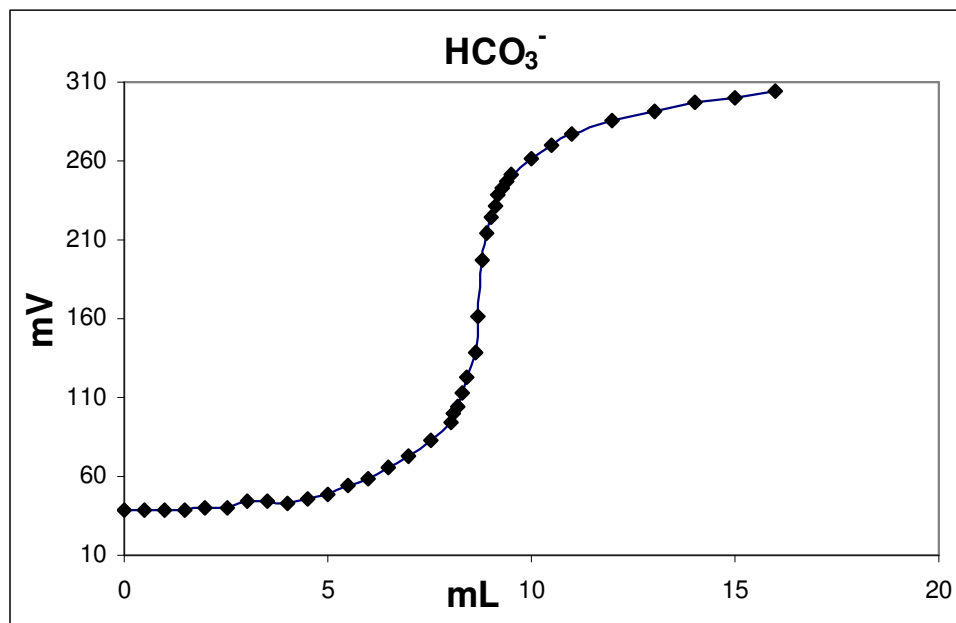


Figure 3.26 Potentiometric titration plot of Pamukkale Antique Pool groundwater sample. (mL titrant volume/ Potential (mV))

Comparative results of spectral, potentiometric and indicator based titrimetric methods were shown in Table 3.2. In spectral method PVC doped Y 10, Y 11 and Y 13 dyes were used as indicator.

Table 3.2 HCO_3^- concentrations determined by spectral and potentiometric method.

HCO_3^- Analysis in Real-Groundwater Samples	Y 10		Y 11		Y 13	
	In fresh sample (M)	After a storage of 7 days(M)	In fresh sample (M)	After a storage of 7 days(M)	In fresh sample (M)	After a storage of 7 days(M)
Potentiometric method	----	$1,53 \times 10^{-2}$	----	$1,53 \times 10^{-2}$	----	$1,53 \times 10^{-2}$
Titration with indicator metil orange (HCO_3^-)	$1,52 \times 10^{-2}$	$1,50 \times 10^{-2}$	$1,52 \times 10^{-2}$	$1,50 \times 10^{-2}$	$1,52 \times 10^{-2}$	$1,50 \times 10^{-2}$
Spectral method	----	$0,90 \times 10^{-2}$	----	$1,106 \times 10^{-2}$	----	$1,19 \times 10^{-2}$

3.5 Ionic Liquid Media Based Studies

The indicator dyes Y 10, Y 11 and Y 13 were also employed in the water-miscible ionic liquid of 1-ethyl 3-methyl imidazolium tetrafluoroborate. The ionic liquid doped indicator dyes were tested with different concentrations of HCO_3^- solutions in the concentration range of 4×10^{-8} – 3.5×10^{-3} M.

Figures from 3.20 to 3.24 show absorption based spectral responses and related calibration curves of Y10, Y11 and Y13 after exposure to standard HCO_3^- solutions.

Interestingly, in the ionic liquid media the indicator dyes exhibited decreasing signal intensity upon exposure to increasing concentrations of HCO_3^- .

The calibration graphs can be concluded as linear. Therefore, the ionic liquid media provided a new matrix for HCO_3^- sensing with Y 10, Y 11 and Y 13 dyes.

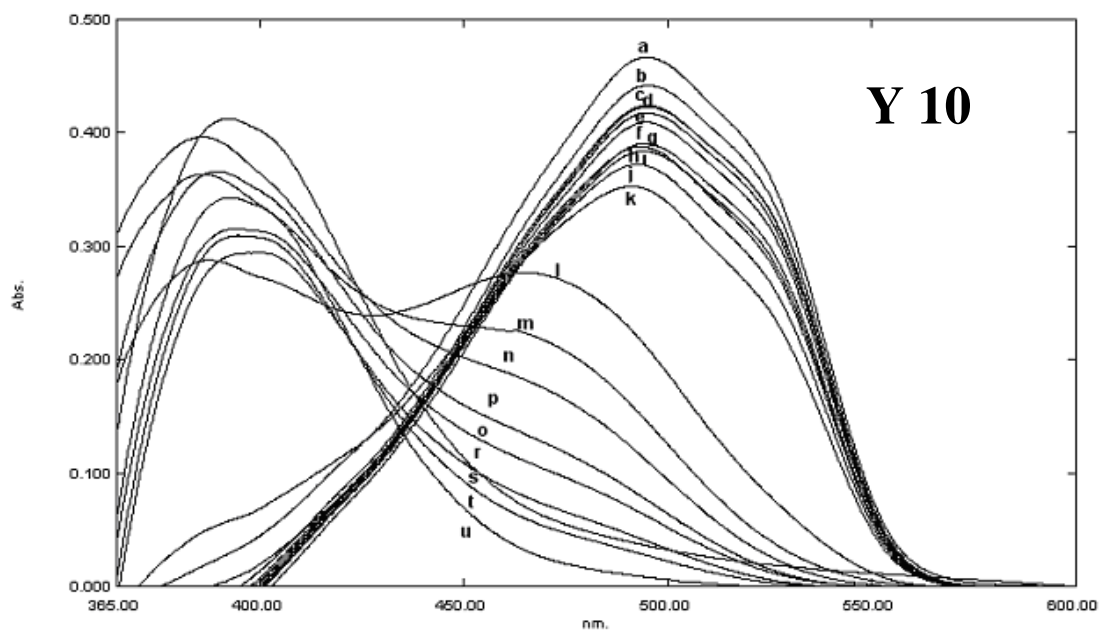


Figure 3.20 Absorption based response of Y 10 to different concentrations of HCO_3^- in ionic liquid media (a) Blank (ionic liquid); (b) 4×10^{-8} M; (c) 4.4×10^{-7} M; (d) 8.4×10^{-7} M; (e) 4.83×10^{-6} M; (f) 4.43×10^{-5} M; (g) 4.82×10^{-5} M; (h) 8.76×10^{-5} M; (i) 4.77×10^{-4} M; (j) 5.16×10^{-4} M; (k) 7.11×10^{-4} M; (l) 1.1×10^{-3} M; (m) 1.5×10^{-3} M; (n) 1.9×10^{-3} M; (p) 2.3×10^{-3} M; (o) 2.7×10^{-3} M; (r) 3.1×10^{-3} M; (s) 3.5×10^{-3} M HCO_3^- .

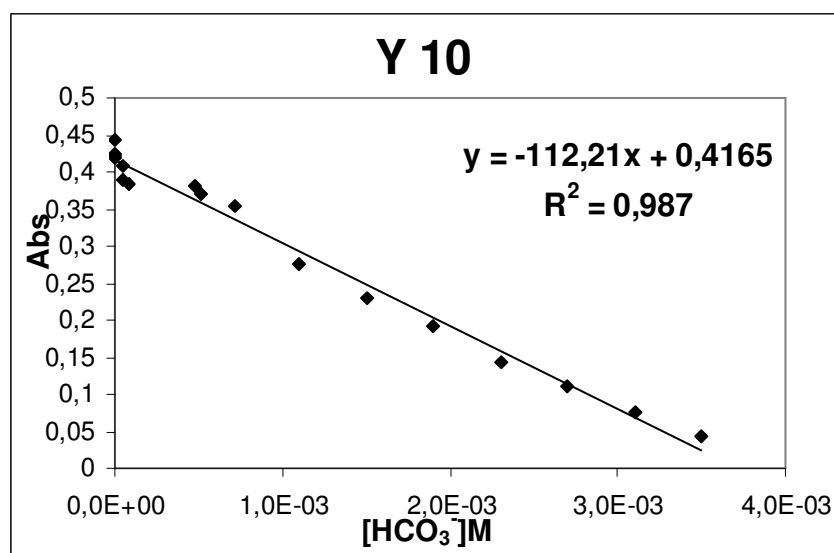


Figure 3.21 Absorption based calibration plot of ionic liquid dissolved Y 10 for HCO_3^- test solutions.

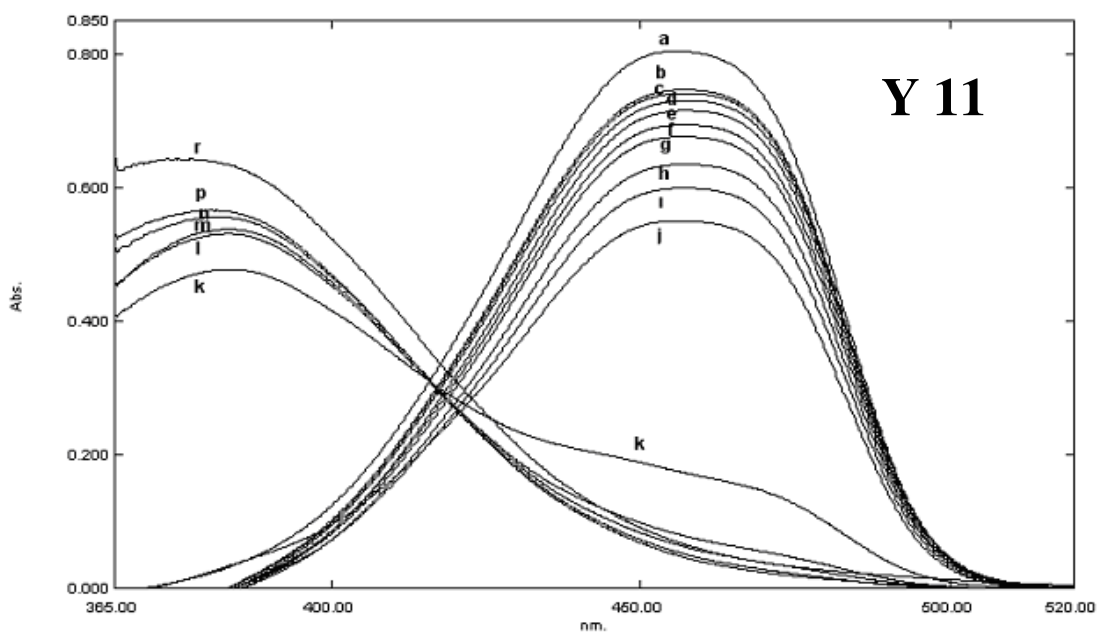


Figure 3.22 Absorption based response of Y 11 to different concentrations of HCO_3^- in ionic liquid media (a) Blank (ionic liquid); (b) 4×10^{-8} M; (c) 4.4×10^{-7} M; (d) 8.4×10^{-7} M; (e) 4.83×10^{-6} M; (f) 4.43×10^{-5} M; (g) 4.82×10^{-5} M; (h) 8.76×10^{-5} M; (i) 4.77×10^{-4} M; (j) 5.16×10^{-4} M; (k) 7.11×10^{-4} M; (l) 1.1×10^{-3} M; (m) 1.5×10^{-3} M; (n) 1.9×10^{-3} M; (p) 2.3×10^{-3} M; (o) 2.7×10^{-3} M; (r) 3.1×10^{-3} M; (s) 3.5×10^{-3} M HCO_3^- .

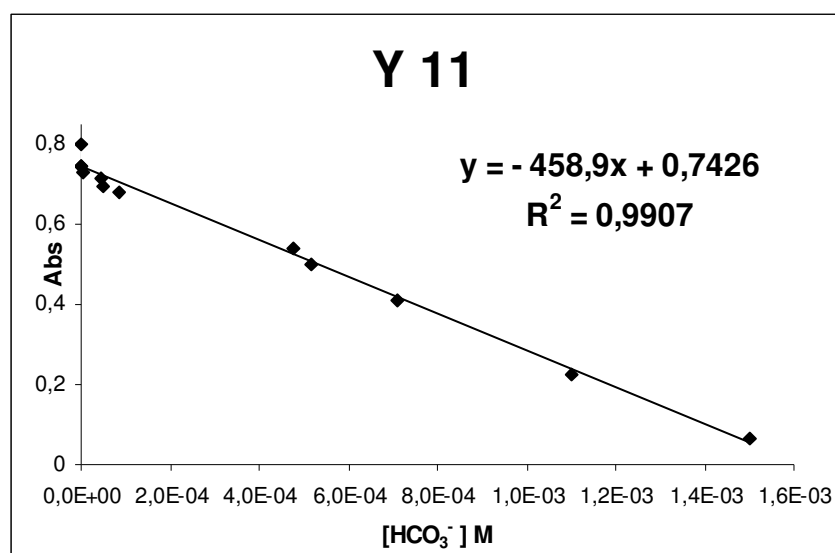


Figure 3.23 Absorption based calibration plot of ionic liquid dissolved Y 11 f or HCO_3^- test solution

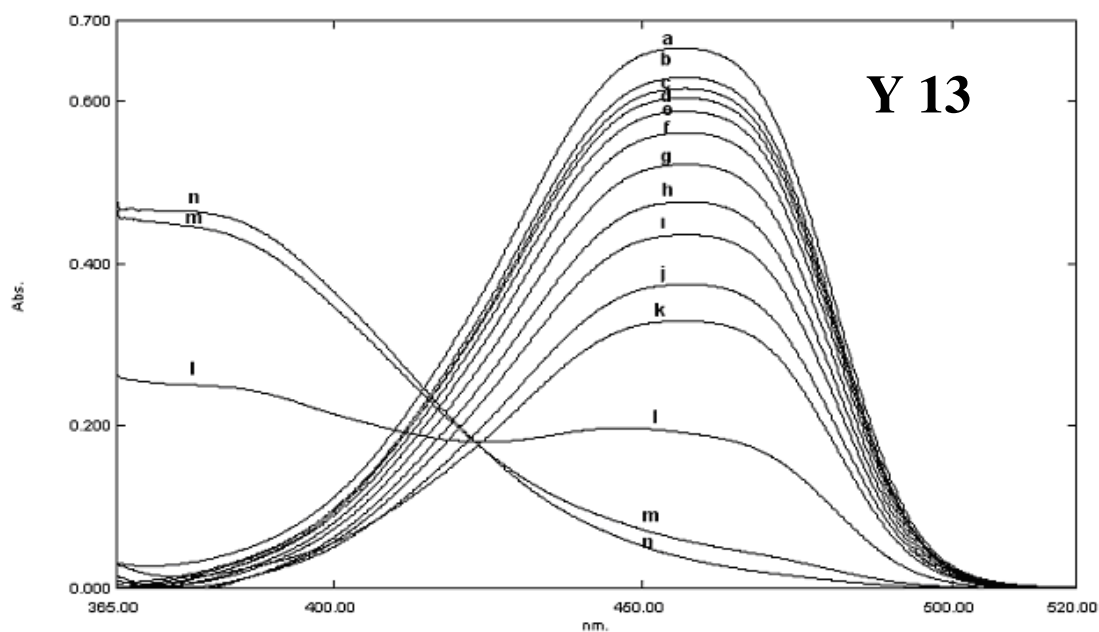


Figure 3.24 Absorption based response of Y 13 to different concentrations of HCO_3^- in ionic liquid media (a) Blank (ionic liquid); (b) 4×10^{-8} M; (c) 4.4×10^{-7} M; (d) 8.4×10^{-7} M; (e) 4.83×10^{-6} M; (f) 4.43×10^{-5} M; (g) 4.82×10^{-5} M; (h) 8.76×10^{-5} M; (i) 4.77×10^{-4} M; (j) 5.16×10^{-4} M; (k) 7.11×10^{-4} M; (l) 1.1×10^{-3} M; (m) 1.5×10^{-3} M; (n) 1.9×10^{-3} M; (p) 2.3×10^{-3} M; (o) 2.7×10^{-3} M; (r) 3.1×10^{-3} M; (s) 3.5×10^{-3} M HCO_3^- .

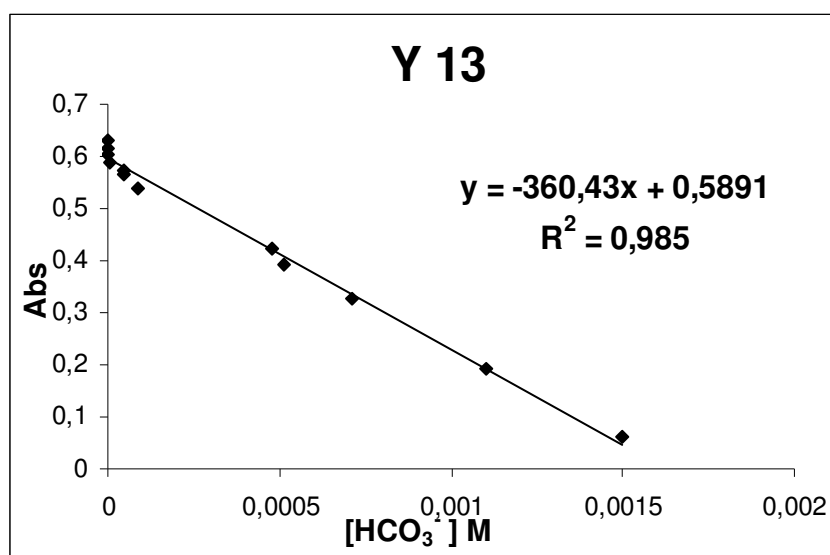


Figure 3.25 Absorption based calibration plot of ionic liquid dissolved Y 13 for HCO_3^- test solutions.

3.6 Response of PVC Doped Y 10, Y 11 and Y 13 to Different Cations and Anions

Response of PVC doped Y 10, Y 11 and Y 13 to polyvalent metal ions was investigated by exposure to 10^{-5} M solutions of Ca^{2+} , Ag^+ , Ni^{2+} , Al^{3+} , Mn^{2+} , Bi^{2+} , Co^{2+} , Hg^+ , Hg^{2+} , Pb^{2+} , Cd^{2+} , Zn^{2+} , Mg^{2+} , Sn^{2+} , Fe^{2+} , Fe^{3+} , Cu^{2+} and H^+ . Figure 3.26, 3.27 and 3.28 reveals intensity-based response of Y 10, Y 11 and Y 13 to the metal cations in acetic acid/acetate buffered solutions at pH 5.0. The most notable source of interference to the pH sensitivity of Y 10 arised from Al^{3+} , Hg^+ , Hg^{2+} and Fe^{3+} at neutral or slightly acidic pHs. The potential interferents for Y 11 are Ni^{2+} , Al^{3+} , Hg^+ , Hg^{2+} , and Fe^{3+} ; and for Y 13 are Bi^{2+} , Hg^+ , Hg^{2+} , and Fe^{3+} . Spectroscopic responses to metal ions are dependent on many factors, including pH, temperature, viscosity, and the presence of other ions.

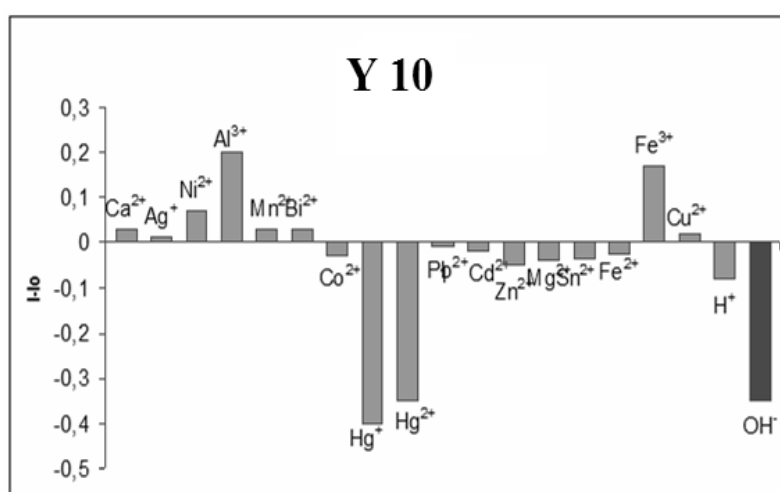


Figure 3.26 Metal-ion response tests for Y 10. Results are plotted as relative signal changes, $(I - I_0)/I_0$, where I is the absorbance intensity of the sensor membrane after exposure to ion-containing solutions and I_0 is the absorption intensity of the sensor slide in ion-free buffer solution.

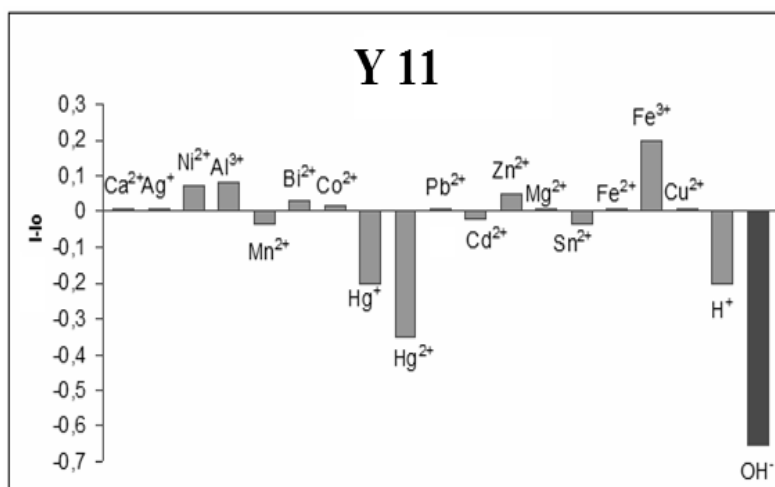


Figure 3.27 Metal-ion response tests for Y 11. Results are plotted as relative signal changes, $(I - I_0)/I_0$, where I is the absorbance intensity of the sensor membrane after exposure to ion-containing solutions and I_0 is the absorption intensity of the sensor slide in ion-free buffer solution.

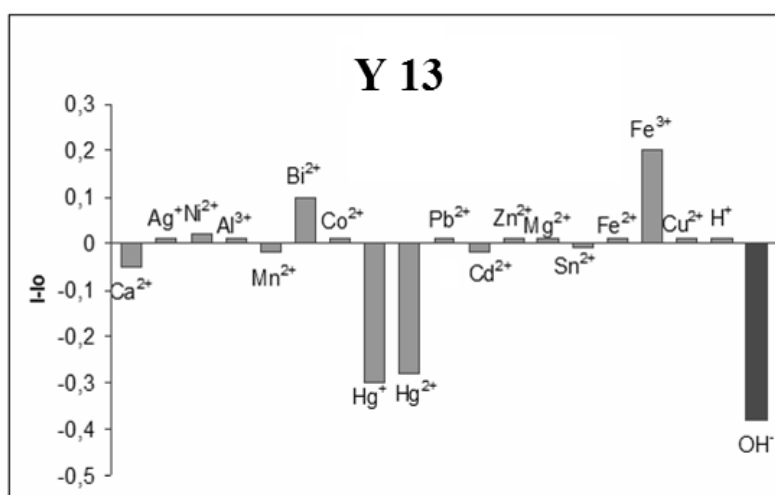


Figure 3.28 Metal-ion response tests for Y 13. Results are plotted as relative signal changes, $(I - I_0)/I_0$, where I is the absorbance intensity of the sensor membrane after exposure to ion-containing solutions and I_0 is the absorption intensity of the sensor slide in ion-free buffer solution.

Response of PVC doped thin films of Y 10, Y 11 and Y 13 was also investigated by exposure to Fluoride (20 mg/L), Chloride (30mg/L), Nitrite (100mg/L), Bromide (100 mg/L), Nitrate (100mg/L), Phosphate (150 mg/L) and Sulfate (150mg/L). It was pleasing that; none of the employed ions produced a significant response when interfaced with dye doped PVC membranes.

CHAPTER FOUR

CONCLUSION

In this part of the thesis, simultaneous ion chromatographic analysis of seven different anions (Fluoride, Chloride, Nitride, Bromide, Nitrate, Phosphate, Sulfate) in real groundwater samples were performed by ion chromatography method. Some validation tests and the optimum conditions for the determination of anions were studied. Analysis of anions was performed by injection of samples to the chromatographic system after filtration and/or dilution. The precision and accuracy of the method were tested at three different concentration levels for each standard. In order to evaluate effectiveness of the method certified reference standards at three different dilution levels were applied initially to the ion chromatography. Subsequently, the same instrumental approach was applied to field samples. Anion concentrations of known certified reference standards (CRS), their calibration related data and results obtained from control samples are presented. The final calibration curves of CRS resulted in >99.99 % correlation coefficient values.

Recovery studies were performed by adding standards in to the geothermal and drinking water samples. For geothermal water samples recovery tests was performed between two successive months. Precision was also assessed as the percentage relative standard deviation (%RSD) of both repeatability (within-day) and reproducibility (between-day and different concentrations) for groundwater samples. SD and RSD values of 220 real groundwater samples acquired during 8 months were evaluated.

Peak asymmetry (EP) is a factor regarding with peak symmetry and its value should be around %10 of the peak height. A peak asymmetry value of 1-1.05 points out excellent peak symmetry. Where the asymmetry values in the range of 1.2-2 are acceptable, the higher ones are unacceptable. Except that of fluoride, all asymmetry values were found to be acceptable. The asymmetry values of low concentrations of fluoride exhibited a little bit deviation from the acceptable values.

The resolution of a column provides a quantitative measure of its ability to separate two analyte. A resolution value of 1.5 means essentially complete separation of peaks. The resolution values were calculated with respect to SO_4^{2-} and were found to be 12.25, 6.49, 7.98, 4.9, 3.55 and 4.8 for F^- , Cl^- , NO_2^- , Br^- , NO_3^- and PO_4^{3-} respectively. From Table 3 it can be concluded that the resolution performance of the column is very satisfactory for our working conditions.

The efficiency of chromatographic columns increases as the number of plates (N) becomes greater and the plate height becomes smaller. Efficiencies in terms of plate numbers can vary from a few hundred to several hundred thousand. Plate number of $N > 2000$ is a desirable value. In our case number of plates are 4450, 12134, 11037, 12473, 12188, 7799 and 10079 for F^- , Cl^- , NO_2^- , Br^- , NO_3^- , PO_4^{3-} and SO_4^{2-} respectively which are quite good for all calibration points.

Precision can be determined by replicating a measurement. In this work, precision of the retention times was evaluated with six replicate measurements for each standard. Average retention times were found to be 3.8112, 6.7035, 8.5385, 11.4423, 13.6102, 15.7833 and 19.3097 min. for Fluoride, Chloride, Nitrite, Bromide, Nitrate, Phosphate and Sulfate respectively. Their standard deviations were in the range of 0.0034 – 0.0903 min. which is less than %0.5.

The recovery studies were performed by adding standards in to the geothermal groundwater and drinking water samples. For groundwater samples recovery tests was performed between two successive months. The groundwater samples were treated with different concentrations of certified reference standards which were diluted in the ratio of 1:8, 1:6 and 1:4. The amount of the added certified reference standards were kept in the range of calibration limits.

In real groundwater samples, the deviations observed in recovery values were less than 10%, except that of Fluoride. However, in Fluoride the deviations may extend up to 17%. This can be attributed to the complexation tendency of Fluoride with metal cations.

Drinking water samples exhibited excellent recovery values with respect to groundwater samples. This can be referred to the rich heavy metal content of groundwater samples which is a strongly possible reason for interferences.

Seven different anions (Fluoride, Chloride, Nitride, Bromide, Nitrate, Phosphate, and Sulfate) in geothermal water samples, that were collected daily during eight months (June 2007- January 2008) from Denizli Pamukkale Antique Pool, were tested and analyzed with ion chromatographic method. Fluoride, Chloride and Sulfate were found to be major ions in Pamukkale geothermal water samples. Nitrite and Nitrate were under limit of detection (LOD) of the instrument. Bromide and Phosphate concentrations were found to be zero. For 26 consecutive measurements, the average value of Fluoride concentration was found to be 1.4750 ppm. SD and RSD of the measurements were calculated as 0.1146 ppm and 7.7706 % respectively.

Average concentrations of Chloride and Sulfate were found to be 13.7169 ppm and 662.8689 ppm respectively. Sulfate measurements were performed after 1:4 dilution.

SD and RSD of Chloride were 0.4373 ppm and 3.1881 % respectively. SD and RSD values of Sulfate were 6.8312 ppm and 1.0305 %. Among them, Fluoride measurements resulted with the highest SD and RSD. In case of Chloride and Sulfate SD and RSD values were satisfactory.

In the second chapter, spectrophotometric, titrimetric and potentiometric bicarbonate (HCO_3^-) analysis results of groundwater samples of Pamukkale Antique Pool were given. New indicator dyes namely (N, N'-bis(4-dimethylaminobenzylidene)benzene-1,4-diamine(Y-10), 4-[4-(dimethylamino)phenylmethylene]amino acetophenone (Y-11) and 4-(4-(dimethylamino)phenyl)methyleneamino benzonitrile (Y-13)) were offered for absorption based analysis of HCO_3^- anion. The indicator dyes were characterized in the different solvents of ethanol (EtOH), dichloromethane (DCM), tetrahydrofurane (THF) and Toluene/Ethanol (To: EtOH) mixture (80:20)), in solid matrix of PVC and

in Ionic Liquid media. Maximum absorption wavelength (λ_{abs}) and molar extinction coefficients (ϵ) of the indicators were determined with UV-Vis spectrophotometer in all of the employed matrices. Acidity constant values of three different indicator dyes were calculated in ethanol and polyvinylchloride for HCO_3^- sensing purposes. The calculated acidity constants were found to be proper for HCO_3^- sensing. Cross sensitivities of the indicator dyes to other cations was also tested and evaluated. For all of the employed dyes the bicarbonate responses were excellent both in PVC and ionic liquid media.

REFERENCES

An introduction to ion chromatography.(n.d.).Retrieved December 8, 2007, from (http://www.metrohm.com.cn/administrator/resource/upfile/ic_theory_20041011_e.pdf)

Basic UV-Vis theory, concepts and applications. (n.d.). Retrieved May 20, 2008, from <http://www.molecularinfo.com/MTM/UV.pdf>

Bakker, E. & Simon, W. (1992). Selectivity of ion-sensitive bulk optodes. *Anal. Chem.*, 64 (17), 1805-1812.

Buytenhuys, F. A. (1981). Ion chromatography of inorganic and organic ionic species using refractive index detection, *Journal Of Chromatography*, 218, 57.

Chakrapani, G., Murty, D.S.R., Mohanta, P.L., & Rangaswamy, R. (1998). Sorption of PAR-metal complexes on activated carbon as a rapid preconcentration method for the determination of Cu, Co, Cd, Cr, Ni, Pb and V in ground water. *Journal Of Geochemical Exploration*, 63 (2), 145-152.

Chemistry of Ion Exchange Polymers. (n.d.). Retrieved June 15, 2008, from <http://www.rpi.edu/dept/chem-eng/Biotech-Environ/IONEX/styrene.html>

Chrompack. Inc.. Bridgewater. New Jersey. Chrompack Topics. Vol. 8 (1981).

Cochrane, R. A., & Hillman, D. E. (1982). Analysis of anions by ion chromatography using ultraviolet detection. *Journal Of Chromatography*, 241, 392.

- Dahlen, J., Karlsson, S., Backstrom, M., Hagberg, J., & Pettersson, H. (2000). Determination of nitrate and other water quality parameters in groundwater from UV/Vis spectra employing partial least squares regression. *Chemosphere*, 40 (1), 71-77.
- Denkert, M., HacEzell, L., Schill, G., & Sjogren, E. (1981). Reversed-phase ion-pair chromatography with UV-absorbing ions in the mobile phase. *Journal Of Chromatography*, 218, 31.
- Dionex Reference Library. (2007). [Recorded by Dionex Corporation], On [CD].
- Downey, S. W., & Hieftje, G. M. (1983). Replacement ion chromatography with flame photometric detection. *Analytica Chimica Acta*, 153, 1.
- Fritz, J.S., & Gjerde, D.T. (2000). *Ion chromatography* (3th ed.) Germany: Wiley-WHC
- Freed, D. J. [1975]. Flame photometric detector for liquid chromatography. *Analytical Chemistry*, 47, 186.
- Goodkin, L., & Fritz, J. S. (1974). Separation and determination of tin by liquid-solid chromatography *Analytical Chemistry*, 46, 959.
- Goodkin, L., Seymour, M. D., & Fritz, J. S. (1975). Ultraviolet spectra of metal ions in 6M hydrochloric acid. *Talanta*, 22, 245.
- Grabinski, A. A. (1981). Determination of arsenic(III), arsenic(V), monomethylarsonate, and dimethylarsinate by ion-exchange chromatography with flameless atomic absorption spectrometric detection. *Analytical Chemistry*, 53, 966.

- Gustavo González, A., Angeles Herrador, M., G. Asuero, Agustín. (1998). Intra-laboratory testing of method accuracy from recovery assays. *Talanta*, 48, 729–736.
- Haddad, P.R., & Heckenberg, A.L. (1982). High-performance liquid chromatography of inorganic and organic ions using low-capacity ion-exchange columns with indirect refractive index detection. *Journal of Chromatography A*, 252, 177-184
- Henshall, A., Rabin, S., Statler, J., & Stilian, J. (1992). Recent development in ion chromatography detection: the self-regenerating suppressor. *American Laboratory*, 24, 20R.
- Hershcovitz, H., Yarnitsky, Ch., & Schmuckler, G. (1982). Ion chromatography with potentiometric detection. *Journal of Chromatography*, 252, 113.
- Introduction to IonPac . AS9-HC/AG9-HC chromatography.* (n.d.). Retrieved October 11, 2007, from http://www1.dionex.com/en-us/webdocs/4347_31267-07_Manual,IP,AS9-HC_V28.pdf
- Ion chromatography.* (n.d.). Retrieved November 27, 2007, from http://www.colorado.edu/chemistry/chem5181/Lectures/C5_IC_TLC.pdf
- Komy, Z. R. (1993). Determination of trace-metals in Nile river and ground-water by differential-pulse stripping voltammetry. *Mikrochimica Acta*, 111 (4-6), 239-249.
- Lakowicz, J. R. (1993). *Principles of Fluorescence Spectroscopy*. Plenum Press: New York and London
- Lerchi, M., Bakker, E., Rusterholz, B., & Simon, W. (1992). Lead-selective bulk optodes based on neutral ionophores with subnanomolar detection limits. *Anal. Chem.*, 64 (14), 1534-1540.

- Liu. Y., Wu. D., Li. J., & Ga. R. (1999). Determination of trace iron(III) and molybdenum(VI) in ground water by pyrocatechol resin-phase spectrophotometry. *Spectroscopy And Spectral Analysis*, 19 (5), 694-696.
- Lockridge, J. E., & Fritz, J.S. (1990). Decontamination of water using a nitrate-selective ion-exchange resin. *United States Patent 4944878*.
- Muller, J. (1999). Determination of inorganic arsenic(III) in ground water using hydride generation coupled to ICP-AES (HG-ICP-AES) under variable sodium boron hydride (NaBH₄) concentrations. *Fresenius Journal Of Analytical Chemistry*, 363 (5-6), 572-576.
- Niedzielski, P. (2005). The new concept of hyphenated analytical system: Simultaneous determination of inorganic arsenic(III), arsenic(V), selenium(IV) and selenium(VI) by high performance liquid chromatography-hydride generation-(fast sequential) atomic absorption spectrometry during single analysis. *Analytica Chimica Acta*, 551 (1-2), 199-206.
- Oter, O. (2007). Investigation of Sensor Characteristics of Some Chromoionophore Structures in Polymer and Sol-Gel Matrices. Dokuz Eylul University Graduate School of Natural and Applied Sciences: Izmir
- Owen, T. *Fundamentals of modern UV-Visible Spectroscopy*, Retrieved May 10, 2008, from https://www.ucursos.cl/medicina/2007/2/TM1BIOQ22/1/material_docente/objeto/144797%20-
- Ozcan. A., & Yilmaz. S. (2005). Determination of boron in the waters of Troia by inductively coupled plasma-atomic emission spectrometry (ICP-AES). *Journal Of The Serbian Chemical Society*, 70 (10), 1219-1227.
- Parker, C. A. (1968). *Photoluminescence of Solutions*. Elsevier: Amsterdam.

- Parvinen, P., & Lajunen, L.H.J. (1999). Determination of chloride in drinking and ground water by AlCl₃ molecular absorption spectrometry using graphite furnace atomic absorption spectrometer. *Talanta*, 50 (1), 67-71.
- Pepper, R. W. *Chemistry research*. (1953). (77). England : Her Majesty's Stationary Office.
- Polesello, S., Valsecchi, S., Cavalli, S., & Reschiotto, C. (2001). Ion-chromatographic screening method for monitoring arsenate and other anionic pollutants in ground waters of Northern Italy. *Journal Of Chromatography A*, 920 (1-2), 231-238.
- Ricci, G.R., Shepard, L. S., Colovos, G., & Hester, N. E. (1981). Ion chromatography with atomic absorption spectrometric detection for determination of organic and inorganic arsenic species, *Analytical Chemistry*, 53, 610-613.
- Saari-Nordhaus, R., & Anderson, J.M. Jr. (1992). Applications of an alternative stationary phase for the separation of anions by chemically suppressed ion chromatography. *Journal Of Chromatography A*, 602, (1-2), 15-19.
- Saari-Nordhaus, R., Henderson, I.K., & Anderson, J.M. Jr. (1991). Universal stationary phase for the separation of anions on suppressor-based and single-column ion chromatographic systems. *Journal Of Chromatography*, 546, 88-89.
- Samatya, S., Kabay, N., Yuksel, U., Arda, M., & Yuksel, M. (2006). Removal of nitrate from aqueous solution by nitrate selective ion exchange resins. *Reactive & Functional Polymers* 66 (11), 1206-1214.
- Schmidt, W. (1994). *Optische Spektroskopie*. VCH: Weinheim.
- Seiler, K. & Simon, W. (1992). Theoretical aspects of bulk optode membranes. *Anal. Chim. Acta*, 266, 73-87.

- Seymour, M. D., & Fritz, J. S. (1973). Rapid, selective method for lead by forced-flow liquid chromatography. *Analytical Chemistry*, *45*, 1632.
- Seymour, M. D., Sickafoose, X. P., & Fritz, J. S. (1971). Application of forced-flow liquid chromatography to the determination of iron. *Analytical Chemistry*, *43*, 1734.
- Skoog, D.A., & Leary, J.J. (1992). Ion Chromatography. In *Principles of instrumental analysis* (4th. ed.) (654–655–656) USA: Saunders College
- Small, H., & Miller, T. E., Jr. (1982). Indirect photometric chromatography. *Analytical Chemistry*, *54*, 457-462.
- Small, H., Stevens, T. S., & Bauman, W. G. (1975). Novel ion-exchange chromatographic method using conductimetric detection. *Analytical Chemistry*, *47*, 1801
- Soto-Chinchilla, J.J., Garcia-Campana, A.M., Gamiz-Gracia, L., & Cruces-Blanco, C. (2006). Application of capillary zone electrophoresis with large-volume sample stacking to the sensitive determination of sulfonamides in meat and ground water. *Electrophoresis*, *27* (20), 4060-4068.
- Stevens, T. S., Davis, J. C., & Small, H. (1981). Hollow fiber ion exchange suppressor for ion chromatography. *Analytical Chemistry*, *53*, 1488-1492.
- Stillian, J. (1985). An improved suppressor for ion chromatography. *LC Magazine*, *3*, 802-805.
- Strasburg, R. F., Fritz J. S., Berkowitz, J. & Schmuckler, G. (1989). Injection peaks in anion chromatography. *Journal of Chromatography*, **482** (2), 343-350.

Strong, D. L., & Dasgupta, P.K. (1989). Electroalytic membrane suppressor for ion chromatography. *Analytical Chemistry*, 61, 939-945.

Stumm, W., & Morgan J.J. (1970). *Aquatic chemistry an introduction emphasizing chemical equilibria in natural water*. (1-554-555) USA: Wiley-Interscience

The Anion Micro Membrane Suppressor, (n.d.)

http://www1.dionex.com/enus/columns_accessories/accsup/cons5339.html

The Jablonski Diagram. (n.d.). Retrieved June 8, 2008, from <http://www.photobiology.info/graphics/photochem13.gif>

The Micro Membrane Suppressor, (n.d.)

http://www1.dionex.com/enus/columns_accessories/accsup/cons5339.html

The Separation Mechanism.(n.d.). Retrieved December 10, 2007, from http://www5.gelifesciences.com/APTRIX/upp00919.nsf/Content/LabSep_EduC~LC_tech~IEX~IEXBasic~IEXTheSepM?OpenDocument&hometitle=LabSep

The principle of ion exchange chromatography. (n.d.). Retrieved December 18, 2007, from

http://www.rmpr.cnrs.fr/j1pr/5__TECHNIQUES_DE_PURIFICATION/ION_EXCHANGE.SWF

Vaaramaa, K., & Lehto, J. (2003). Removal of metals and anions from drinking water by ion exchange. *Desalination*, 155 (2), 157-170.

Walton W.C., (1970). *Groundwater resource evaluation*. McGraw-Hill Education (441-442)

- Warth, L.M., Cooper, R.S., & Fritz, J.S.(1989). Low-capacity quaternary phosphonium resins for anion chromatography. *Journal of chromatography*, 479, 401-409.
- Weiss, J. *Handbook of Ion Chromatography*. Retrieved May 26, 2008, from http://media.wiley.com/product_data/excerpt/19/35272870/3527287019.pdf
- Weiss, J. (1995). *Ion chromatography* (2nd ed.) (43). Germany : Weinheim, VCH.
- Woolson, E.A., & Aharonson, N. (1980). Separation and detection of arsenical pesticide residues and some of their metabolites by high-pressure liquid chromatography-graphite furnace atomicabsorption spectrometry. *Journal - Association of Official Analytical Chemists*, 63, 523.
- Yoshida, K., & Haragachi, H. (1984). Determination of rare earth elements by liquid chromatography/ inductively coupled plasma atomic emission. *Analytical Chemistry*, 56, 2580-2585.